C H A P T E R - 4

PREPARATION AND CHARACTERISATION OF POLYPROPYLENE/NYLON-6 BLENDS

CHAPTER - 4

PREPARATION AND CHARACTERISATION OF POLYPROPYLENE/NYLON-6 BLENDS

In this chapter the synthesis and characterisation of various binary and ternary blends of PP/NY-6 is discussed. The blending has been carried out mainly to improve the mechanical properties, toughness, processibility and to reduce water absorption extent of NY-6. Before discussing the preparation and characterisation of blends, the basic toughening mechanism, conforming to various theoretical models for the prediction of the tensile modulus and tensile strength, is discussed.

4.1 TOUGHENING MECHANISM

The tougheness of many plastics can be improved by blending it with other polymeric components having low modulus values. When this polymeric component i.e., elastomeric phase is highly dispersed in the polymer matrix, it acts as an effective stress concentrator. The stress concentrations produced by elastomeric particles give the initiation sites for the various deformations, i.e., crazing; shear yielding in the form of shear band and elastic deformation. Crazing is the first step towards fracture in the polymers. Under sufficiently high stress, the fibrilar structure of crazes breaks down and a true crack forms. Large amount of energy is absorbed in the formation of a single craze. In the toughened plastic multiple crazes are formed. So a considerable amount of energy is absorbed during the fracture. As multiple crazing is always associated with stress whitening [1], it can be easily identified.

Elastic deformation and shear yielding are also very important energy absorbing processess. According to Bulknell [2], shear yielding besides acting as an energy absorbing process, also functions as a craze stopper. As the number of shear bands increase, the length of the newly formed crazes decreases. Thus, shear yielding is not only the deformation mechanism but it appears to be an integral part of toughening mechanism.

Depending upon the structure and concentration of the dispersed phase and matrix any of the above mentioned deformation mechanism can be more effective.

4.1.1 Factors affecting toughening mechanism

Toughening mechanism of the blends is expressed in terms of fracture behaviour. Hence factors affecting fracture behaviour are discussed below.

4.1.1.a Adhesion

The adhesion between the dispersed phase and matrix plays an important role in determining the final impact strength of resultant blends. If the adhesion between the two phases is inadequate a void is formed at the interface and a crack formation is initiated. If one such crack is developed it is transferred from one particle to other with little hinderance from poorly anchored particles in its path. Thus, under impact condition, the material will show very poor impact behaviour. However, according to Wu [3] strong adhesion does

not always ensure toughening. The optimum adhesion required should be such that, the elastomeric particles are not detached from matrix during fracture.

4.1.1.b Particle size

The size of the dispersed particles has a noticable effect on the toughness of the blends. For each type of polymeric blends there appears to be an optimum particle size for toughening. Impact strength falls drastically if average particle diameter is reduced below the optimum value. The smaller particles are unable to initiate the craze formation and also to control craze growth effectively. Again the particle size must exceed the craze thickness to prevent the dispersed phase from becoming encapsulated in the growing craze. Impact strength also falls drastically if the particle size is increased above the optimum diameter due to increased distance between neighbouring particles resulting into increase in craze size. Again the higher particle size can limit the shear bending and cavitation process. Therefore, the lower particle size of dispersed phase is favoured. Here smaller particles are small to control crazing directly, but they are large enough to control it indirectly by initiating shear yielding.

4.1.1.c Matrix ligament thickness

The matrix ligament thickness is the average surface to surface interparticle distance. According to Wu [4] for pseudo ductile matrix, the matrix ligament thickness should

be always lower than criticle matrix ligament thickness (Tc), for achieving the improved toughening with the soft dispersed phase. Tc is the characteristic of the matrix alone at a given temperature and rate of deformation, but independent of domain size and volume fraction of the dispersed phase. According to Wu [4] if matrix ligament thickness is thinner than Tc a plane strain to plain stress transition occurs resulting into the ligament shear yield and hence blend toughening. On the other hand, if the ligament is thicker than Tc, such transition does not occur and matrix ligament shows brittleness.

4.1.1.d The dispersed phase properties

The stress for elastomer required to cavitate in a triaxial stress state decreases with decreasing its tensile modulus. Thus, the elastomer having lower tensile modulii are more edffective in improving impact behaviour.

4.2 THEORETICAL MODELS

4.2.1 Theoretical models for the tensile modulus of heterogeneous blends

Many theories have been proposed for predicting the tensile modulus of heterogeneous blends. According to Dickie [5] these theories can be divided into three groups which can predict the modulus - composition dependance.

(i) Mechanical coupling model,

(ii) Self consistent model,

(iii) Bounds on modulus model.

In principle, mathematical models describing the mechanical response in terms of properties of blends constituents allow identification of responses that can be accounted for on purly mechanical ground.

(i) Mechanical coupling model : The mechanical coupling model is an empirical expression, containing an adjustable parameter. It furnishes a convient frame work for empirical curves fitting and systematic phenomenological description of blend behaviour. The major drawback for use of this model is attributing a physical meaning to the adjustable parameter as it is not morphologically or mechanically realistic model.

(ii) Self consisting model : The self consisting model is based on the following assumptions;

- perfect adhesion exists between the matrix and the inclusion (dispersed phase),
- negligible interaction takes place between the dispersed phase particles and
- dispersed phase particles embedded in matrix are spherical in shape and are isotropic morphologically and mechanically.

Based on these, Kerner's [6] model was originally developed for the shear modulus of a composite consisting of particulates and polymer matrix. However, this model is useful for the prediction of the tensile modulus of a certain class of heterogeneous blend systems. When the matrix and

inclusion have the same Poisson's ratio, the Kerner's model for a system having perfect adhesion at the boundary may be written as :

$$E_b = E_m \left\{ \frac{\phi_d E_d/[(7-5\nu_m) E_m + (8-10\nu_m) E_d] + \phi_m/15(1-\nu_m)}{\phi_d E_m/[(7-5\nu_m) E_m + (8-10\nu_m) E_d] + \phi_m/15(1-\nu_m)} \right\} \quad (1)$$

Here E is the tensile modulus, ϕ is the volume fraction and ν is Poisson's ratio. The subscripts b, m and d refer to the blend, the matrix and the dispersed phase respectively. The Poisson's ratio for Nylon-6 and PP are 0.4 and 0.35 respectively. These values are close enough to use the Kerner's equation in the above form.

For the polymeric system in which dispersed phase particles are loosely bound, $E_d \cong 0$ and eq. (1) is reduced to

$$\frac{1}{E_b} = \frac{1}{E_m} \left[1 + \frac{15 (1 - \nu_m) \phi_d}{(7 - 5\nu_m) \phi_m} \right] \quad (2)$$

It should be noted that in the Kerner's derivation only particle-matrix adhesion, but no particle-particle interaction was assumed. Therefore, the Kerner's model may not be applicable to the polymer blend systems in which strong interaction between dispersed phase and matrix may exist.

For such type of polymer systems, Nielson [7] suggested a modification of the Kerner's model.

According to Nielson [7],

(i) For a rigid polymer dispersed in a rubber matrix :

$$\frac{E_b}{E_m} = \frac{1 + AB\,\phi_d}{1 - B\,\psi\,\phi_d} \qquad (3)$$

in which,

$$B = \left(\frac{E_d}{E_m} - 1\right) \Big/ \left(\frac{E_d}{E_m} + A\right); \qquad \psi = 1 + \left(\frac{1 - \phi_{max}}{\phi^2_{max}}\right)\phi_d$$

(ii) For rubber inclusion in a rigid matrix :

$$\frac{E_m}{E_b} = \frac{1 + AB_i\,\phi_d}{1 - B_i\,\psi\,\phi_d} \qquad (4)$$

where,

$$B_i = \left(\frac{E_m}{E_d} - 1\right) \Big/ \left(\frac{E_m}{E_d} + A\right); \qquad \psi = 1 + \left(\frac{1 - \phi_{max}}{\phi^2_{max}}\right)\phi_d$$

ϕ max is the maximum packing volume and can be considered as a scale of interaction between two phases. A small value of ϕ max represents a large extent of the interface, which is immobilised by dispersed phase. The constant A in eq. (3) and eq. (4) takes in to account the geometry of the particulate phase. For spherical dispersed phase particles and for the two phases having the same Poisson's ratio, the constant A is $(7 - 5\,\nu_m)/(8 - 10\,\nu_m)$ for eq. (3) and $(8 - 10\,\nu_m)/(7 - 5\,\nu_m)$ for eq. (4).

The approach of self consistant model for the prediction of the tensile modulus values of various blends, mainly relies on the simplified assumptions about the morphology and physical behaviour of the blends. It predicts approximate but single valued modulus for each blend.

(iii) Bound on modulus model : According to Paul [8], the bounds on modulus model represents an alternate approach based on the variational principle to bound the strain energy and thus to place upper and lower limits on the modulii of the blends.

According to Paul upper limit is given by,

$$E_b = (1 - \phi_d) E_m + \phi_d E_d \qquad (5)$$

and lower limit by,

$$E_b = 1 \Big/ \left(\frac{1 - \phi_d}{E_m} + \frac{\phi_d}{E_d} \right) \qquad (6)$$

4.2.2 Theoretical model for the tensile strength of heterogeneous blends

Compared to well-developed theories for predicting the tensile modulus of polymer blends, relatively little is available for predicting theoretically the tensile strength of polymer blends. According to Kunori and Geil [9] and Nielson [7], the poor tensile strength of a blend is attributed to the failure of the adhesion between the

dispersed phase and the matrix through crazing. The crazing or void depends on the area occupied by the dispersed phase in the blends.

When there is no adhesion between the constituents of a polymer blend, the tensile strengh of the polymer blend can be represented by

$$\sigma_b = \sigma_m (1 - \phi_d) \quad (7)$$

in which σ_b and σ_m are the tensile strengths of the blend and the matrix, respectively, and ϕ_d is the fraction of area occupied by the dispersed phase. On the other hand, when strong adhesion exists between the constituent components, the dispersed phase also contributes to the tensile strength of the blend and eq. (7) can be modified as,

$$\sigma_b = \sigma_m (1 - \phi_d) + \sigma_d \phi_d \quad (8)$$

where, σ_d denotes the tensile strength of dispersed phase.

Latter in this chapter an attempt is made to fit the experimental data in the various models discussed here.

4.3 EXPERIMENTAL

Some of the properties of PP and Nylon-6 used in this study are given in Table 4.1.

Prior to use, NY-6 grannules were dried at 105^{o}C for 3 h to ensure that they are free from moisture.

Table 4.1

Properties of Polypropylene and Nylon-6.

Property	PP	NY-6
Melt flow index, g/10 min	10.0	30.0
Density, g/cm^3	0.89	1.125
Supplier	Indian Petro-Chemicals Co. Ltd. Vadodara, India.	Gujarat State Fertilizer Co. Ltd. Vadodara, India.

4.3.1 Preparation of the blends

All the blends of PP and NY-6 were prepared by melt mixing technique. The Brabender plasticorder system coupled with single screw extruder (L/D = 16) was used for the preparation of the blends. All the temperatures were controlled by thermocouples. The extrudate was obtained in the form of a thread, which was quenched in water, dried and granulated. For all the blends, during mixing, the initial extrudate was discarded in order to ensure steady operation and to flush out impurities from the extruder to ensure the resulting blend free from any impurities adhered to the extruder.

All the binary PP/NY-6 blends and ternary PP/NY-6/grafted PP blends (grafted PP as compatibiliser) of various compositions were prepared by single step mixing process. The composition of blends prepared is given in Table 4.2 and 4.3. The mixing was carried out by keeping the temperatures of three zones at 190^{o}C, 220^{o}C and 235^{o}C respectively. The die temperature was kept at 230^{o}C. The screw speed was kept at 30 r.p.m.

4.3.2 Specimen preparation

Prior to molding, the extrudats were cut into 3 to 5 mm pellets and the pellets were dried to avoid the plasticising and hydrolysing effect of moisture on nylon-6. Then the compounded pellets were injection molded to obtain the samples for the measurements of their tensile strength, izod impact strength and flexural strength. All the samples were prepared according to ASTM standards. A Windsor injection

Table 4.2

Various compositions of PP/NY-6 binary blends and PP/NY-6/PP-g-BA ternary blends.

Blend Code	PP % (w/w)	Ny-6 % (w/w)	Blend Code	PP % (w/w)	NY-6 % (w/w)	PP-g-BA (D.G.=2.9%) % (w/w)	Blend Code	PP % (w/w)	Ny-6 % (w/w)	PP-g-BA (D.G.=2.9%) % (w/w)
PP	100	-	B_1	73.2	24.4	2.4	C_1	71.4	23.8	4.8
A_1	75	25	B_2	58.5	39.0	2.4	C_2	57.1	38.1	4.8
A_2	60	40	B_3	48.8	48.8	2.4	C_3	47.6	47.6	4.8
A_3	50	50	B_4	39.0	58.5	2.4	C_4	38.1	57.1	4.8
A_4	40	60	B_5	24.4	73.2	2.4	C_5	23.8	71.4	4.8
A_5	25	75					D_1	68.2	22.7	9.1
Ny-6	0	100					D_2	45.5	45.5	9.1
							D_3	22.7	68.2	9.1

Table 4.3

Various compositions of PP/Ny-6/PP-g-MAH and PP/Ny-6/PP-g-(BA-co-MAH) ternary blends.

Blend Code	PP % (w/w)	Ny-6 % (w/w)	PP-g-MAH (D.G.=5.4%) (w/w)	Blend Code	PP % (w/w)	NY-6 % (w/w)	PP-g-(BA-co-MAH (D.G.=4.8%) (w/w)
E_1	73.2	24.4	2.4	BM_1	73.2	24.4	2.4
E_2	58.5	39.0	2.4	BM_2	48.8	28.8	2.4
E_3	48.8	48.8	2.4	BM_3	24.4	73.2	2.4
E_4	39.0	58.5	2.4				
				BM_4	71.4	23.8	4.8
E_5	24.4	73.2	2.4				
				BM_5	47.6	47.6	4.8
F_1	71.4	23.8	4.8	BM_6	23.8	71.4	4.8
F_2	51.1	38.1	4.8				
F_3	47.6	47.6	4.8				
F_4	38.1	57.1	4.8				
F_5	23.8	71.4	4.8				
G_1	68.2	22.7	9.1				
G_2	45.5	45.5	9.1				
G_3	22.7	68.2	9.1				

molding machine (SP-3) was used for molding the samples. All the samples were conditioned at room temperature for 72 h prior to the measurements.

4.3.3 Characterisation of the blends

4.3.3.a Tensile properties measurement

Tensile properties of the dumbell shaped test specimens having the dimensions of the narrow portions 57 mm x 13 mm x 3.2 mm were measured according to ASTM-D638 procedure. At least 6-7 specimens were tested for each blend. The specimens which donot break at pre-determined gauge marks or those breaking at obvious fortuitous flaw were discarded. All the testings were carried out at 50 mm/min cross head speed. The full scale load was 500 Kg. Classical stress - strain curves were obtained on the Universal Testing Machine Instron - 1195. The tensile modulus and tensile strength were calculated from the curves.

4.3.3.b Izod impact strength

The test samples having the dimensions of 62.5 x 12.8 x 6.2 mms with a triangular notch of 45^{o} angle and 2.5 mm notch depth were used for the izod impact strength measurements. The measurements were carried out according to ASTM-D256. At least 5 - 7 individual determinations of Impact values were made on each sample.

4.3.3.c Flexural strength

Flexural strength measurements were carried out according to the method described in ASTM-D790. Three point bending system utilizing central loading on doubly supported beam has been used for this measurements. The test samples were of 125 mm length, 12.2 mm width and a 6.2 mm thickness. During testing, the rate of cross head motion was kept at 2.8 mm/min. At least five individual determinations of flexural strength values were made on each sample.

4.3.3.d Rockwell hardness

The test specimen having a thickness of 3 mm were obtained by injection molding. At least five samples were analysed for each blend. The hardness measurements were carried out according to ASTM-D785. For the hardness measurement the R rockwell hardness scale was used.

4.3.3.e Heat deflection temperature (HDT)

The deflection temperature of the blends under flexural load was determined in accordance with ASTM-D648.

The test specimen was tested as a beam, having dimenstions of 125 mm x 12.2 mm x 6.2 mm, with load applied at its center to give maximum fibre stress of 18.20 kpa. The specimen was immersed in a heat transfer medium (silicon oil) and heating was carried out at the rate of 2^{o}C/min. The temperature of the medium was measured when the test bar had a deflection

0.25 mm which is a deflected temperature under flexural load of the test specimen. At least two specimen were analysed for each blend.

4.3.3.f Melt flow index (MFI)

MFI is quoted as weight expelled in g, in 10 mins. MFI is having inverse relationship with molecular weight. It gives an idea about ease of processing.

MFI of PP and nylon-6 and its blends was determined by using a rheometer Deven Port, England. It has a capillary die of length 8 mm, diameter 2 mm and driving weight of 2.65 Kgs.

MFI was taken at a temperature of 230^{o}C. The melt through the die was cut at an interval of 10 sec. and five such samples were taken and weighed. For every composition the experiment was repeated twice and the average values of MFI are reported.

4.3.3.g Thermal analysis

The thermal properties of the homopolymers and blends have been studied using Delta Series DSC7 thermal analyser. Prior to the measurements all the samples were dried and kept in vacuum dessicator and in the presence of anhydrous calcium chloride to avoid any effect of moisture. The following standard procedure was used. The samples were heated upto 250^{o}C at 10^{o}C/min heating rate and were kept at annealing temperature for 5 min. Then the samples were cooled down to room temperature at a cooling rate of 10^{o}C/min. The next

heating run was carried out at 10°C/min. The melting temperature and the heat of fusion ΔH_f of the samples were obtained from the maxima and the area under the melting peaks respectively. The crystallisation temperature was calculated from the cooling thermograms. The % crystallinity of the NY-6 phase, Xc (NY) and of the PP phase, Xc (PP) was calculated by means of the following relations,

$$Xc\ (NY) = \frac{\Delta H_f^{*}\ (NY)}{\Delta H_f^{o}\ (NY)} \times 100; \quad Xc\ (PP) = \frac{\Delta H_f^{*}\ (PP)}{\Delta H_f^{o}\ (PP)} \times 100$$

Where ΔH_f^{*} (NY) and ΔH_f^{*} (PP) are the heat of fusion for NY-6 and PP in the blends respectively. ΔH_f^{o} (NY) and ΔH_f^{o} (PP) are the heat of fusion of 100% crystalline NY-6 and PP respectively. (From the literature [10,11] ΔH_f^{o} (NY) = 45.6 cal/g. and ΔH_f^{o} (PP) = 50 cal./g).

4.3.3.h Water absorption

The test specimens having dimentions of about 64 x 18x 3 mms were taken for the measurements. The test specimens were dried at 50°C in vacuum for 24 h prior to the measurements. The conditioned samples were first cooled, weighed and then suspended in a container of boiling distilled water. After 120 minutes the specimens were removed from water and cooled by immersing in distilled water at room temperature. All the surface water was removed with a dry cloth and the specimens were weighed immediately. At least three specimens were analysed for each sample. The percentage of water absorption was determined as follows;

$$\text{Percentage water absorption} = \frac{\text{Weight of wet sample} - \text{Initial weight of the sample}}{\text{Initial weight of the sample}} \times 100$$

4.3.3.i Dynamic mechanical properties

Measurements of dynamic mechanical properties, the dynamic storage moduli E', loss moduli E" and loss factor tanδ as a function of temperature were measured by using Rheometrics Dynamic Spectrometer, RDS, Rheometrics Inc., N. J. The testing was carried out in three point bending (Flexural). The static and dynamic loads were 2 and 1 Kg. respectively. The frequency was 6.3 rad/sec. and strain was 0.05%. The temperature range used was 25^{o}C to 140^{o}C. The magnitude of the dynamic moduli (E'and E") and tangent of phase angle (tanδ = E"/E') were measured at about every 5^{o}C.

4.3.3.j Scanning electron microscopy

Morphological studies were carried out on two types of samples,

(a) Standard tensile test bars fractured at liquid nitrogen temperature and

(b) Izod test bars fractured at room temperature.

Fractured surfaces to be studied were given a gold coating of about 500 A^{o} thickness in JFC 1100 ion sputtering unit under nitrogen atmosphere, a pressure of 0.1 torr and 10 mA, 15 kV current and voltage respectively. This was necessary to make the samples conducting and to avoid charge buildup. The gold

coated fractured surfaces were observed under JEOL JSM 35C Scanining Electron Microscope operated at 15 kV. The whole set of samples was scanned rapidely at various magnifications and finally 200 and 1000 magnifications were chosen for recording the electron micrographs for detailed study.

SEM study was also carried out for etched samples. The samples were selectively etched by using hot xylene for PP phase and formic acid for nylon phase. First the etching was carried out in formic acid at different time intervals and concentrations of formic acid. Further samples were etched at optimised condition of 30% formic acid and 10 min time interval. For etching of PP phase, samples were kept in boiling hot xylene for 15 min. The etched samples were gold coated and observed under SEM as mentioned above.

4.4 RESULTS AND DISCUSSION

It has been reported by various researchers [10,12,13] that polypropylene (PP) and nylon-6 (NY-6) form immiscible mixtures with each other. We have calculated the second partial derivative of the free energy of mixing (g") using eq. 6 from ch.3 for PP/NY-6 blends with various compositions for the study of miscibility of PP and NY-6. The results are given in Table 4.4.

It can be seen from the results that the g" has negative values for all the compositions of PP/NY-6 blends. Thus, according to F.H.S. theory (ch-3) PP and NY-6 are

Table 4.4

Data for theoretical calculation of g" values for PP/Ny-6 blends.

Sr. No.	Weight fraction of PP	Weight fraction of NY-6	Volume fraction of PP	Volume fraction of Ny-6	g"
1	0.997	0.003	0.998	0.002	-0.174
2	0.995	0.005	0.996	0.004	-0.268
3	0.900	0.100	0.917	0.083	-0.371
4	0.700	0.300	0.753	0.297	-0.394
5	0.500	0.500	0.566	0.434	-0.402
6	0.200	0.800	0.233	0.767	-0.041
7	0.100	0.900	0.127	0.873	-0.412
8	0.005	0.995	0.007	0.993	-0.326
9	0.003	0.997	0.004	0.996	-0.271

thermodynamically immiscible with each other at all the compositions under present study.

4.4.1 PP-g-BA as compatibiliser for PP/NY-6 blends

The synthesis and characterisation of PP-g-butyl acrylate (PP-g-BA) is already discussed in the chapter-2. In this section the potential of PP-g-BA as an compatibiliser for PP/NY-6 blends is discussed.

As it has been mentioned earlier PP and NY-6 form incompatible mixture with each other. When PP-g-BA copolymer was added to PP/NY-6 blends following reaction may take place between the ester group of butyl acrylate and terminal amine groups of NY-6 during melt mixing of PP-g-BA and NY-6 at 235^{o}C.

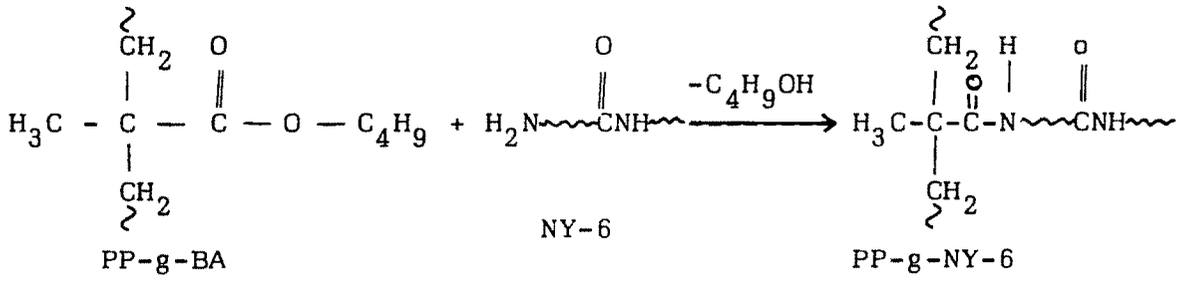

This PP-g-NY-6 can actually act as an interfacial agent for PP/NY-6 blend system.

4.4.2 Evidence of the activity of PP-g-BA as an compatibiliser for PP/NY-6 blends

4.4.2.a Molau's test

For confirmation of the formation of PP-g-NY-6 copolymer and its activity, Molau's test [14] was carried out for PP/NY-6

binary and PP/NY-6/PP-g-BA ternary blends. When formic acid was added to PP/NY-6 blends, NY-6 was observed to be dissolved completely within 1-2 h while PP was observed to be separated and floted on the surface. When the same experiment was carried out with PP/NY-6/PP-g-BA blends a stable emulsion in the presence of formic acid was obtained. According to Molau the formation of stable emulsion in the presence of formic acid can be attributed to the dispersion action of PP-g-NY-6 blends, formed during melt mixing of PP-g-BA and NY-6 at higher temperature and shear rate. Again according to him these graft copolymers have tendency to go to the interface; since their various chains get completely solvated at interface. This arrangement also corresponds to the thermodynamically stable state. At this interface PP chain segment of PP-g-NY-6 copolymer will be joining with the PP phase and NY-6 chain segments with NY-6 phase making the system more compatible. Diagramatically it can be presented as

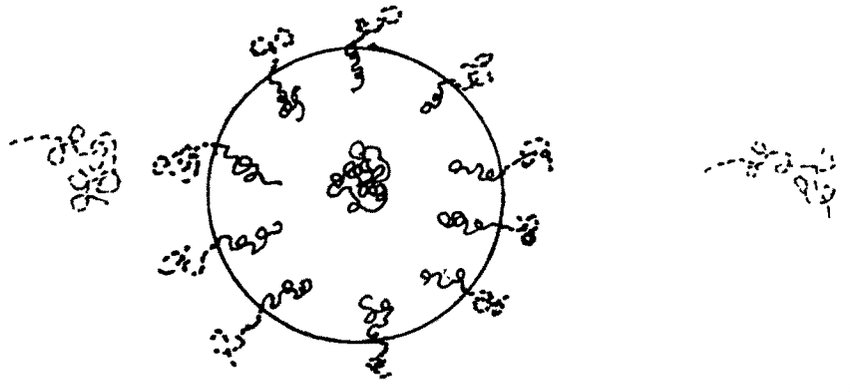

Fig. 4.1 : Digramatic representation of the stabilizing effect of graft copolymers on emulsion.

Coiled polymer chain of PP

Coiled polymer chain of NY-6

Graft polymer chain from PP and NY-6

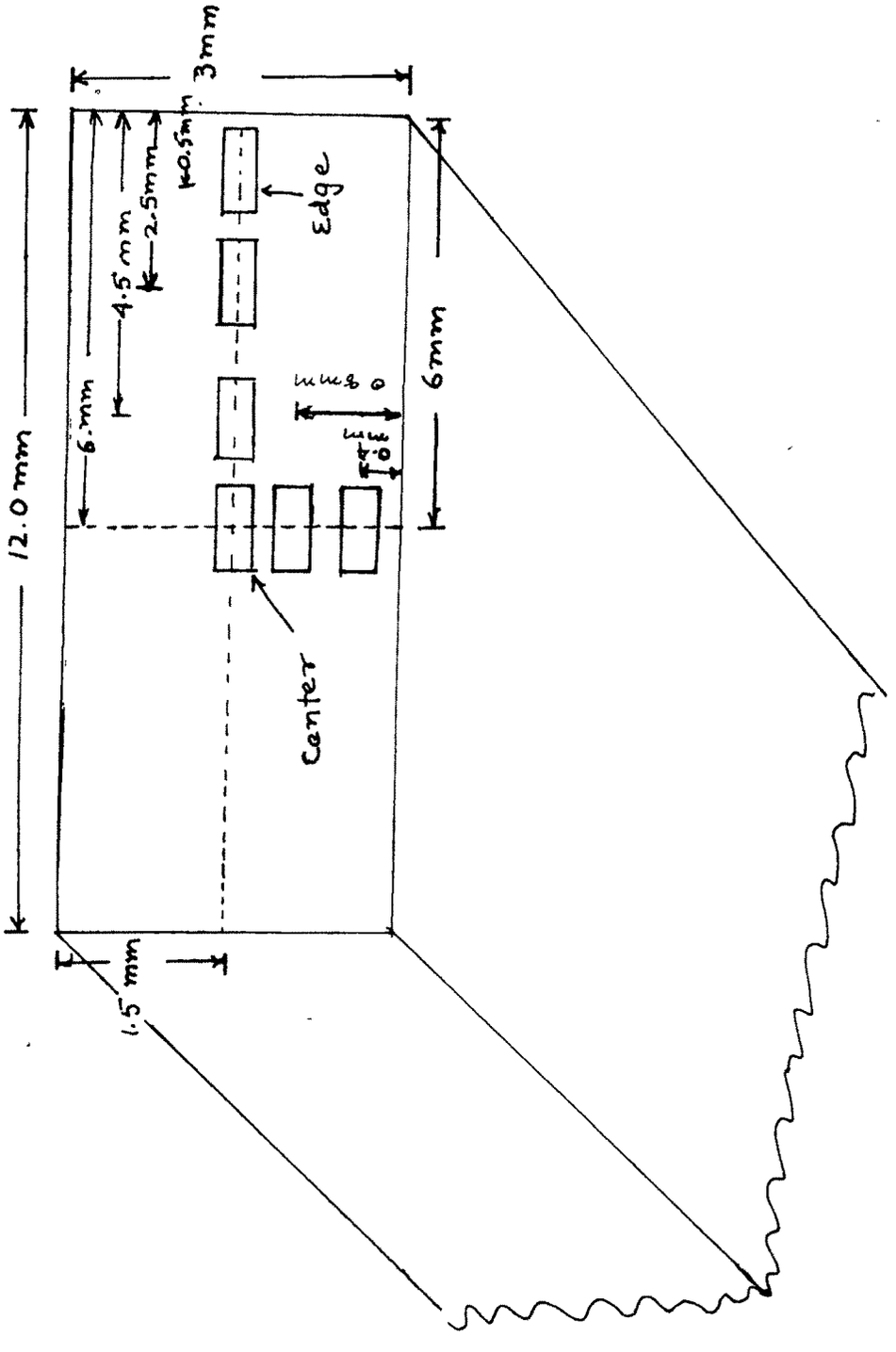

Fig. 4.2 Line drawing showing the details of scanning

Circle : Colloid particle from macromolecule PP surrounded by a solution of macromolecule of NY-6 or Vice Versa.

4.4.2.b Electron microscopy study

Electron micrographs were taken at various positions of the tensile bar fractured surfaces as shown in Fig. 4.2. Only selected micrographs are illustrated during discussion.

Figs. 4.3 and 4.4 show the complete set of micrographs of cryogenically fractured standard tensile bar surfaces of the PP/NY-6 A_1 and A_5 blends respectively with 1000 magnification taken from the different areas of the fractured surface as shown in Fig. 4.2. This gives an idea of morphological changes that have taken place across the cross section of the injection moulded test specimen. The size, shape and distribution of dispersed phase is not uniform throughout the cross section of the specimen (perpendicular to the melt flow direction).

In the Fig. 4.4 it is observed that dispersed phase PP shows lower diffusion towards centre due to the low melt flow index. The shape of the dispersed phase particles is also elongated to some extent only at the peripheri of the specimen. Elongated shape of dispersed phase (NY-6) was also observed in A_1 (Fig. 4.3) blends. But here due to higher melt flow index dispersed phase nylon shows increasing concentration towards centre than at edge.

Center →

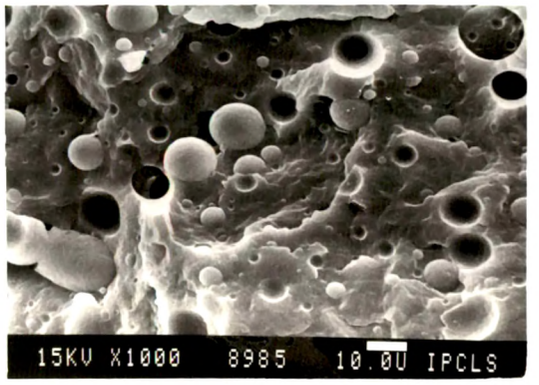

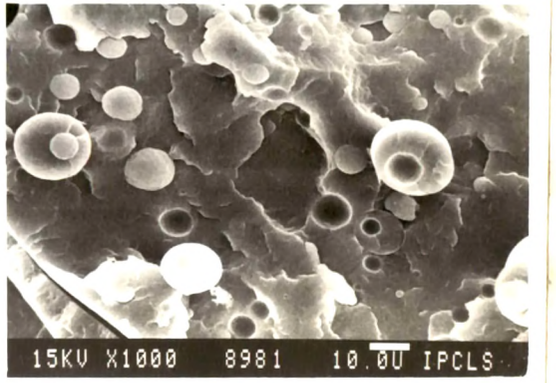

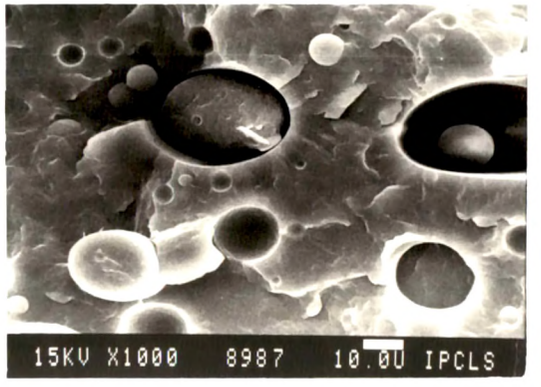

Edge →

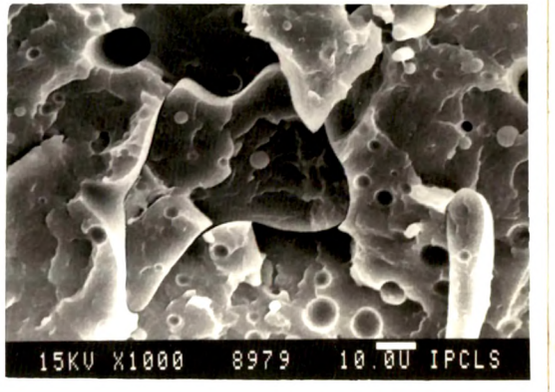

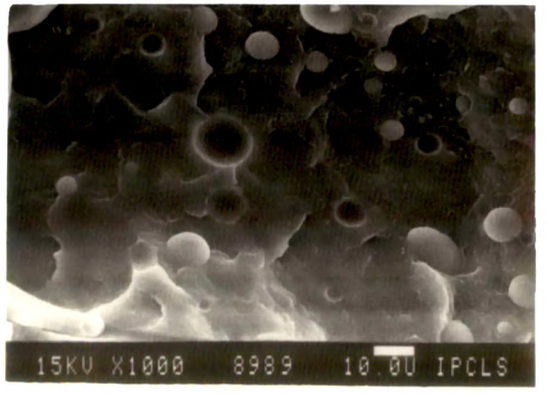

Fig. 4.3 Complate set of SE micrographs of cryogenically fractured blend A_1 (X 1000)

Center →

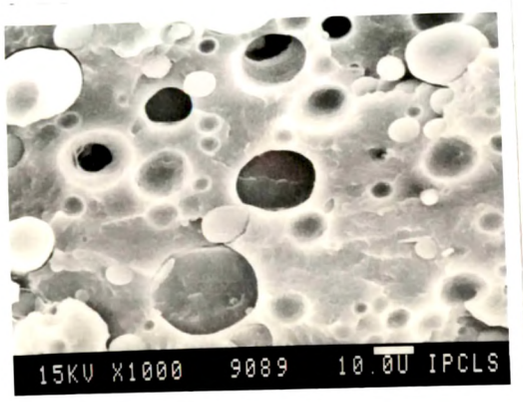

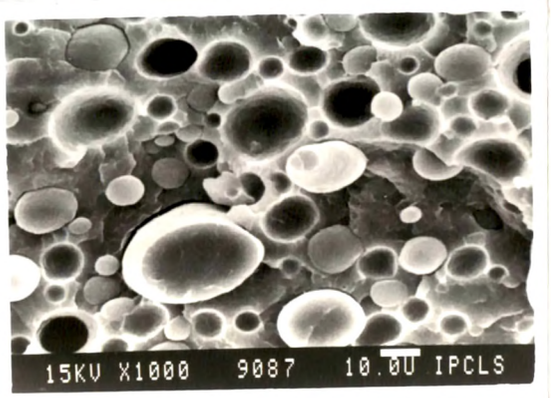

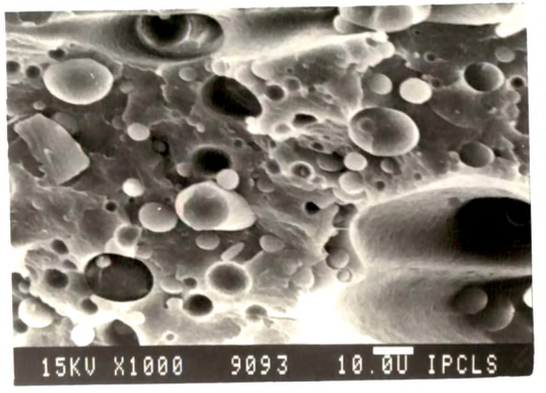

Edge →

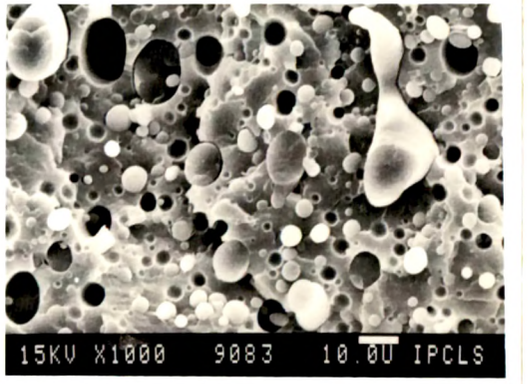

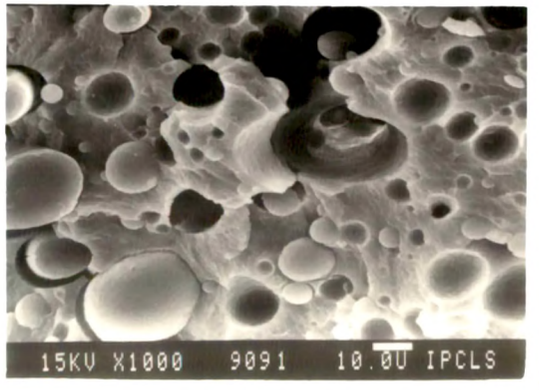

Fig. 4.4 Complate set of SE micrographs of cryogenically fractured blend A_5 (X 1000)

Figs. 4.5 - 4.11, show centre and edge electron micrographs of cryogenically fractured tensile bar surfaces of PP, A_1 - A_5 binary blends and NY-6 respectively at 200 magnification. The particle - matrix morphology is observed for binary A_1, A_4 and A_5 blends in which well shaped spherical particles of NY-6 or PP form a dispersed phase embeded in a continuous matrix phase. Whereas in binary A_2 and A_3 blends the phase inversion is observed.

From the Figs. 4.6 to 4.10, no morphological evidence of good adhesion between the interphase of the matrix and the dispersed phase is seen, as the dispersed phase particles show smooth surface. Large number of domains have been pulled out during fracture process and surface of the holes also appears to be smooth suggesting the poor interfacial adhesion in binary blends. This results into relatively larger size (30-20 μm) of the dispersed particles and relatively smaller contact areas with matrix.

As mentioned above A_2 and A_3 blends (Fig. 4.7 and 4.8) show co-continuous two phase interpenetrating morphology. This composition may attain the maximum contact area [15] and lead to the poorest balance of properties due to very weak mechanical interaction between two phases. The similar observation was made by Liang and Williams [16] and other researchers [12] for PP/Nylon blend systems.

It is observed from these Figs. that at the edge the phase morphology is different than that at the centre. At the edge

CENTER EDGE

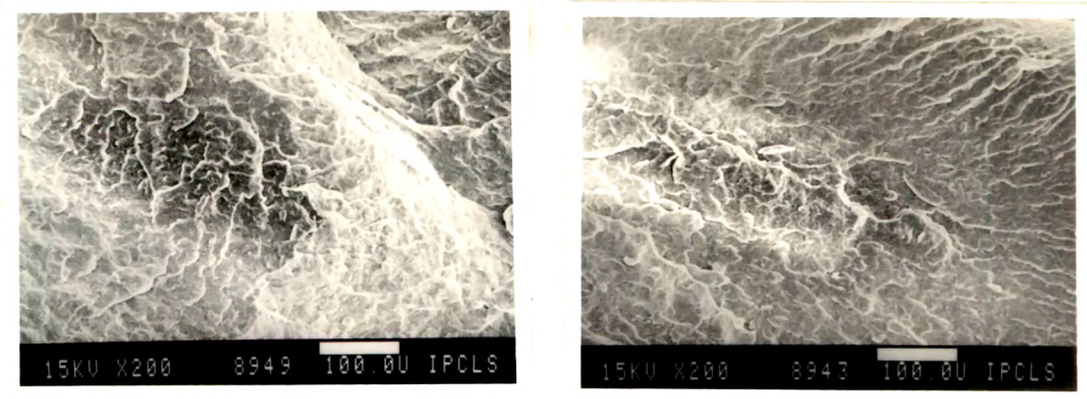

Fig. 4.5 SE micrographs of cryogenically fractured polypropylene (X 200)

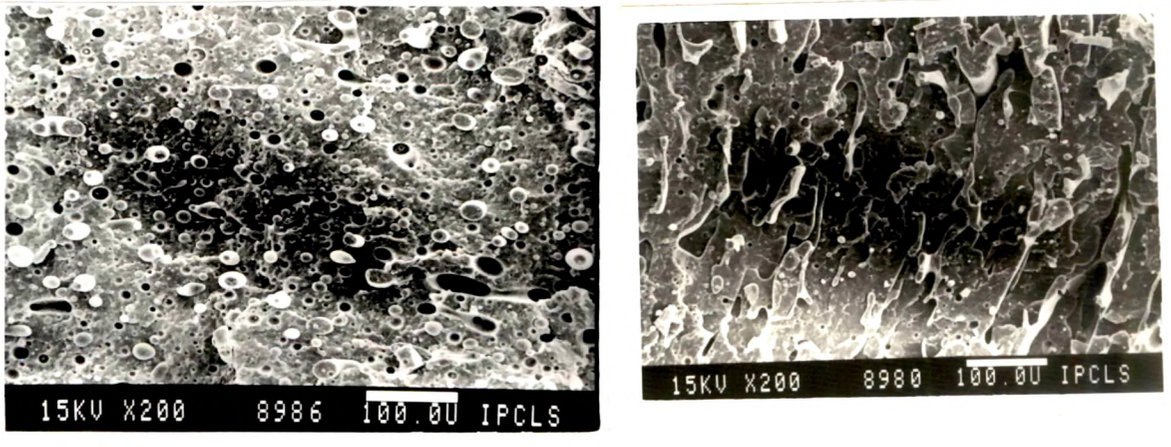

Fig. 4.6 SE micrographs of cryogenically fractured blend A_1 (X 200)

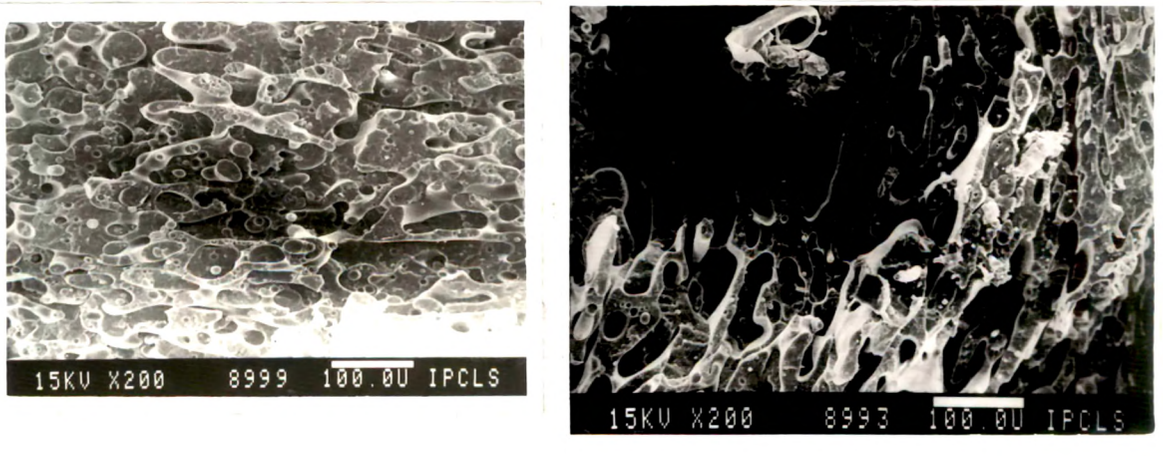

Fig. 4.7 SE micrographs of cryogenically fractured blend A_2 (X 200)

Center Edge

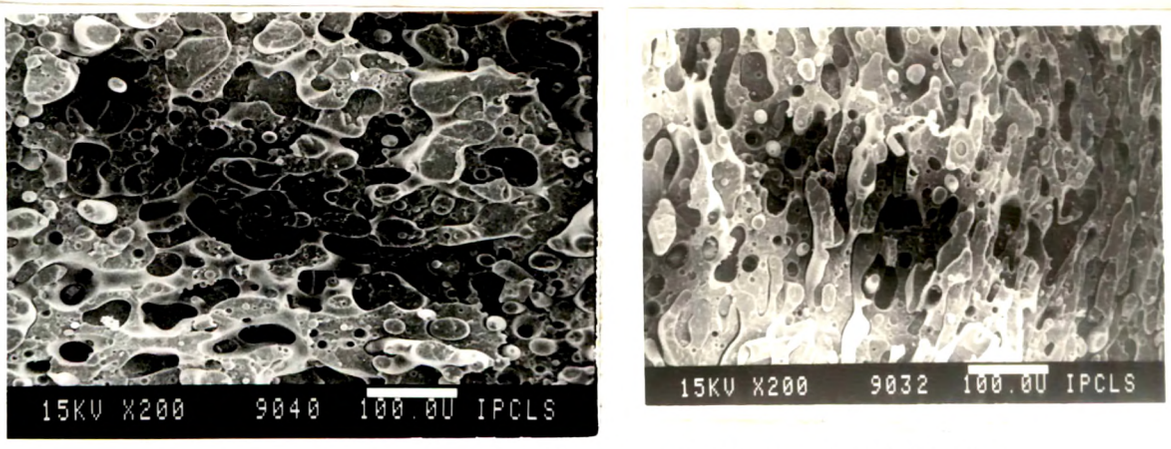

Fig. 4.8 SE micrographs of cryogenically fractured blend A_3 (X 200)

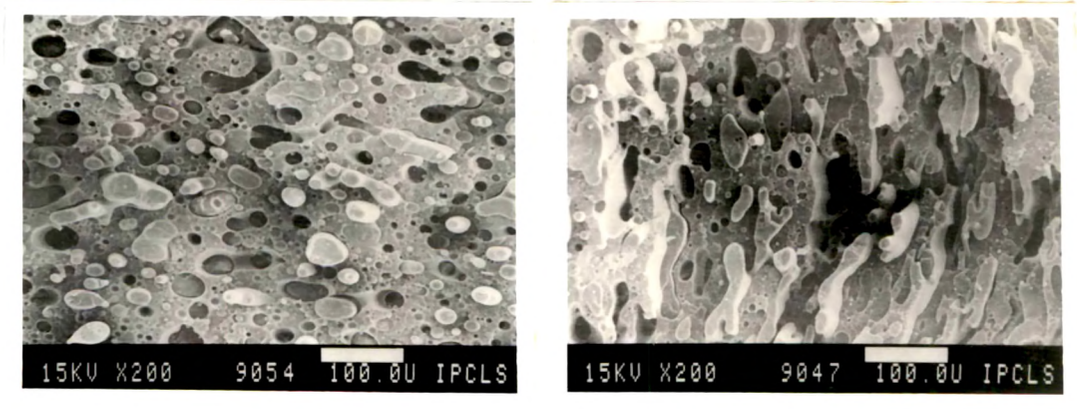

Fig. 4.9 SE micrographs of cryogenically fractured blend A_4 (X 200)

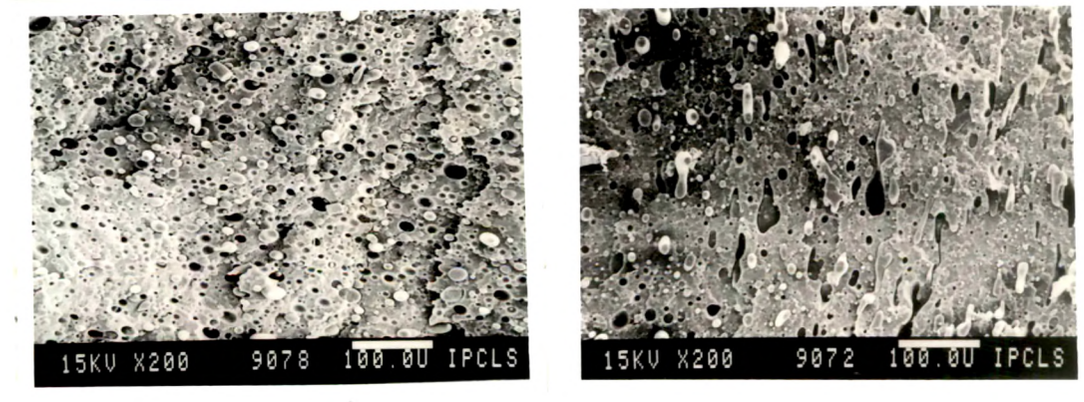

Fig. 4.10 SE micrographs of cryogenically fractured blend A_5 (X 200)

Center

Edge

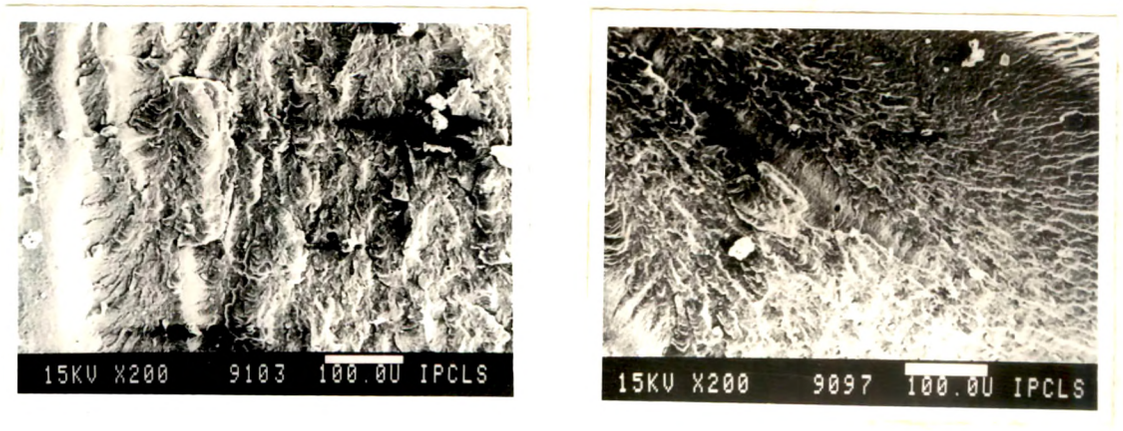

Fig. 4.11 SE micrographs of cryogenically fractured Nylon-6 (X 200)

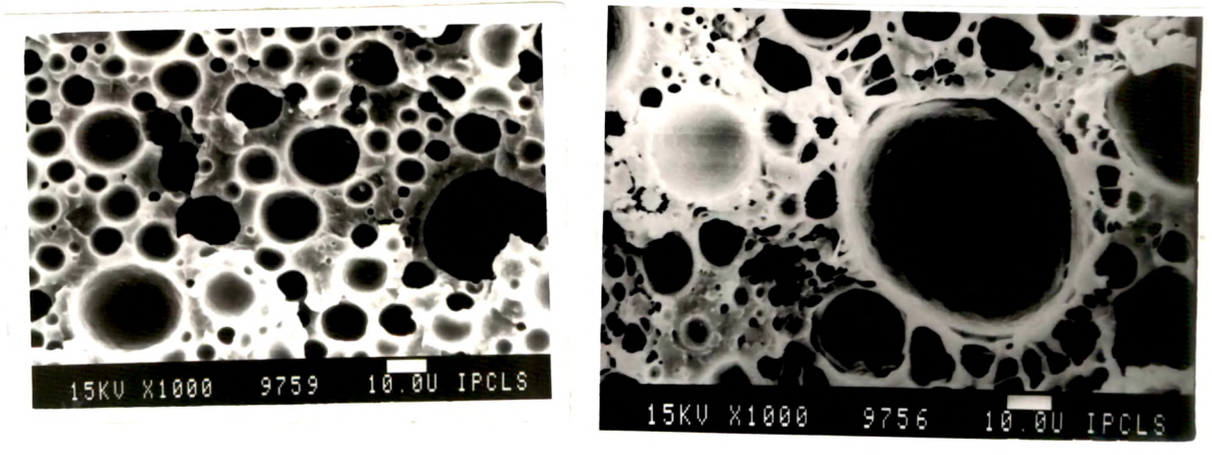

Fig. 4.12 SE micrographs of blend A_5 etched with hot xylene (X 1000)

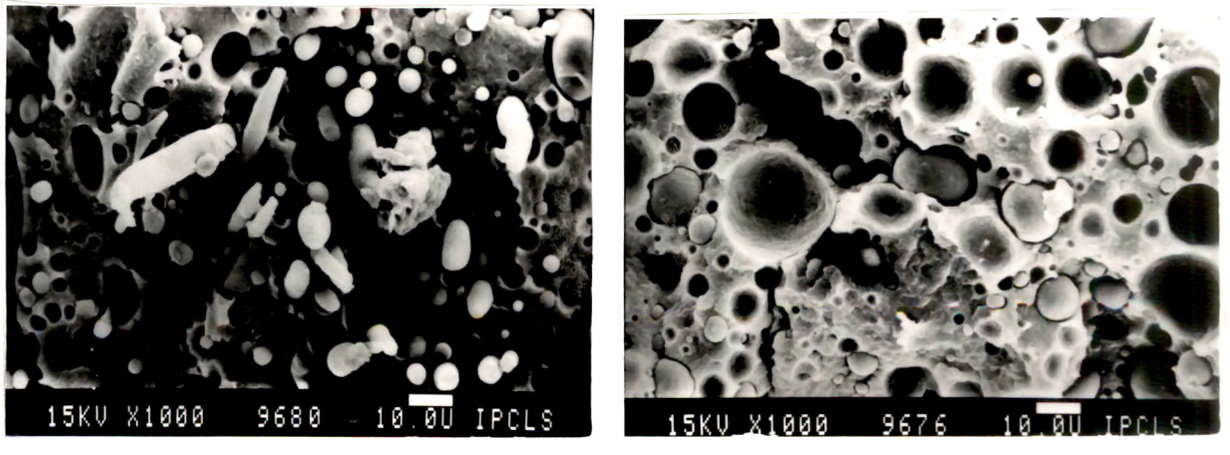

Fig. 4.13 SE micrographs of blend A_5 etched with formic acid (X 1000)

the dispersed phase exhibits nonuniform morphology with cylindrical, thread type or elongated particles. On the other hand, at the centre the dispersed particles are in well defined spherical shape. This may be due to the poor adhesion between dispersed phase and matrix and because of this the dispersed phase and matrix flowing with different viscosity ratio at the edge and at the centre under shear rate.

To identify the individual phases we have selectively etched the surface of impact broken samples with hot xylene for PP phase and formic acid for nylon-6 phase. Fig. 4.12 and 4.13 show the xylene and formic acid etched A_5 blend respectively taken at centre and near to the notch. In xylene etched photograph, the holes represented the removal of PP phase, whereas in formic acid etched photograph the spherical particles and some elongated particles represented the presence of PP phase. The average particle size is given in Table 4.5.

Figs. 4.14, 4.15 and 4.16 show the surface of cryogenically fractured tensile bars for ternary blends B_5, C_5 and D_3 respectively. These micrographs do show a two phase morphology features, but the mixing of the phases has been greatly improved due to compatibilisation. From Fig. 4.14 it is seen that though the particle size is large, the particles are very much adhered to the matrix with the relatively large contact area and the surface of particles as well as the surface of the holes created due to pulling of dispersed phase are rough. In the blend with 4.8% compatibiliser (Fig.

Center

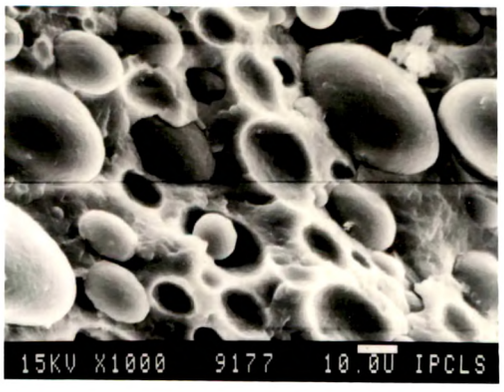

Edge

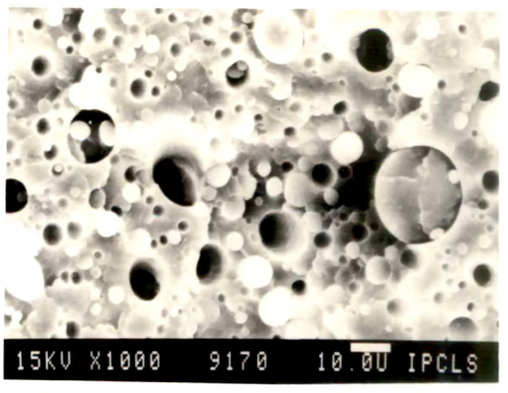

Fig. 4.14 SE micrographs of cryogenically fractured blend B_5 (X 1000)

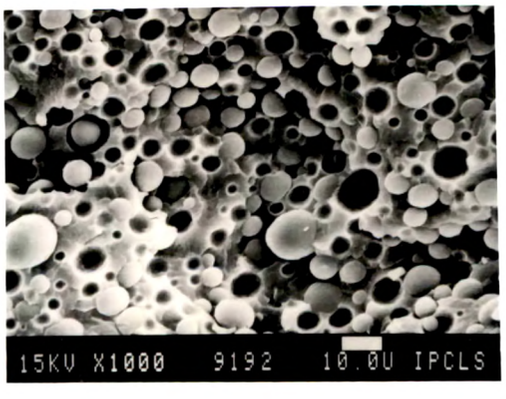

Fig. 4.15 SE micrographs of cryogenically fractured blend C_5 (×1000)

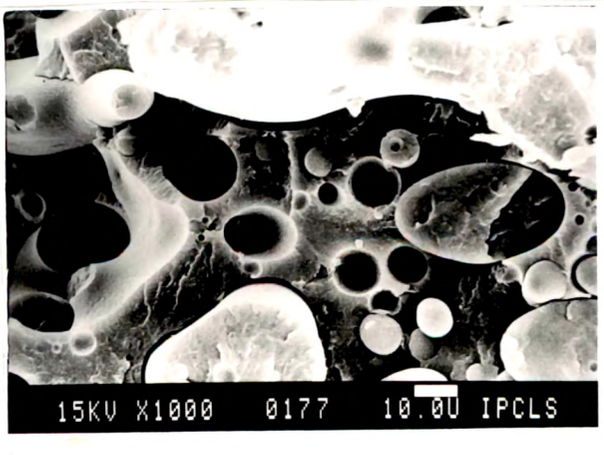

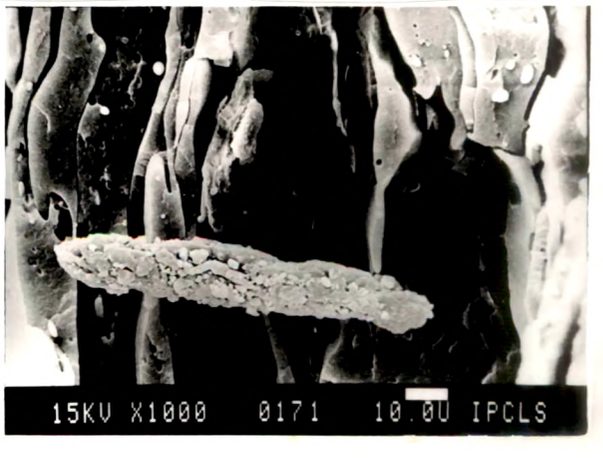

Fig. 4.16 SE micrographs of cryogenically fractured blend D_3 (X 1000)

Table 4.5

Accuracy and precision of the SEM results

Code	Mean diameter of the domains for 30 measurements	Average deviation for 30 measurements	Standard deviation for 30 measurements
	---μm---		
A_1	25.40	0.012	3.126
A_4	30.21	0.0143	2.590
A_5	20.42	0.052	0.1869
B_1	12.75	0.030	0.456
B_4	25.02	0.002	0.565
B_5	6.89	0.043	1.242
C_1	5.46	0.068	1.645
C_4	18.42	0.110	0.789
C_5	3.42	0.0018	0.216
D_3	11.12	0.067	4.137
E_1	0.89	0.089	0.368
G_3	1.05	0.134	0.498

Note : Particle size measurements for E_4, E_5, F_1, F_4, F_5 were not possible.

4.15), the particle size of dispersed phase is still decreased when compared with the corresponding blend containing 2.4% compatibiliser (Fig. 4.14). This is attributed to the increased concentration of compatibiliser imparting greater compatibility to PP and NY-6. This suggests that the PP-g-BA does act as compatibiliser for PP/NY-6 blend systems.

In the PP/NY-6 blends with 9.1% compatibiliser (Fig. 4.16) the phase morphology of blend is drastically changed. The particle size of the dispersed phase is observed to be higher but particles still show adhesion to the matrix. From the Fig. 4.14 and 4.15 it is observed that there is not much difference in phase morphology of the ternary blends at the edge and at the centre as it is seen in binary blends (Fig. 4.10). This also suggest the interfacial activity of PP-g-BA.

Again to measure the particle size we have selectively etched the PP phase by hot xylene. The Figs. 4.17, 4.18, 4.19 show the photographs of xylene etched impact fractured surfaces taken at center and edge for B_5, C_5 and D_3 ternary blends. From the Figs. it is observed that the particle size decreases with increasing PP-g-BA content. On comparision with the corresponding binary blend A_5 it was observed that drastic reduction in particle size takes place when blends are compatibilised with PP-g-BA. However, blend with 9.1% compatibiliser (Fig. 4.19) shows different morphological

Center Edge

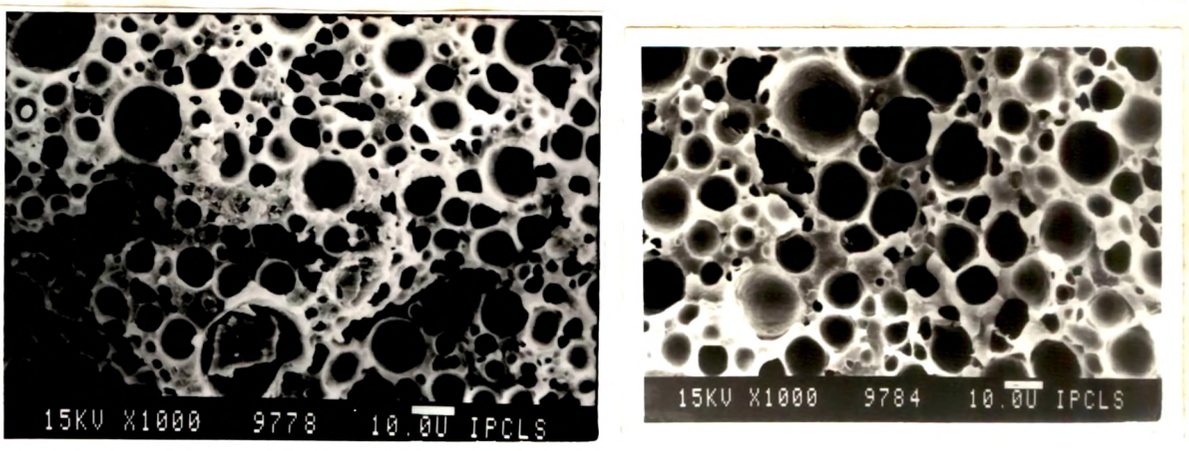

Fig. 4.17 SE micrographs of blend B_5 etched with hot xylene (X 1000)

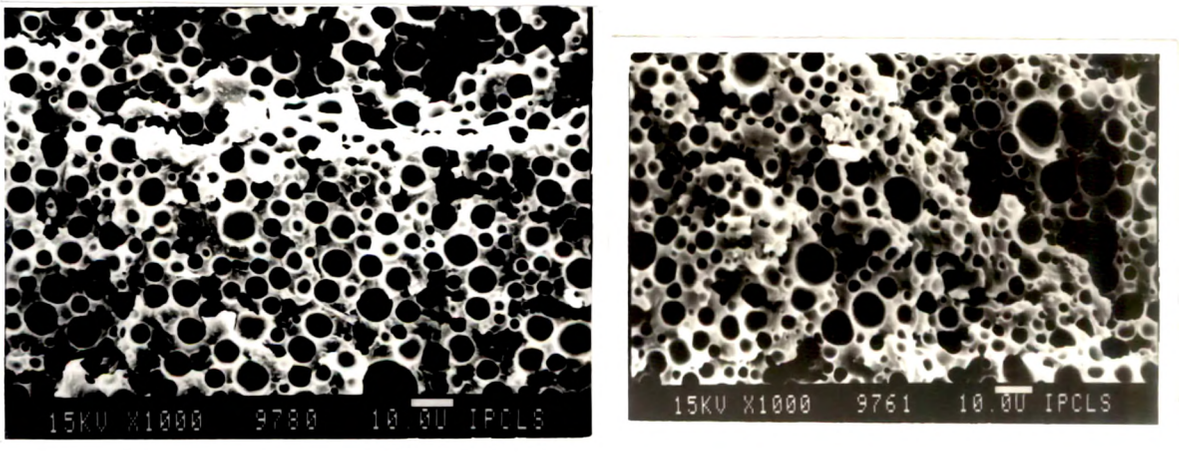

Fig. 4.18 SE micrographs of blend C_5 etched with hot xylene (X 1000)

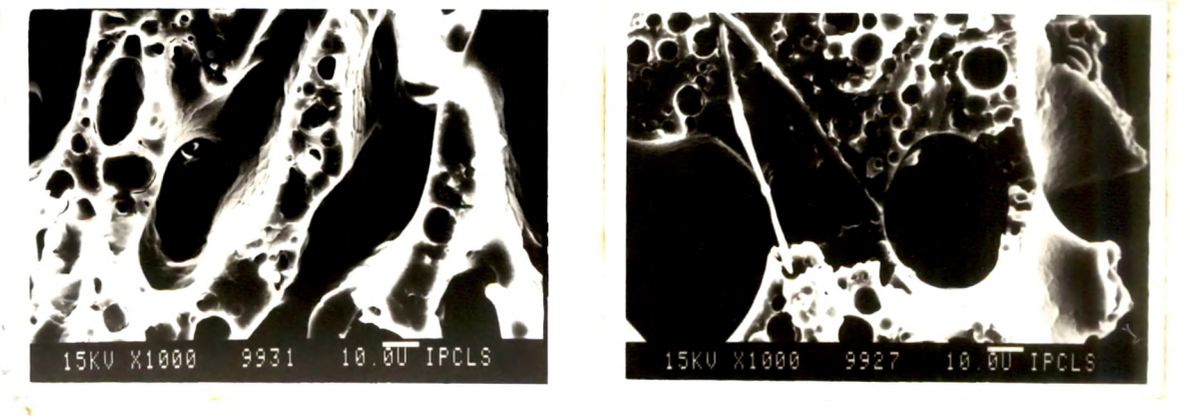

Fig. 4.19 SE micrographs of blend D_3 etched with hot xylene (X 1000)

texture with a considerable increase in the domain size. The average particle size of various ternary blends are given in Table 4.5.

4.4.3 Characterisation of blends

The effect of the blend composition on the mechanical, thermal and dynamic mechanical properties of PP/NY-6 and PP/NY-6/PP-g-BA blends were studied as discussed earlier.

The composition of various blends is given in Table 4.2 and 4.3. The processing conditions of these blends have been maintained throughout the preparation so that comparision of the efficiency of various compatibilisers used can be made.

4.4.3.a Effect of PP-g-BA on tensile properties of PP/NY-6 blends

Stress-strain curves for PP/NY-6, PP/NY-6/PP-g-BA (2.4%) and PP/NY-6/PP-g-BA (4.8%) blends along with that of nylon-6 and polypropylene are illustrated in Figs. 4.20.a, 4.20.b and 4.20.c respectively.

From the figures it is seen that PP and NY-6 show necking behaviour, while in all the three types of blends necking is found to decrease. PP or NY-6 is semicrystalline polymer. During necking it undergoes through the classical spherulitic - fibrous morphological transformation by means of cold drawing. As all the blends contain incompatible or semicompatible dispersed phase, hinderence in cold drawing

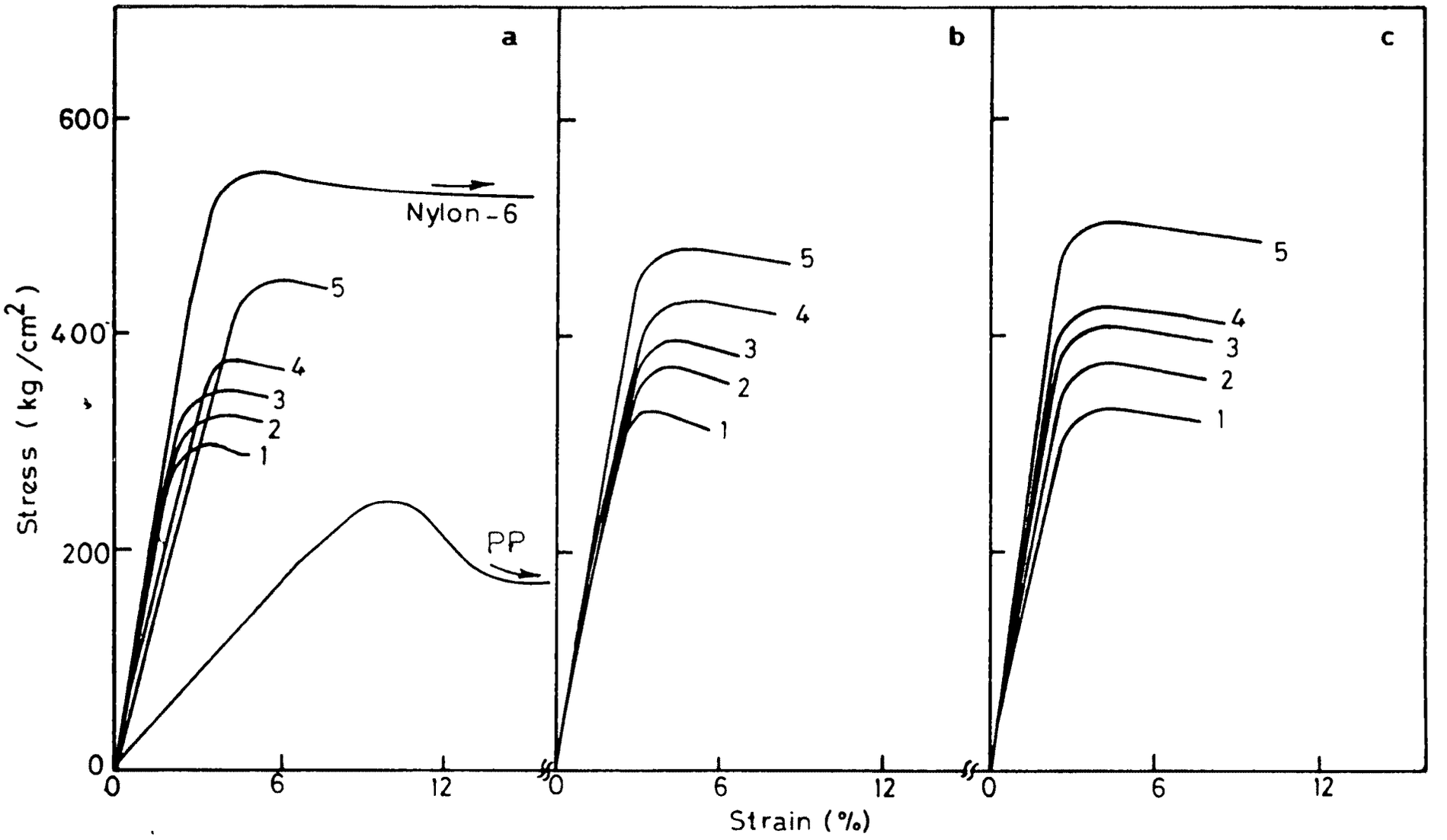

Fig. 4.20 Stress-strain curves for

a) PP/Ny-6 blends : 1, A_1 ; 2, A_2 , 3, A_3 ; 4, A_4 ; 5, A_5

b) PP/Ny-6/PP-gBA (2.4%) blends : 1, B_1 ; 2, B_2 ; 3, B_3 , 4, B_4 ; 5, B_5

c) PP/Ny-6/PP-g-BA (4.8%) blends : 1, C_1 ; 2, C_2 ; 3, C_3 , 4, C_4 ; 5, C_5

will be created. This will result in the decreased necking behaviour. It is also seen that, smoother change in slope of curves takes place.

In Fig. 4.21 the effect of blend composition on the tensile modulus of PP/NY-6, PP/NY-6/PP-g-BA (2.4%), PP/NY-6/PP-g-BA (4.8%) and PP/NY-6/PP-g-BA (9.1%) blends is illustrated. From the results it is concluded that,

(i) in binary blends, as the NY-6 content increases, the tensile modulus goes on increasing.

(ii) the tensile modulus of all the ternary blends is higher than that of binary blends.

(iii) higher values of tensile modulus are observed for the blends containing PP-g-BA (4.8%) compatibiliser.

(iv) The decrease in tensile modulus was observed in the blend containing PP-g-BA (9.1%) compatibiliser.

The increase in tensile modulus with increasing Ny-6 content is due to higher tensile modulus of Ny-6 itself. Whereas presence of compatibiliser in ternary blends improves the homogenity of the system resulting in to improved tensile modulus. Improved homogenity can also be observed from micrographs Fig. 4.14 and 4.15. The blends containing 4.8% compatibiliser give more homogenity to the system resulting into higher tensile modulus. The reduction in the tensile modulus is observed for the 9.1% compatibilised system, indicating that each systems performs better at optimised concentration of compatibiliser.

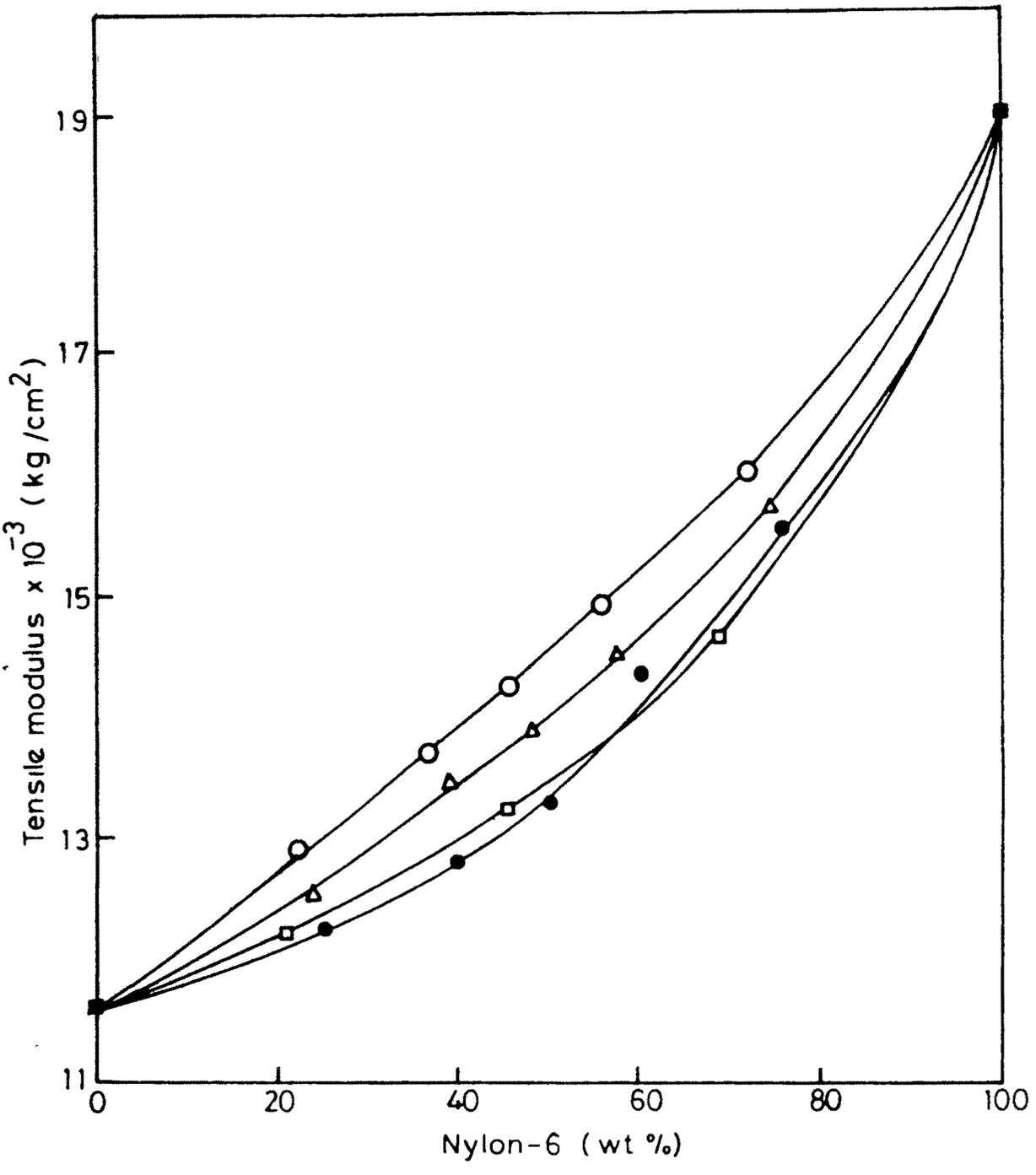

Fig. 4.21 Effect of blend compositionoon tensile modulus for

□ PP/Ny-6-/PP-g-BA (9.1%) blends
○ PP/Ny-6/PP-g-BA (4.8%) blends
△ PP/Ny-6/PP-g-BA (2.4%) blends
● PP/Ny-6 blends

In Figs. 4.22 and 4.23, the tensile modulus values calculated from the various theoretical models discussed earlier in section 4.2 along with experimental values for PP/Ny-6/PP-g-BA (2.4%) and PP/Ny-6/PP-g-BA (4.8%) blends are presented.

Referring to Fig. 4.22 for nylon-6 rich and PP rich blends having 2.4% of compatibiliser the Nielsun's model eq. 3 and eq. 4 and Kerner model eq. 1 for system having perfect adhesion predict the experimental data rather well. On the other hand eq. 2 of Kerner's model for loosely bound inclusion predicts a trend completely opposite to the experimental data. This implise that the discreat nylon or PP phase is not loosely bound to PP or nylon matrix and some adhesive force exists between PP and Ny-6. Here eq. 3 and eq. 4 can be used to fit the experimental data well by adjusting the value of ϕ_{max} = 0.7 for 2.4% compatibilised blends. For PP/Ny-6/PP-g-BA (4.8%) blends, Nielson's model eq. 3 and eq. 4 predicts the experimental data rather well (Fig 4.23) when values of ϕ_{max} are adjusted. The ϕ_{max} values used for calculating tensile modulus with the aid of eq. 3 and eq. 4 are given in Table 4.6. In this case also eq.2 for Kerner's model for loosely bound inclusion shows a trend which is very different than the experimental data. This suggests that PP and Ny-6 are not loosely bound in this system also. From Table 4.6 it can be observed that smaller ϕ_{max} value is required for 4.8% compatibilised blends. It should be noted that a smaller values of ϕ_{max} indicates a larger volume at interface, which is immobilised by the

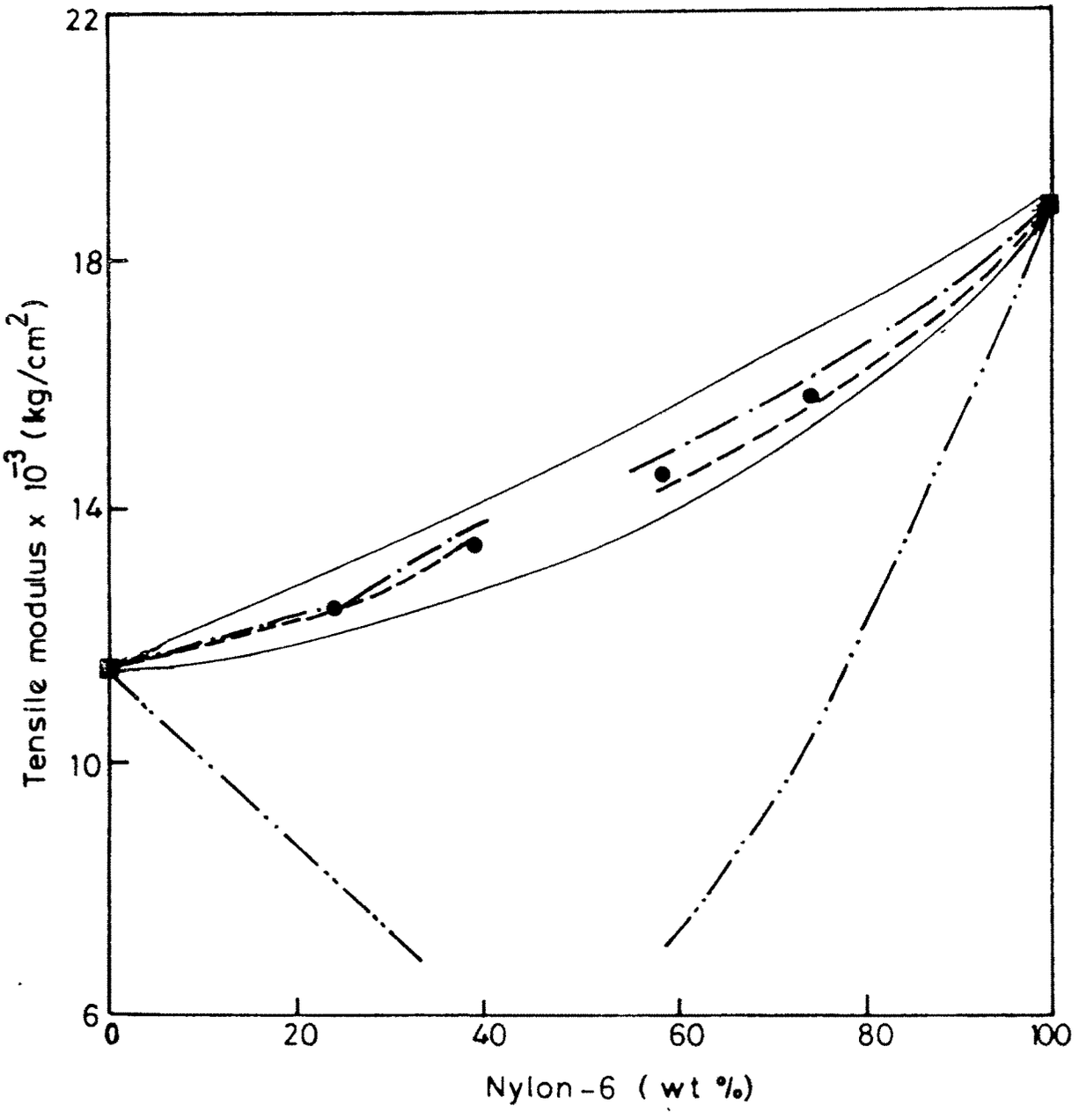

Fig. 4.22 Tensile modulus vesus blend composition for the PP/Ny-6/PP-g-BA (2.4%) blends:

(————), Paul's upper and lower bounds model ;

(—·—·—), Kerner's model with perfect adhesion ;

(— ··—··), Kerner's model with loosely bound inclusion ;

(– – – –), Nielsen's model ; (●) experimental data.

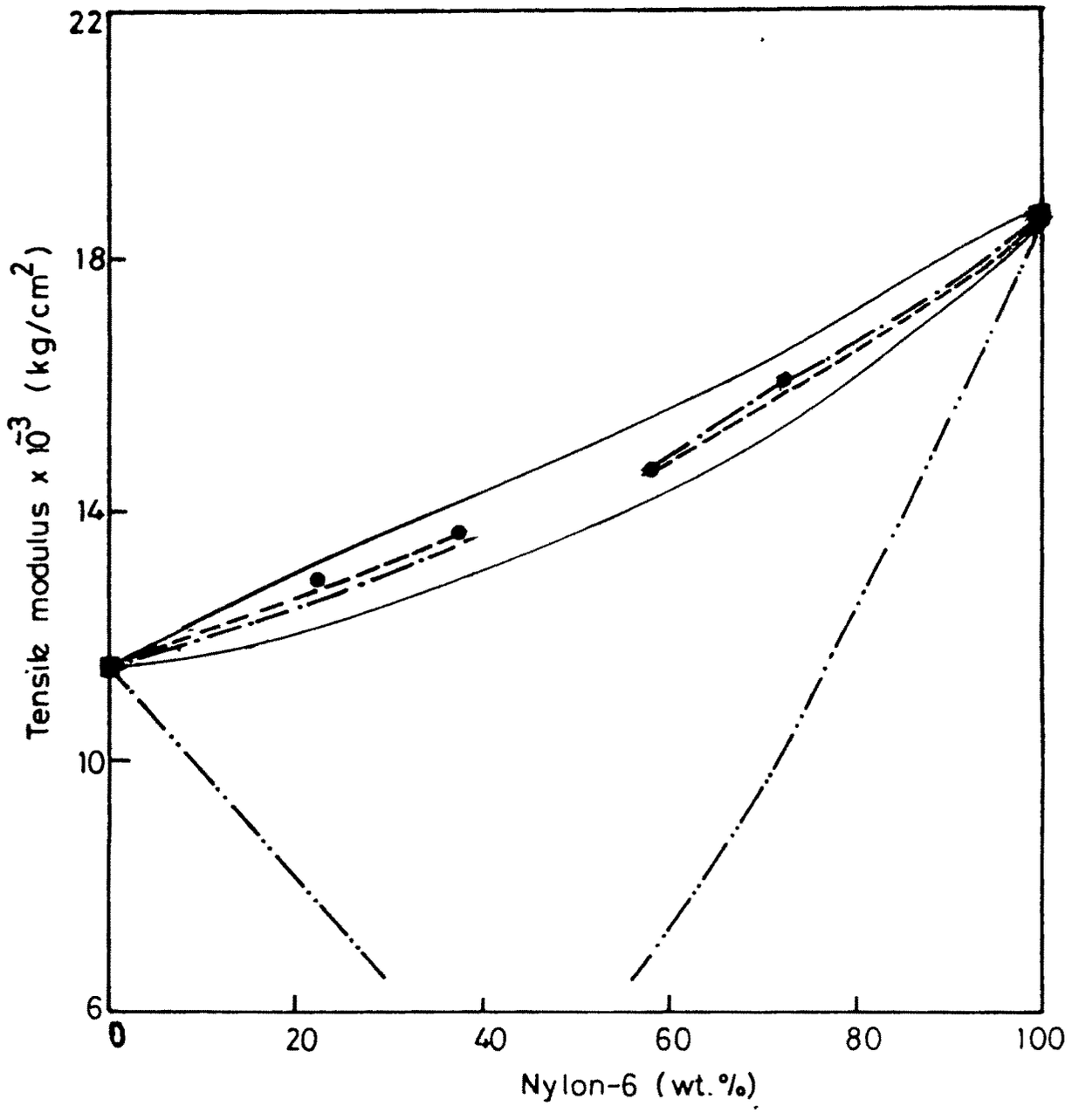

Fig. 4.23 Tensile modulus versus blend composition for the PP/Ny-6/PP-g-BA (4.8%) blends

(—————), Paul's upper and lower bounds model ;
(- ·- ·-· -), Kerner's model with perfect adhesion ;
(— ·· —··), Kerner's model with loosely bound inclusion;
(— — —), Nielsen's model ; (●), experimental data.

Table 4.6

The volume fraction and the maximum packing volume of PP/Ny-6/PP-g-BA (4.8%) blends.

Code No.	Volume fraction of PP	ϕ_{max}
C_1	0.801	0.45
C_2	0.671	0.50
C_4	0.485	0.65
C_5	0.334	0.55

Table 4.7

Rockwell hardness values of various binary (PP/Ny-6) and ternary (PP/Ny-6/PP-g-BA) blends

Code No.	Rockwell hardness	Code No.	Rockwell hardness	Code No.	Rockwell hardness
PP	80	B_1	86	C_1	88
A_1	84	B_2	91	C_2	93
A_2	90	B_3	95	C_3	96
A_3	95	B_4	101	C_4	102
A_4	99	B_5	105	C_5	107
A_5	104				
Ny-6	115				

dispersed phase in the blends. The results from the electron micrographs as well as tensile modulus agree with this fact.

It should be noted here that for both the PP/Ny-6/PP-g-BA (2.4%) and PP/Ny-6/PP-g-BA (4.8%) blends, the calculations for predicting the tensile modulus on the basis of various models were done considering PP/Ny-6/PP-g-BA blends as the two phase systems. Ny-6 was taken as one phase and mixture of PP and PP-g-BA has been taken as another phase. As the per cent grafting in PP-g-BA is low the tensile modulus of mixture of PP and PP-g-BA will not be much different than that of PP alone. Therefore, in our study, the tensile modulus of the mixture of PP + PP-g-BA was taken as that of PP.

In Figs. 4.24 and 4.25 the effect of composition on the tensile strength and flexural strength of all PP/Ny-6 blends containing 0%, 2.4%, 4.8% and 9.1% compatibiliser is shown. In binary blends the tensile strength and flexural strength increases linearly with the amount of Ny-6 as Ny-6 has higher tensile strength. It is also seen from the Figs. 4.24 and 4.25 that tensile and flexural strength of ternary blends compatibilised with 2.4% and 4.8% PP-g-BA are higher than that of binary PP/Ny-6 blends. This can be attributed to the improved homogenity of the system, which is clearly observed in the electron micrographs Figs. 4.14 and 4.15. In ternary blend with 9.1% compatibiliser the tensile and flexural strength was observed to decrease. This may be due to the presence of higher amount of PP-g-BA which imparts softness

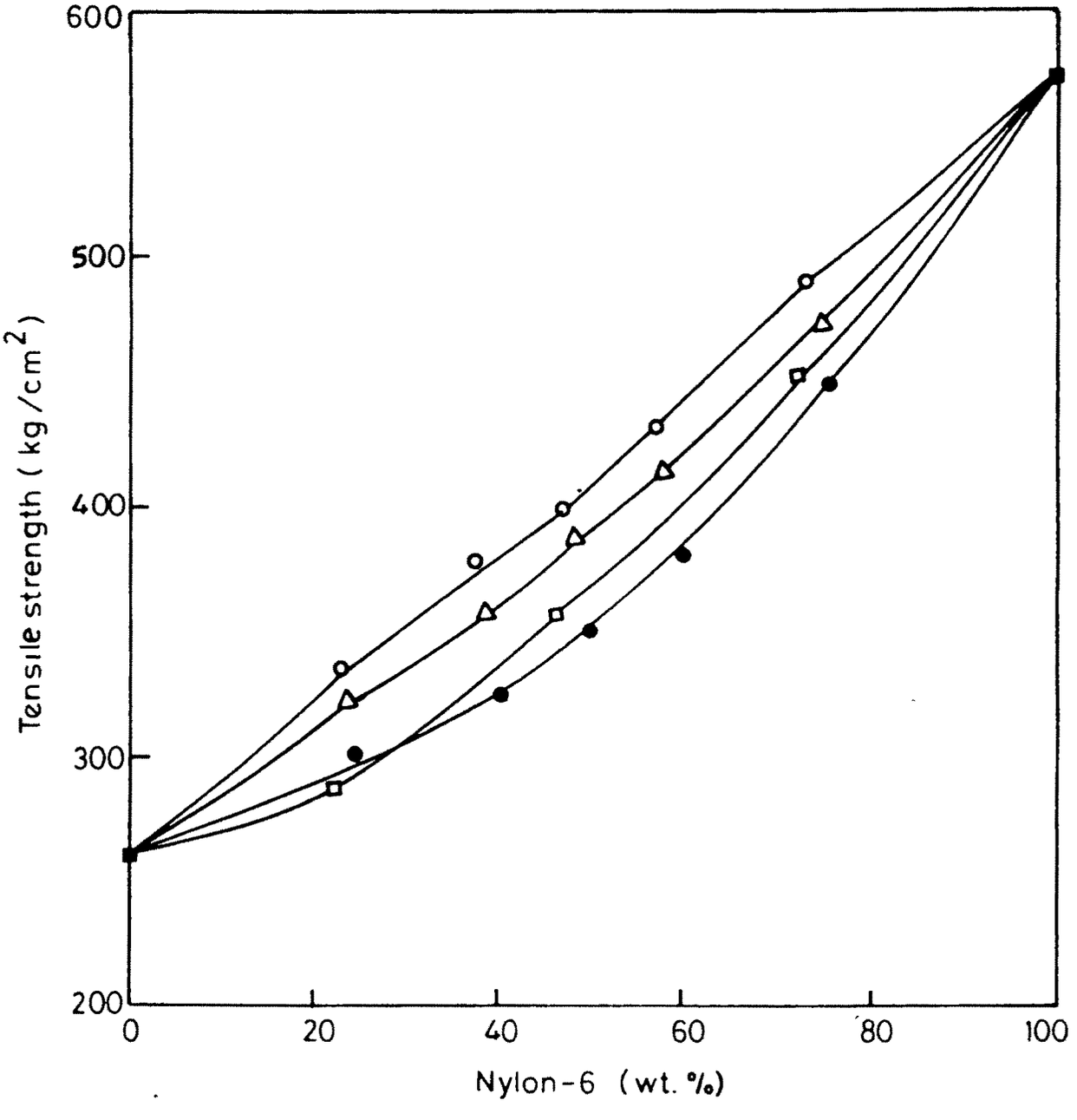

Fig. 4.24 Effect of blend composition on tensile strength for

- □ PP/Ny-6/PP-g-BA (9.1%) blends
- ○ PP/Ny-6/PP-g-BA (4.8%) blends
- △ PP/Ny-6/PP-g-BA (2.4%) blends
- ● PP/Ny-6 blends

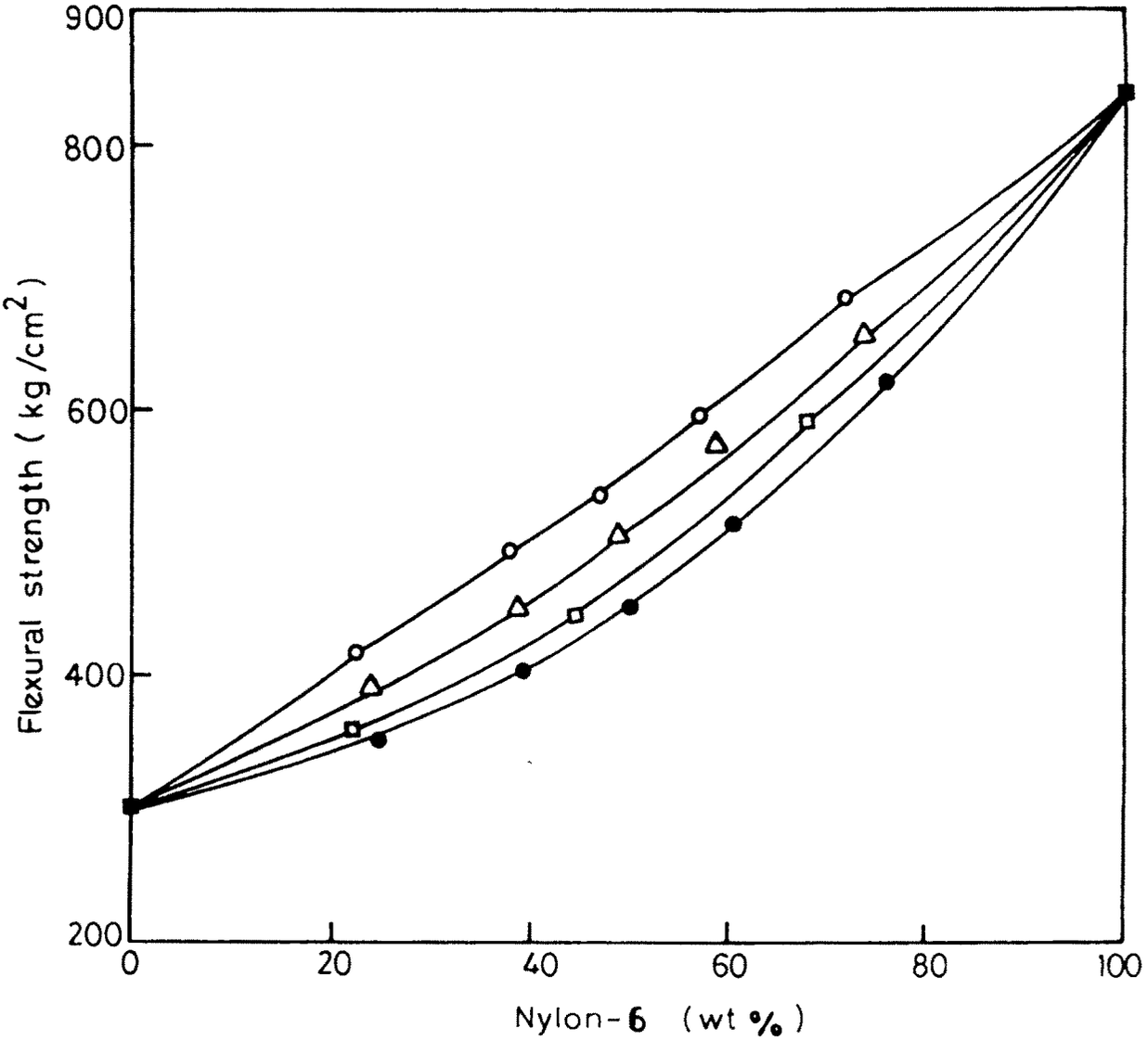

Fig. 4.25 Effect of blend composition on flexural strength for

□ PP/Ny-6/PP-g-BA (9.1%) blends
○ PP/Ny-6/PP-g-BA (4.8%) blends
△ PP/Ny-6/PP-g-BA (2.4%) blends
● PP/Ny-6 blends

to the resultant blend and gives lower tensile and flexural strength. The softening effect of LDPE was observed by Rawal et al. [17,18] in the Ny-6/LDPE/LDPE-g-BA (2.4%) and (4.8%). They observed decreased tensile and flexural strength of the blend with 4.8% compatibiliser than that with 2.4% compatibiliser and binary blends.

In Fig. 4.26, the theoretical prediction of tensile strength on the basis of Nielson's model is illustrated. The Nielson's model eq. 8 predicts the experimental data rather well for the blends containing 2.4% of PP-g-BA compatibiliser.

4.4.3.b Impact properties

Fig. 4.27 illustrates the impact strength of PP/Ny-6, PP/Ny-6/PP-g-BA (2.4%), PP/Ny-6/PP-g-BA (4.8%) and PP/Ny-6/PP-g-BA (9.1%) blends as a function of blend composition. According to simple mixture rule, here impact strength linearly increases with increasing Ny-6 content in PP/Ny-6 binary blends. Experimental results obtained were consistant with the theoretical predictions. The results obtained for the notched impact strength of ternary blends showed maximum value at higher Ny-6 concentration. Addition of 4.8% PP-g-BA compatibiliser to PP/Ny-6 showed ~50% improvement in impact strength.

Unlike LDPE/Ny-6/LDPE-g-BA blends [17,18] in the system under present study impact strength increases with increasing concentration of compatibiliser but decreases at 9.1% concentration of compatibiliser. The improvement in impact

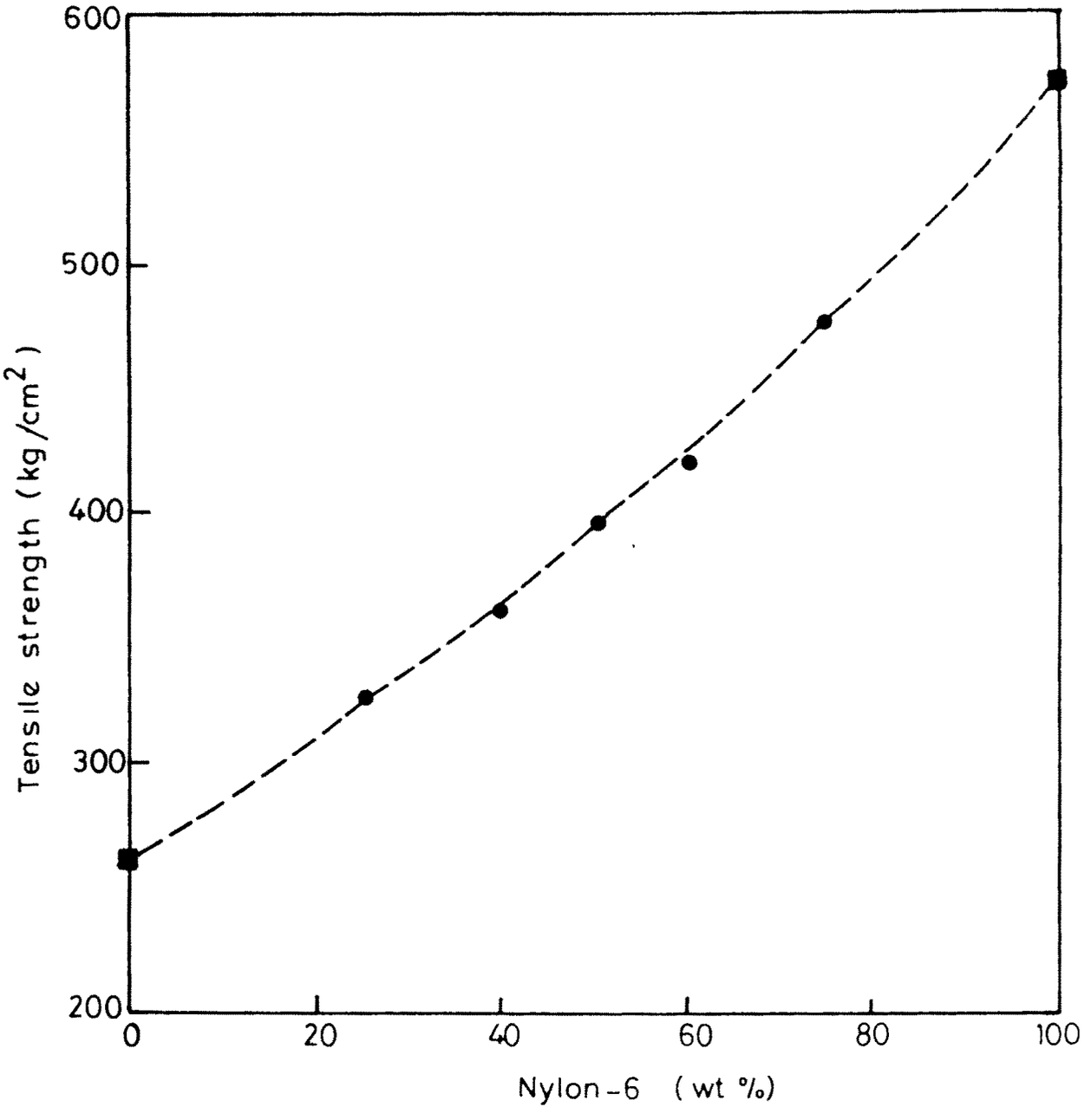

Fig. 4.26 Tensile strength versus blend composition for PP/Ny-6/PP-g-BA (2.4%): (- - - - -), theoretical prediction based on the tensile strength proposed by Nielsen ; (●), experimental data.

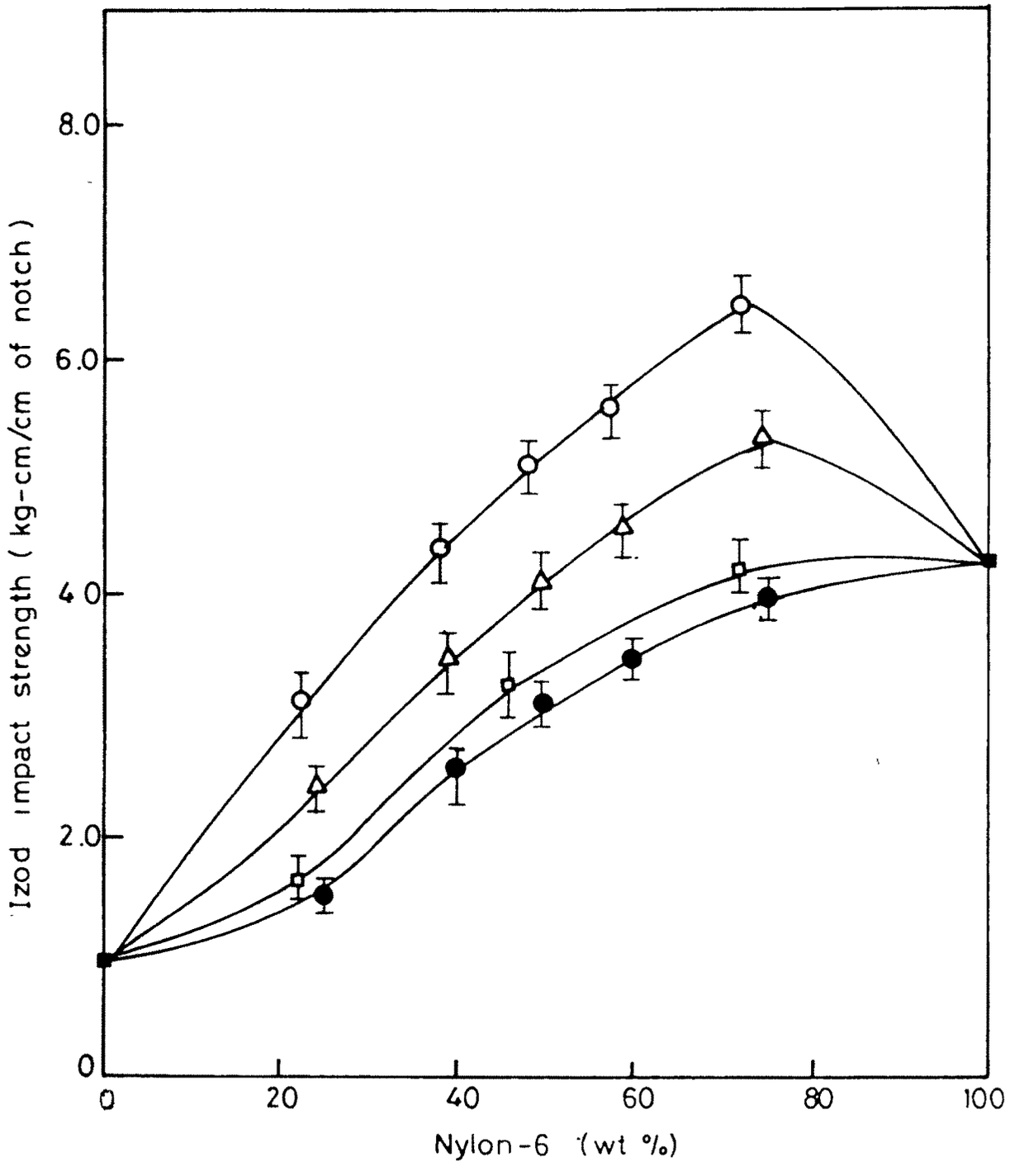

Fig. 4.27 Effect of blend composition on impact strength for

- □ PP/Ny-6/PP-g-BA (9.1%) blends
- ○ PP/Ny-6/PP-g-BA (4.8%) blends
- △ PP/Ny-6/PP-g-BA (2.4%) blends
- ● PP/Ny-6 blends

strength may be due to the improved homogenity of the system. The increase in impact strength is more pronounced at higher concentration of Ny-6.

It can be inferred from the Fig. 4.10 that in PP/Ny-6 blends, dispersed particles have average diameter of 20 μm and are uniformly distributed throughout the matrix. It should be also pointed out that there is no evidence of adhesion between the Ny-6 and PP. The effect of particle size and adhesion between two phases on the final impact strength of the blend is already discussed in section 4.1.1. Thus, in PP/Ny-6 blends due to larger particle size and lower adhesion between the dispersed phase and matrix, poor impact behaviour is observed. In ternary blends, due to interfacial activity of PP-g-BA, observed drastic reduction in the average diameter of dispersed phase particles (Table 4.5) imparts higher impact strength to the ternary blends than to binary blends. In PP/Ny-6/PP-g-BA (4.8%) blends better homogenity is achieved (Fig. 4.15) over PP/Ny-6/PP-g-BA (2.4%) blends (Fig. 4.14) due to further reduction in dispersed phase particle size. But again at 9.1% compatibiliser the average particle size of dispersed phase is increased (Fig. 4.16) resulting into lower impact strength.

4.4.3.c Melt flow index (MFI)

From the Fig. 4.28 it can be inferred that all binary and ternary blends show lower melt flow index than that of Ny-6. It is seen from the Fig. 4.28 that ternary PP/Ny-6/PP-g-BA

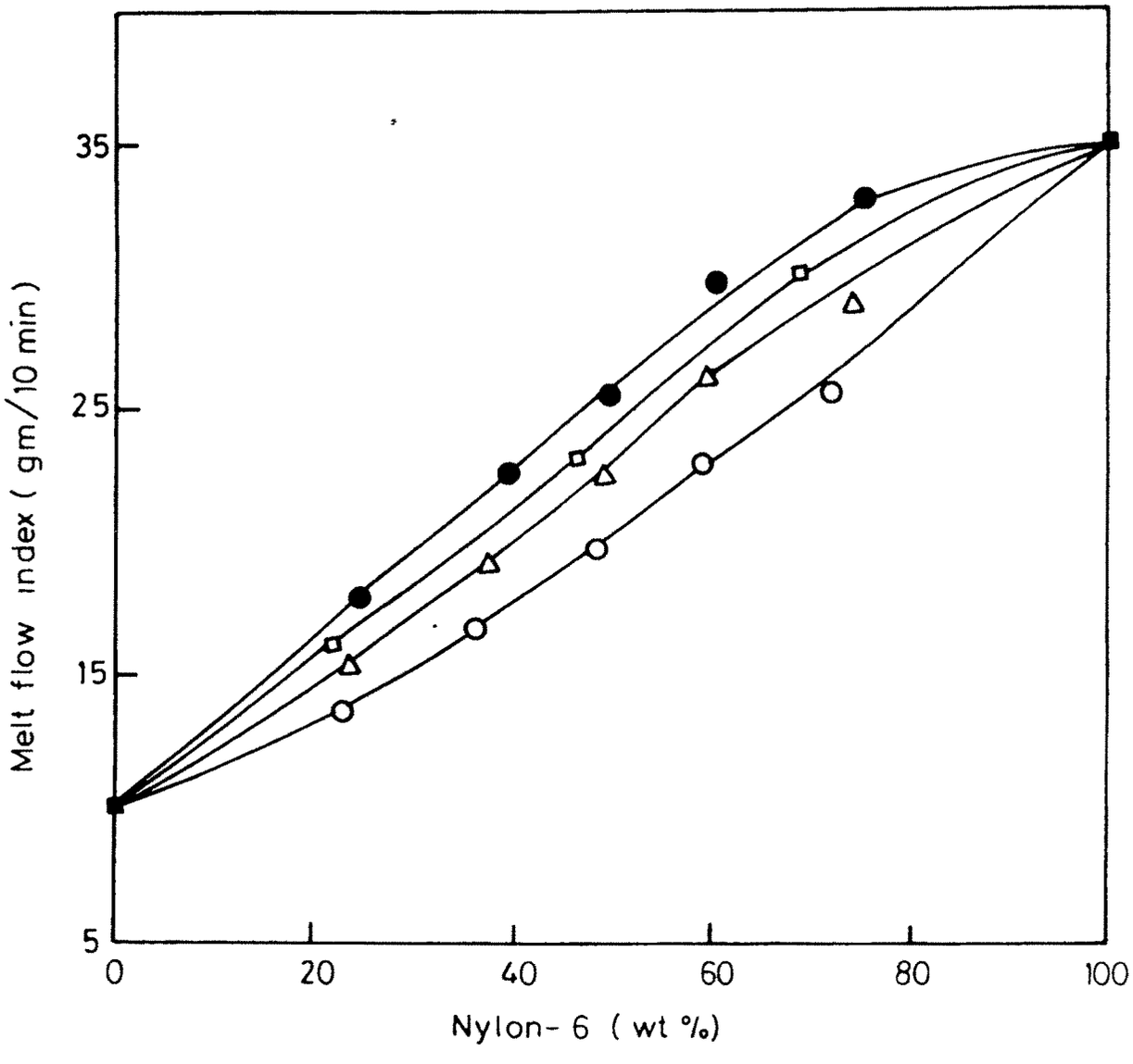

Fig. 4.28 Effect of blend composition on melt flow index for

□ PP/Ny-6/PP-g-BA (9.1%) blends
○ PP/Ny-6/PP-g-BA (4.8%) blends
△ PP/Ny-6/PP-g-BA (2.4%) blends
● PP/Ny-6 blends

(2.4%) and PP/Ny-6/PP-g-BA (4.8%) blends have lower MFI values than coresponding binary blends. But the blends having 9.1% PP-g-BA compatibiliser have higher MFI than other ternary blends. Due to high MFI of nylon-6, the MFI of binary blends increases with Ny-6 content in the blend. On the other hand, in ternary blends, due to structural changes such as formation of graft copolymer (i.e., PP-g-Ny-6) during melt mixing, MFI vlaues decrease.

4.4.3.d Rockwell hardness

Rockwell hardness test measures the ability of the material for its rebound efficiency and residual indentation after load is removed. In Table 4.7 the rockwell hardness values for all types of blends are given.

From the Table 4.7 it can be inferred that all the blends have lower Rockwell hardness values than that of Ny-6. This is due to the presence of PP, with lower rockwell hardness value, in the blend system. From the Table 4.7 it can also be seen that the ternary blends have some what higher Rockwell hardness values than that of binary blends. Among the ternary blends, PP/Ny-6/PP-g-BA (4.8%), blends have slightly higher hardness values than PP/Ny-6/PP-g-BA (2.4%) blends. However, the difference in the Rockwell hardness values for all the binary and ternary blends is not significant.

4.4.3.e Heat deflection temperature (HDT)

Heat deflection temperature of polymer can be considered as the upper temperature limit at which the material can support the load for any appreciable deflection. Thus, it is an important property for a polymer from the application point of view. In Table 4.8 the effect of composition on heat deflection temperature (HDT) is given for all the blends.

It can be observed from results given in Table 4.8 that all blends have higher HDT values than that of Ny-6. HDT values of ternary blends are not showing much improvement over binary blends.

4.4.3.f Thermal properties

The representative melting curves for PP/Ny-6 and PP/Ny-6/PP-g-BA (4.8%) are shown in Figs. 4.29.a and 4.29.b. From the results obtained (Fig. 4.30) it is seen that the extent of Ny-6 or PP does not affect the thermal properties of the binary blends. But addition of PP-g-BA to the binary blends showed significant change in melting temperature. From the Fig. 4.30 it is observed that the melting temperature of PP and Ny-6 remain unaffected in binary blends. But for the ternary blends, PP/Ny-6/PP-g-BA (2.4%) the melting temperatures are shifted to somewhat lower side 161^{o}C - 163^{o}C for PP and 222.5^{o}C - 224^{o}C for Ny-6. In PP/Ny-6/PP-g-BA (4.8%) blends the melting temperatures for PP and Ny-6 are shifted further towards lower side ~159^{o}C and ~221^{o}C

Table 4.8

Heat distortion temperature (HDT) of various binary (PP/Ny-6) and ternary (PP/Ny-6/PP-g-BA) blend systems.

Code No.	HDT (^{o}C)	Code No.	HDT (^{o}C)	Code No.	HDT (^{o}C)
PP	67.0	B_1	70.2	C_1	73.2
A_1	66.0	B_2	70.0	C_2	72.4
A_2	66.2	B_3	71.3	C_3	70.4
A_3	66.4	B_4	67.4	C_4	70.6
A_4	65.0	B_5	69.5	C_5	71.1
A_5	64.1				
Ny-6	62.2				

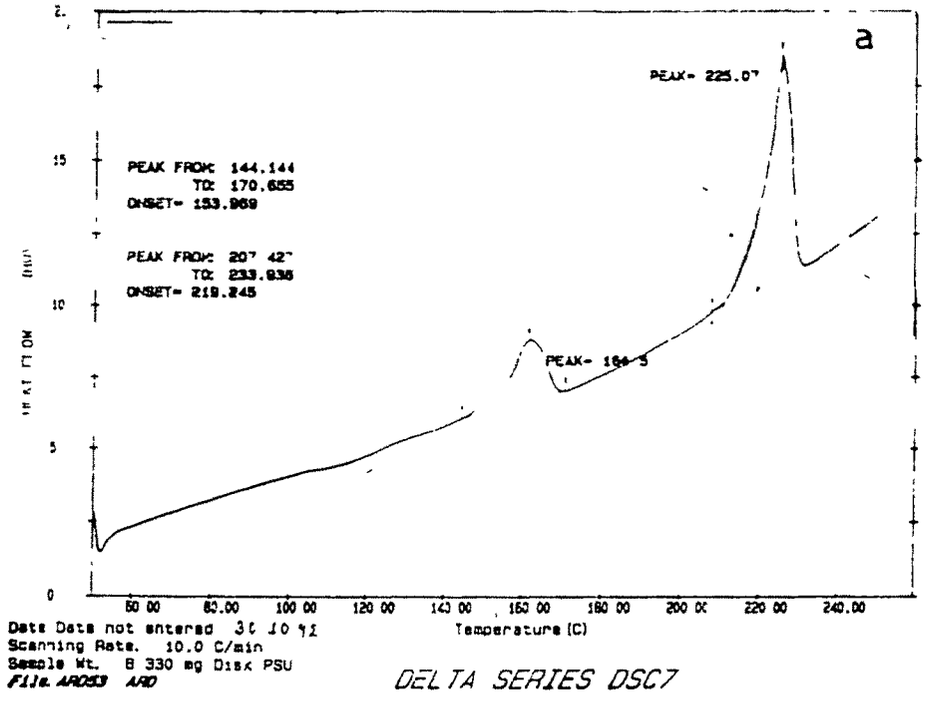

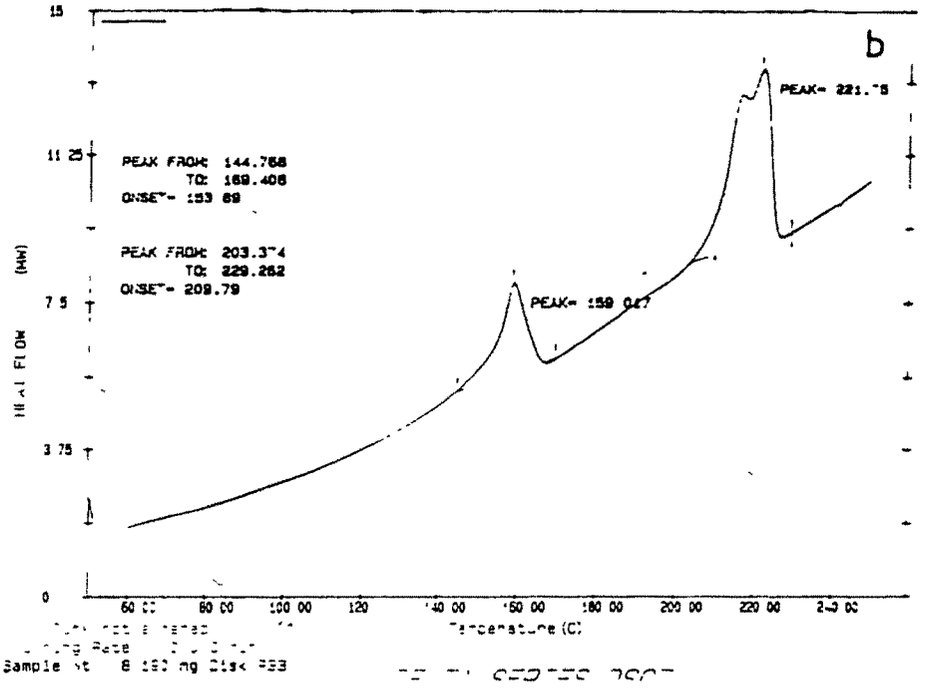

Fig. 4.29 DSC melting curves for

a. blend A_5; b. blend C_5

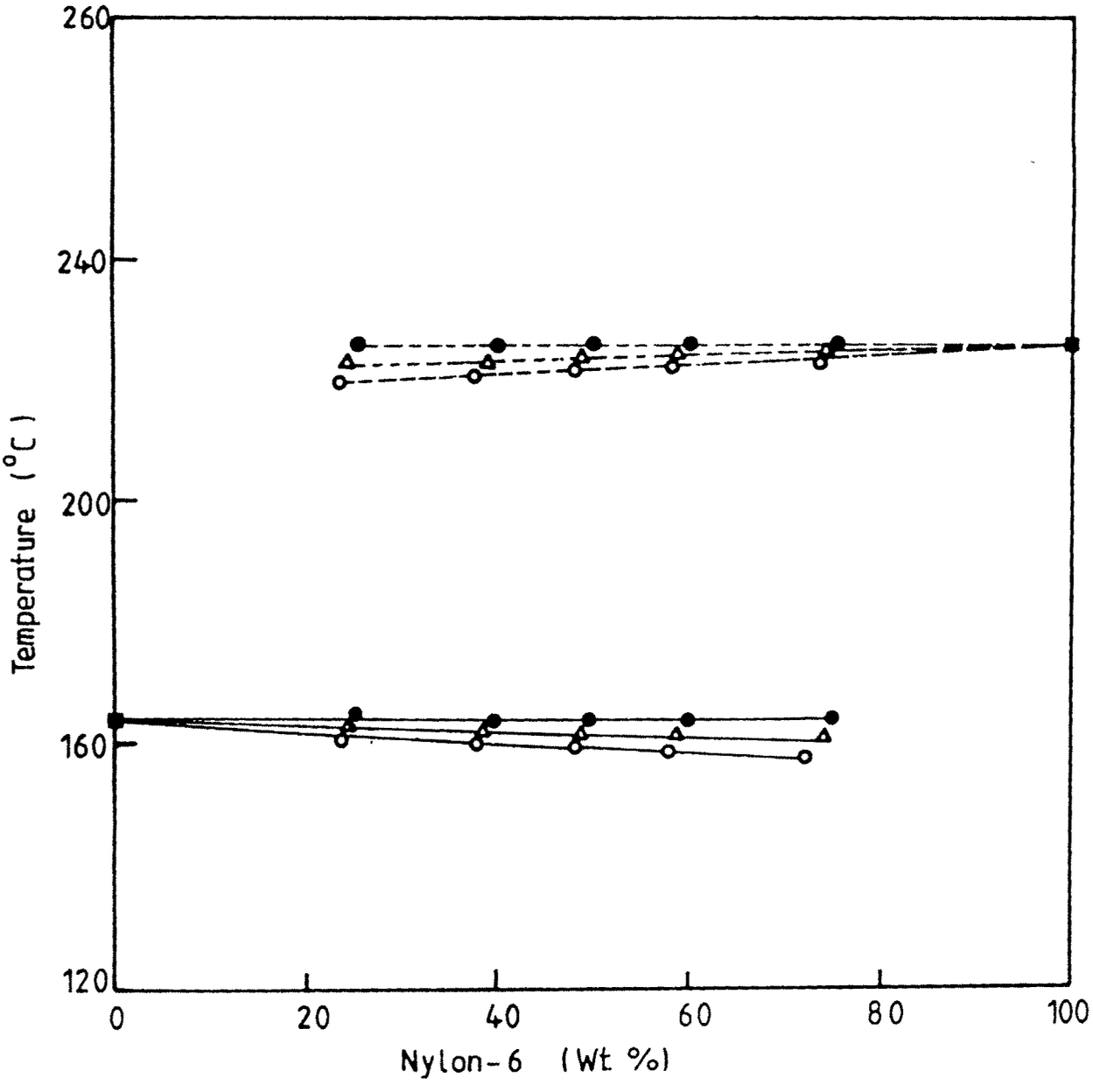

Fig. 4.30 Effect of blend composition on melting temperature (●——●) Tm (PP) and (●- - - -●), Tm (Ny-6) in PP/Ny-6 blends ; (△——△), Tm (PP) and (△- - -△) Tm (Ny-6) in PP/Ny-6/PP-g-BA (2.4%) blends ; (○——○) Tm (PP) and (○ - - -○) Tm (Ny-6) in PP/Ny-6/PP-g-BA (4.8%) blends.

respectively. Similar observation was reported by Nishio et al. [19].

Percent crystallinity of the blends was calculated as discussed in section 4.3.3.g. The percent crystallinity versus Ny-6 content for all types of blends are presented in Fig. 4.31. From the Fig. 4.31 it is observed that in binary PP/Ny-6 blends the percent crystallinity of PP and Ny-6 are not influenced by each other's presence. Whereas in ternary blends both PP and Ny-6 show lower percent crystallinity. It has already discussed that in PP/Ny-6/PP-g-BA ternary blends, the reaction between the free amine group of Ny-6 and ester group of PP-g-BA takes place during melt mixing resulting into formation of PP-g-Ny-6. These grafted chains of Ny-6 creat hinderance in the polymer chain packing in crystals. As a result the reduction in the percent crystallinity of both PP and Ny-6 is observed. Similar results were obtained by Rawal et al. [17,18] for the PE/Ny-6/PE-g-BA.

4.4.3.g Dynamic mechanical property

Due to non availability of low temperature device we were not able to find out the β- and γ-relaxation of pure PP and PP component in the blends and also γ-transition peak of pure Ny-6 and Ny-6 in the blends. However, we could find out β-transition peak for Ny-6.

The temperature dependence of the dynamic loss moduli (E") and the loss factor ($\tan\delta$) at 6.3 rad sec^{-1} for the non

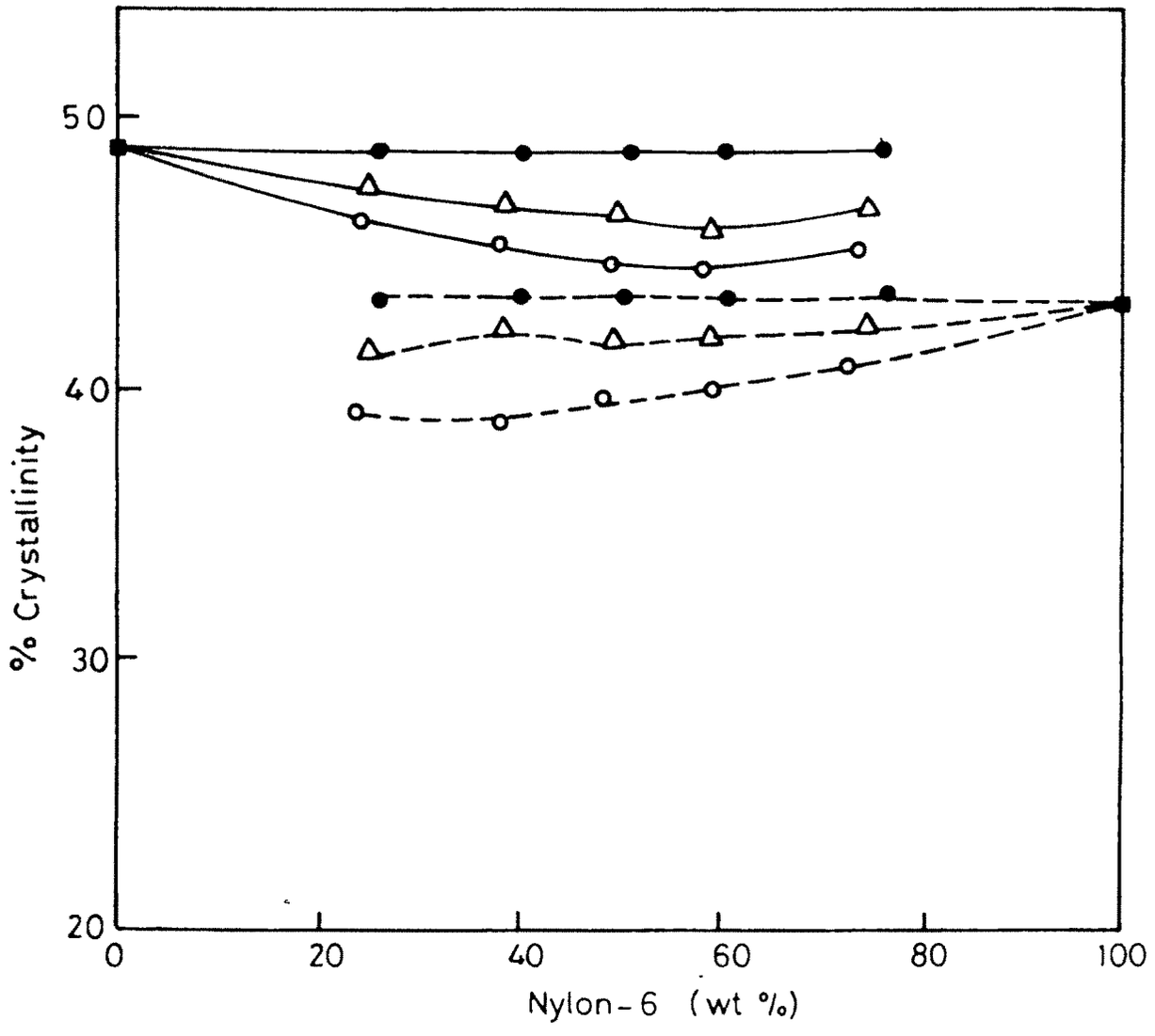

Fig. 4.31 Effect of blend composition on % crystallinity : (●——●), % crystallinity of PP and (●- - -●), % crystallinity of Ny-6 in PP/Ny-6 blends ; (△——△), % crystallinity of PP and (△- - -△), % crystallinity of Ny-6 in PP/Ny-6/PP-g-BA (2.4%) blends ; (○——○), % crystallinity of PP and (○- - -○), % crystallinity of Ny-6 in PP/Ny-6/PP-gBA (4.8%) blends

compatibilised PP/Ny-6 blends (A_1, A_3 and A_5) is given in Figs. 4.32.a and 4.32.b respectively.

The loss factor curves (tan δ) and loss modulus curves (E") shown in Fig. 4.32 for the non compatibilised blends exhibit fairly sharp relaxation peak at 60^{o}C which correspond to the glassy temperature of Ny-6. This indicates weak mechanical interaction between PP and Ny-6 phases in the blends. The Fig. 4.33.a and 4.33.b summarise the dynamic mechanical data, the loss moduli (E") and the loss factor (tan δ) respectively for compatibilised blend PP/Ny-6/PP-g-BA (4.8%). From the results obtained it is seen that the use of PP-g-BA produces blends with different dynamic mechanical properties due to an improvement in comatibility between the PP phase and Ny-6 phase in the blends.

The loss modulus E" data from Fig. 4.33.a indicates that the compatibilised blends differ from the non compatibilised blends in the β-relaxation process of Ny-6 phase in the blends. Here the β-transition temperature (Peak maxima) of Ny-6 phase in the blend is slightly shifted to lower temperature and the peaks become broader, while in non compatibilised blends at the corresponding compositions well shaped peak of β-relaxation is retained. These results are in agreement with the E" data published by Utracki and Summut [20] for commercial alloys of compatibilised PP-Ny-6 (40/60) blends.

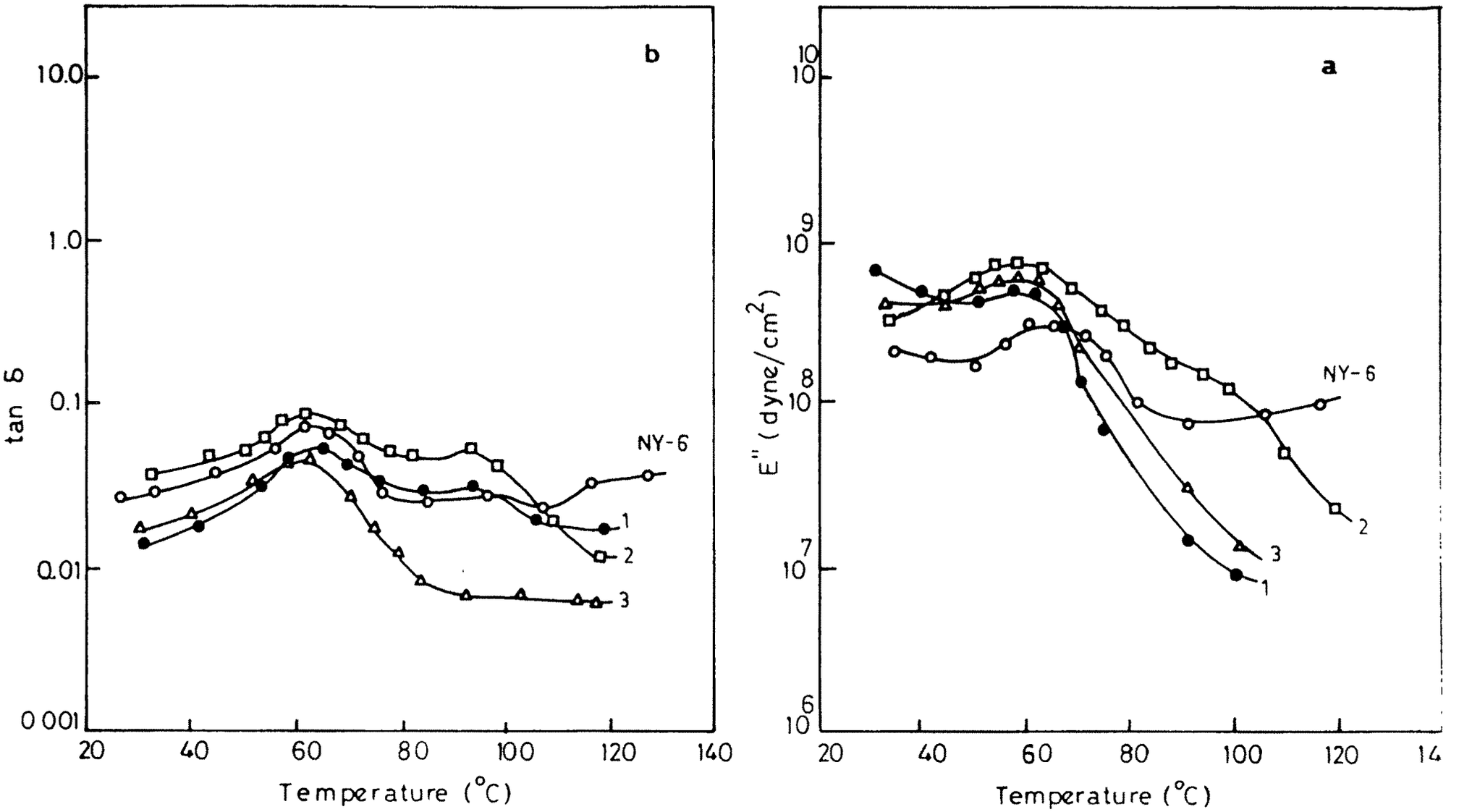

Fig. 4.32 β-relaxation for Ny-6 phase in non compatibilised blends (PP/Ny-6 blends)

a) loss modulus (E") : 1, A_1 ; 2, A_3 ; 3, A_5 b) loss factor (tanδ) : 1, A_1 ; 2, A_3; 3, A_5

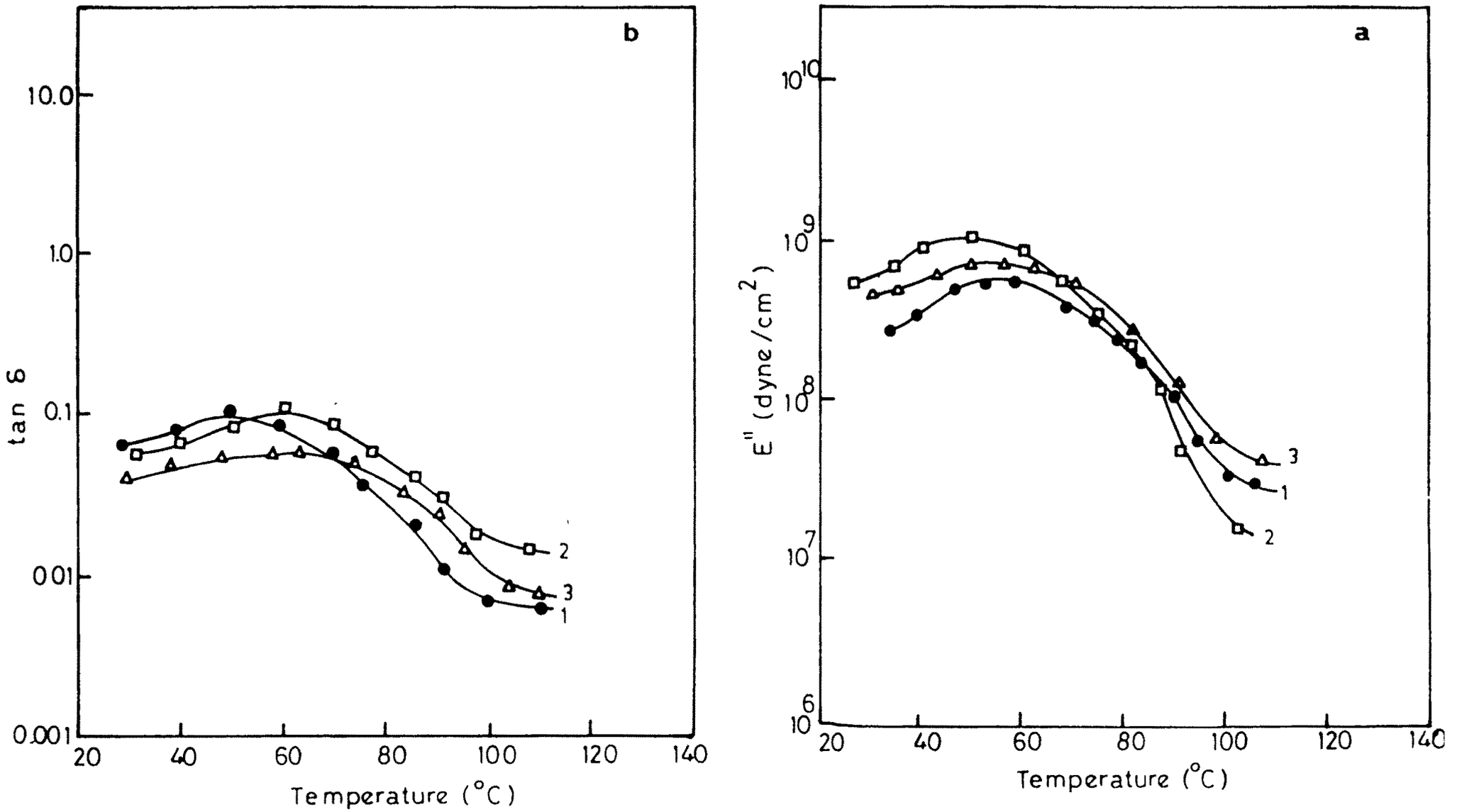

Fig. 4.33 β-relaxation for Ny-6 phase in compatibilised blends [PP/Ny-6/PP-g-BA (4.8%)]

a) loss modulus (E") : 1, C_1 ; 2, C_3 ; 3, C_5 b) loss factor (tenδ) : 1, C_1 , 2, C_3 ; 3, C_5

The loss factor tan δ (E"/E') spectra for compatibilised blends are given in Fig.4.33.b. In comparision with non compatibilised blends, the β-transition peak maxima of the Ny-6 phase in compatibilised blends is broader. Similar results were obtained by Liang and Williams [16], with Ny-11/PP system with PP-g-AA as compatibiliser.

4.4.3.h Water absorption

From Fig 4.34 it can be inferred that all types of blends have lower water absorption than that of Ny-6. Due to hydrophobicity of PP, it contributes to reduction in water absorption extent of the blends. From Fig. 4.34 it can also be observed that the ternary blends absorb less water than binary blends. Water susceptibility of Ny-6 is mainly due to the presence of amine groups. In PP/Ny-6/PP-g-BA blends ester groups of butyl acrylate get interacted with free amine groups of Ny-6. As a result the number of free amine groups in Ny-6 is reduced. Hence, with increased concentration of PP-g-BA in blends higher reduction in water absorption extent was observed. This can also be taken as an additional indication of interfacial activity of PP-g-BA for PP/Ny-6 blends. Similar results were obtained by Rawal et al. [17,18] for the PE/NY-6/PE-g-BA blends.

4.4.4 PP-g-MAH as compatibiliser for PP/NY-6 blends

The efficiency of the PP-g-MAH as an interfacial agent for PP/Ny-6 system has been evaluated. The synthesis and

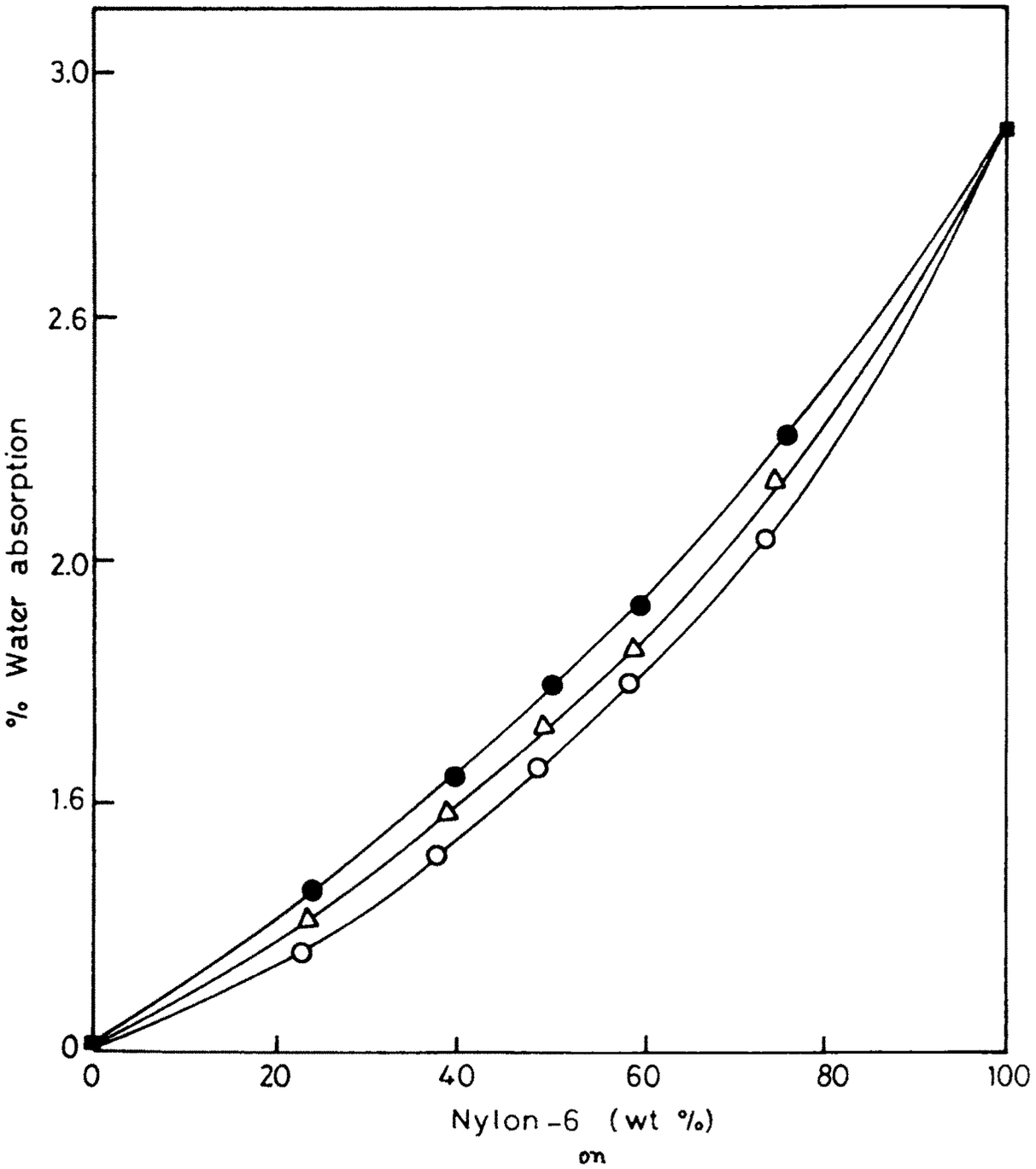

Fig. 4.34 Effect of blend composition on % water absorption

○ PP/Ny-6/PP-g-BA (4.8%) blends

△ PP/Ny-6/PP-g-BA (2.4%) blends

● PP/Ny-6 blends

characterisation of PP-g-MAH is already discussed in the Chapter 2.

As mentioned earlier, when PP-g-MAH is added to PP/Ny-6 blends, the anhydride group of maleic anhydride reacts with the free amine groups of Ny-6 during melt mixing at 235°C resulting into amide linkages between nylon-6 and PP. The amide linkages can become imide linkages by the loss of water with the ring closure[22]. Thus, formation of PP-g-Ny-6 during melt mixing is assumed.

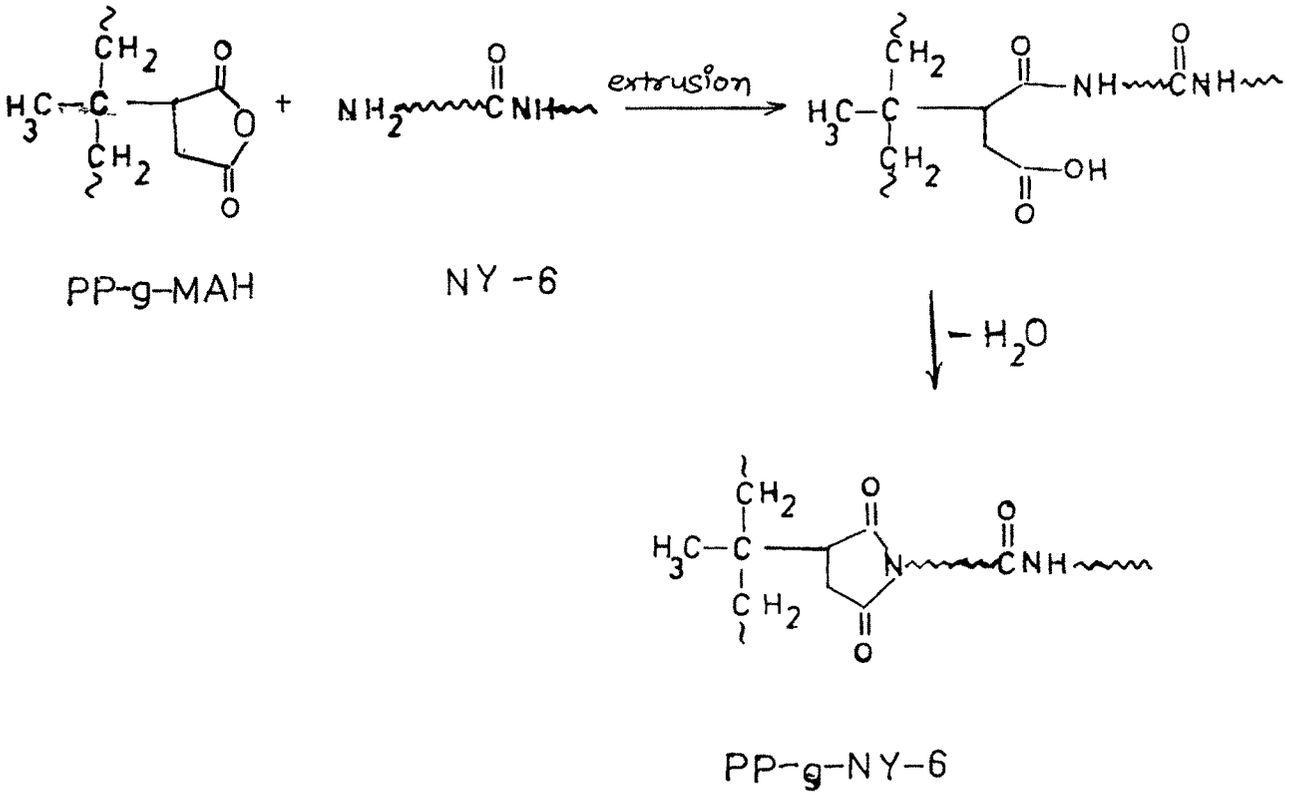

In the support of this statement Molau's test described earlier in section 4.3.2.a was carried out. On the addition of formic acid to the blend containing 2.4%, 4.8% and 9.1%

compatibiliser (PP-g-MAH), colloidal solution was obtained. This positive Molau's test indicates the formation of PP-g-Ny-6 in PP/Ny-6/PP-g-MAH blends.

4.4.4.a Microscopy study

Figs. 4.35, 4.36 and 4.37 show the morphology of E_5, F_5 and G_3 blends of cryogenically fractured tensile bar surfaces respectively. The spherical particles appearing in binary A5 blends (Fig. 4.10) have completely disappeared in the ternary blends. The resulting morpholoy is very much like nylon-6. In Fig. 4.35 very small particles are observed but in Fig. 4.36 and 4.37 it is very difficult to identify the dispersed phase and matrix.

For the calculation of particle size impact broken surfaces were etched selectively with hot xylene for PP phase. The micrographs for E_5, F_5 and G_3 blends are given in Figs. 4.38, 4.39 and 4.40 respectively. It is observed from Fig. 4.38 that the particle size of dispersed phase is very small 0.89 μm - 1 μm. But in the Fig. 4.39 it is very difficult to identify the etched pp phase. This suggests the high interfacial activity of PP-g-MAH for PP/Ny-6 blend system. Again for the blends containing 9.1% compatibiliser (Fig. 4.40) small holes were observed ($\sim$1 μm) due to etching of PP phase from the blend. The results obtained are similar to those for PP/Ny-6/PP-g-BA systems under present study. However, higher homogenity is observed for PP-g-MAH compatbiliser than that for PP-g-BA compatibiliser in PP/NY-6 blend systems.

Center

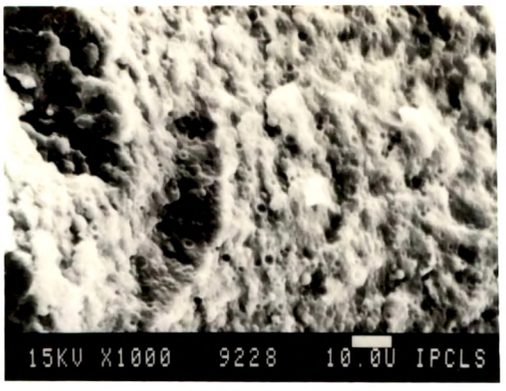

Edge

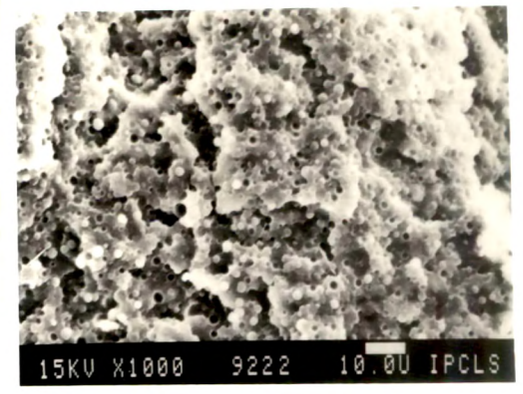

Fig. 4.35 SE micrographs of cryogenically fractured blend E_5 (X 1000)

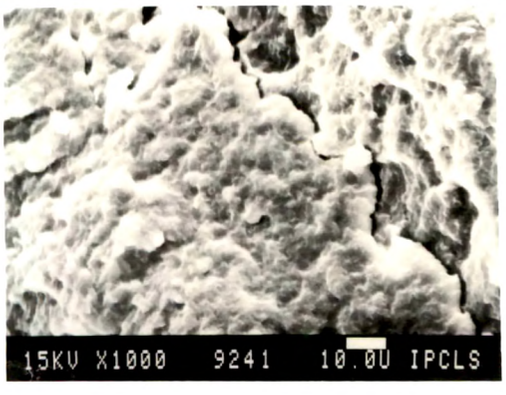

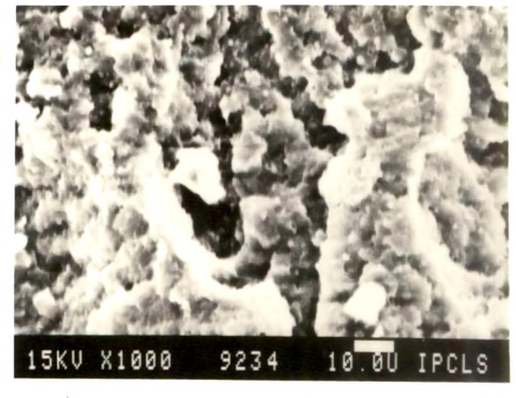

Fig. 4.36 SE micrographs of cryogenically fractured blend F_5 (X 1000)

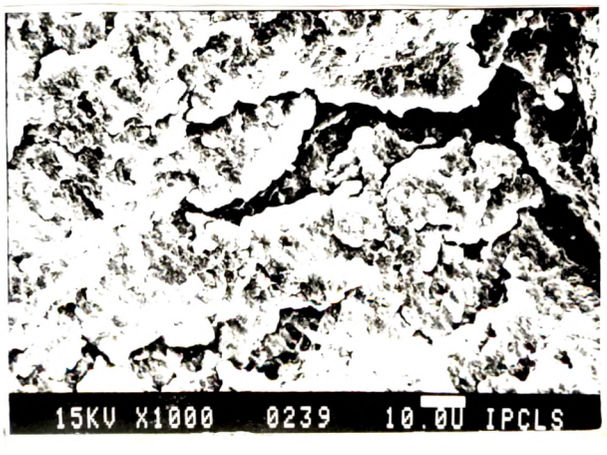

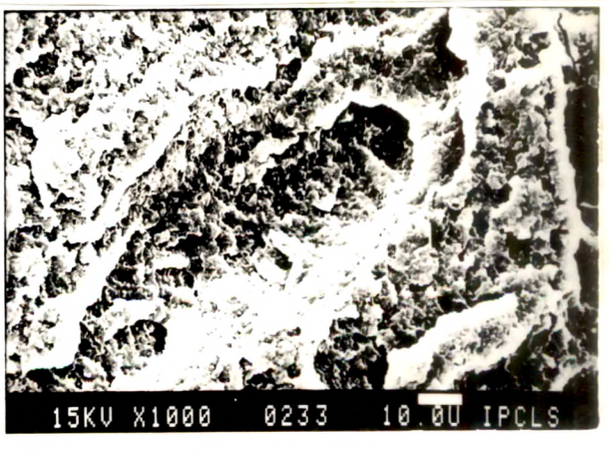

Fig. 4.37 SE micrographs of cryogenically fractured blend G_3

Center Edge

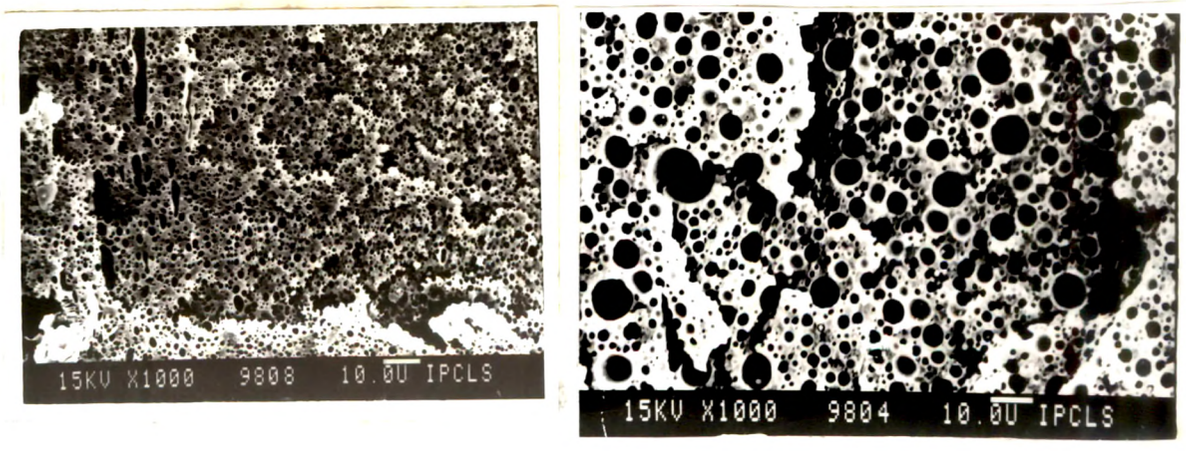

Fig. 4.38 SE micrographs of blend E_5 etched with hot xylene (X 1000)

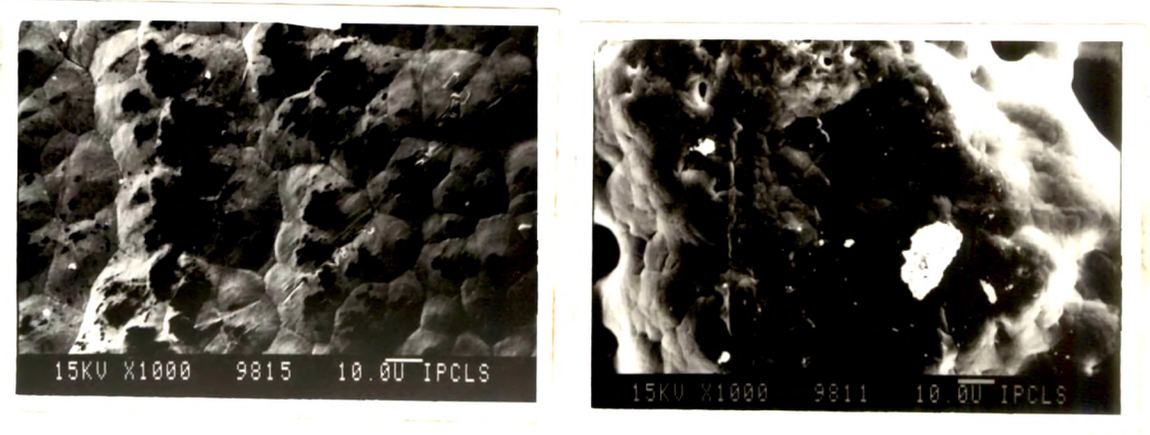

Fig. 4.39 SE micrographs of blend F_5 etched with hot xylene (X 1000)

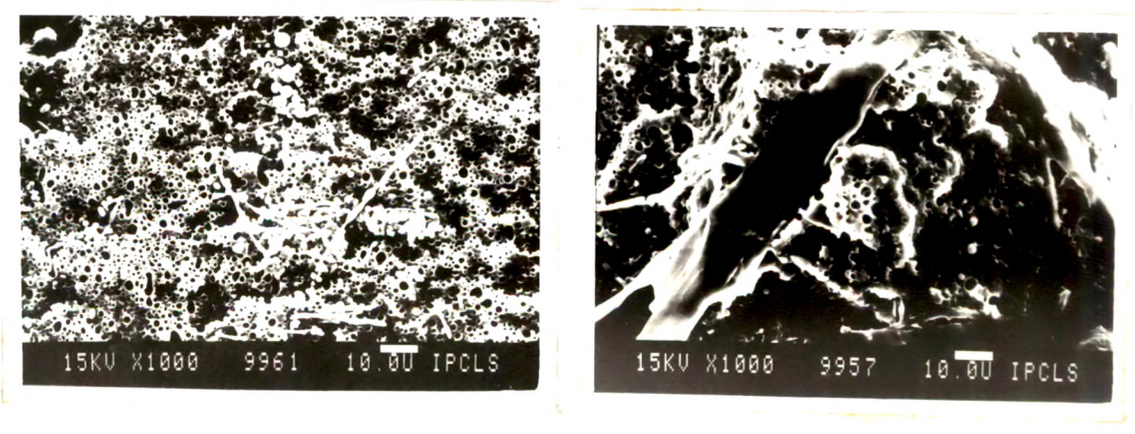

Fig. 4.40 SE micrographs of blend D_3 etched with hot xylene (X 1000)

4.4.4.b Tensile properties

Typical stress-strain curves for PP/Ny-6/PP-g-MAH (2.4% and 4.8%) blends are given in Fig. 4.41.a and 4.41.b. From the results obtained it is inferred that like PP/Ny-6/PP-g-BA blend systems here also no necking behaviour is observed.

In Figs. 4.42, 4.43 and 4.44 the dependence of the tensile modulus, tensile strength and flexural strength on the composition is illustrated. It is observed that performance of PP/Ny-6 blend is strongly influenced by the addition of PP-g-MAH (2.4%, 4,8% and 9.1%).

The over all improvement in all these properties was observed for ternary blends containing PP-g-MAH interfacial agent when compared with binary PP/Ny-6 blends. While comparing with corresponding PP/Ny-6/PP-g-BA blends, it was observed that PP/Ny-6/PP-g-MAH blends show higher tensile modulus, tensile strength and flexural strength. This may be attributed to improved homogenity due to the presence of more reactive maleic anhydride groups present in PP/Ny-6/PP-g-MAH blends. On comparision of electron micrographs for PP/Ny-6/PP-g-BA (2.4%) (Fig. 4.14) and corresponding PP/Ny-6/PP-g-MAH (2.4%) blends (Fig. 4.35), the marked difference in homogenity of two blends can be clearly seen.

4.4.4.c Impact strength

Referring to Fig.4.45 it can be observed that all the ternary blends have higher impact strength than binary blends. From

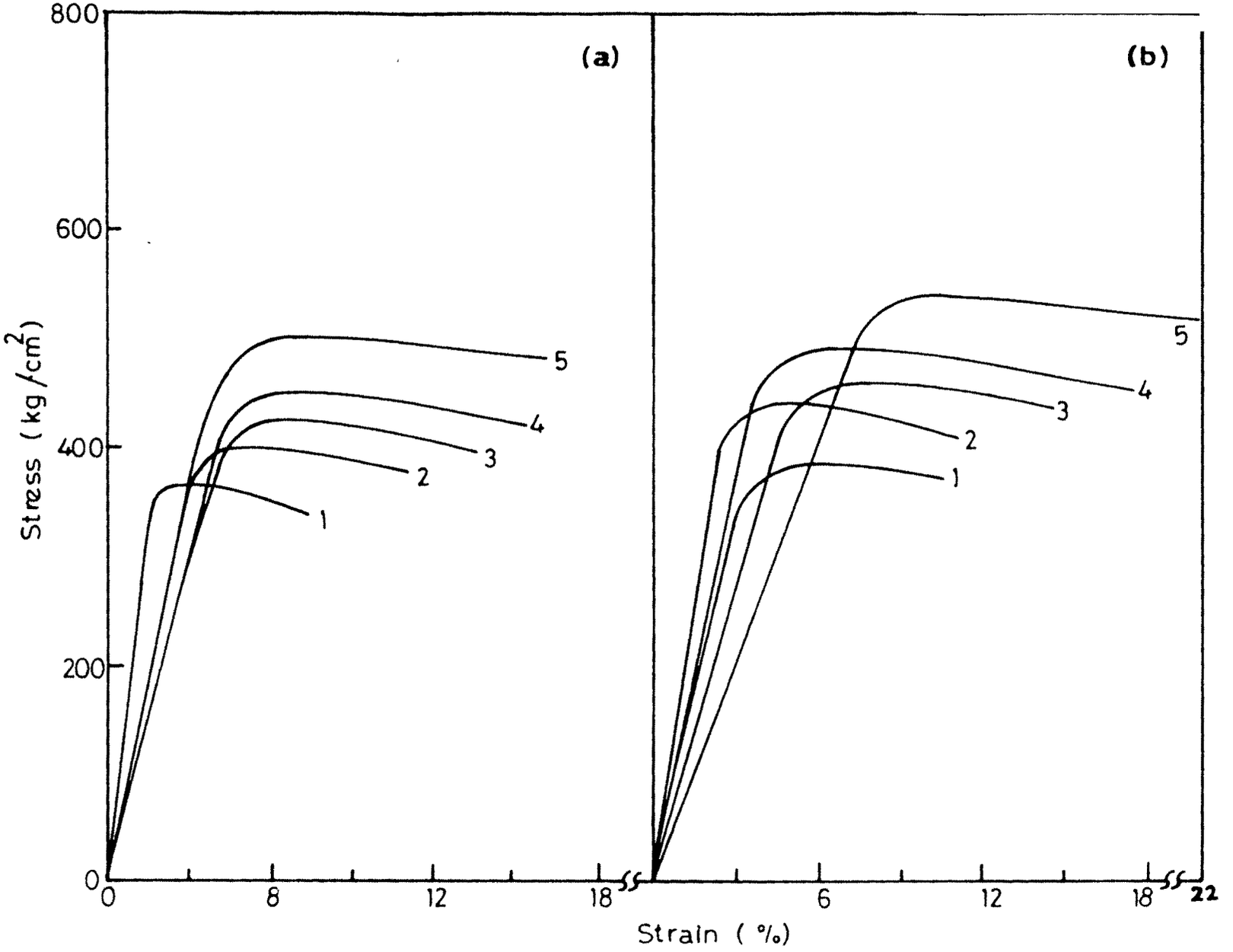

Fig. 4.41 Stress versus strain curves for

a) PP/NY-6/PP-g-MAH (2.4%) : 1, E_1 ; 2, E_2 ; 3, E_3 , 4, E_4 ; 5, E_5

b) PP/Ny-6/PP-g-MAH (4.8%) : 1, F_1 ; 2, F_2 ; 3, F_3 ; 4, F_4 ; 5, F_5

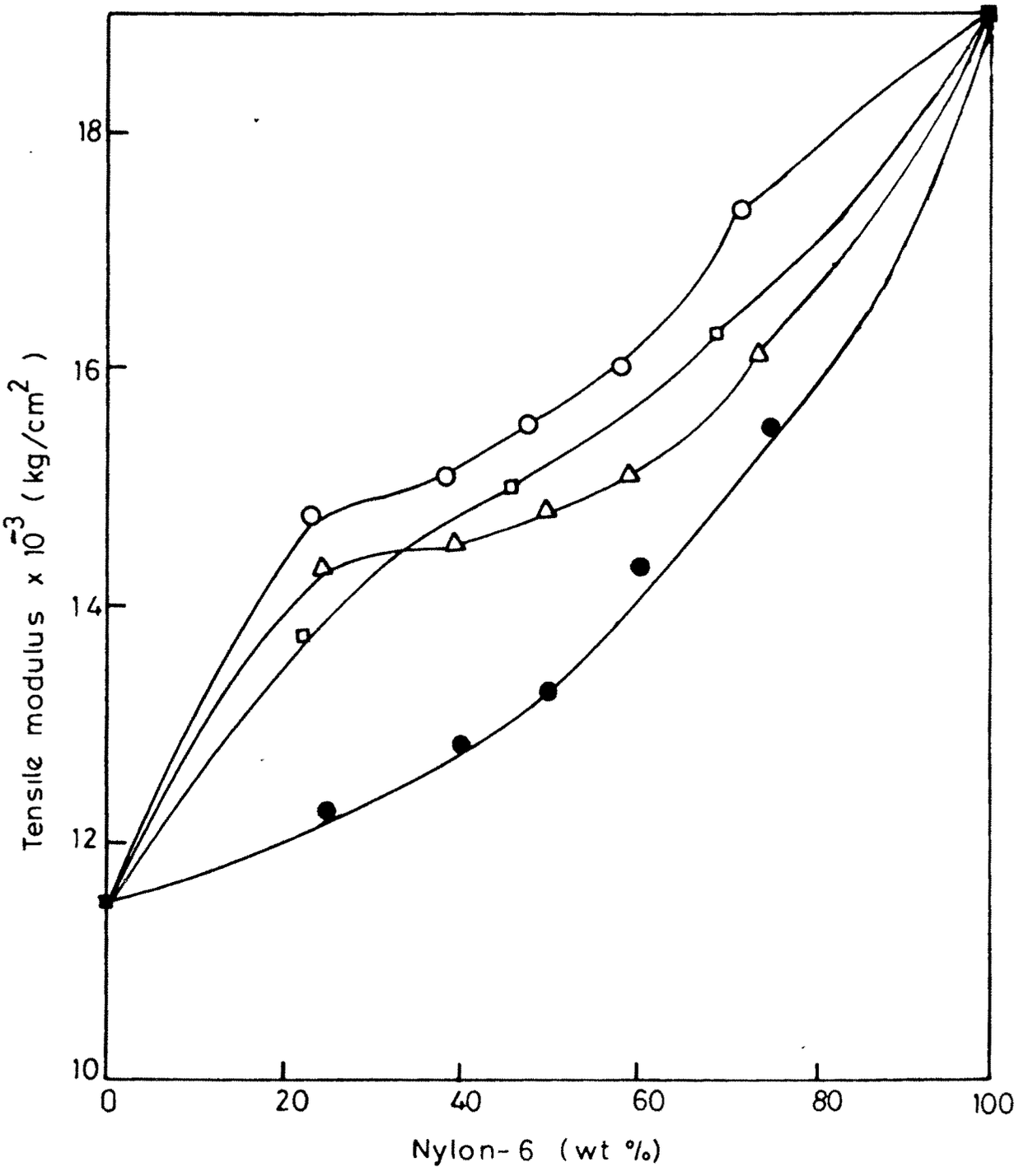

Fig. 4.42 Effect of blend composition on tensile modulus for
□ PP/Ny-6/PP-g-MAH (9.1%) blends
○ PP/Ny-6/PP-g-MAH (4.8%) blends
△ PP/Ny-6/PP-g-MAH (2.4%) blends
● PP/Ny-6 blends

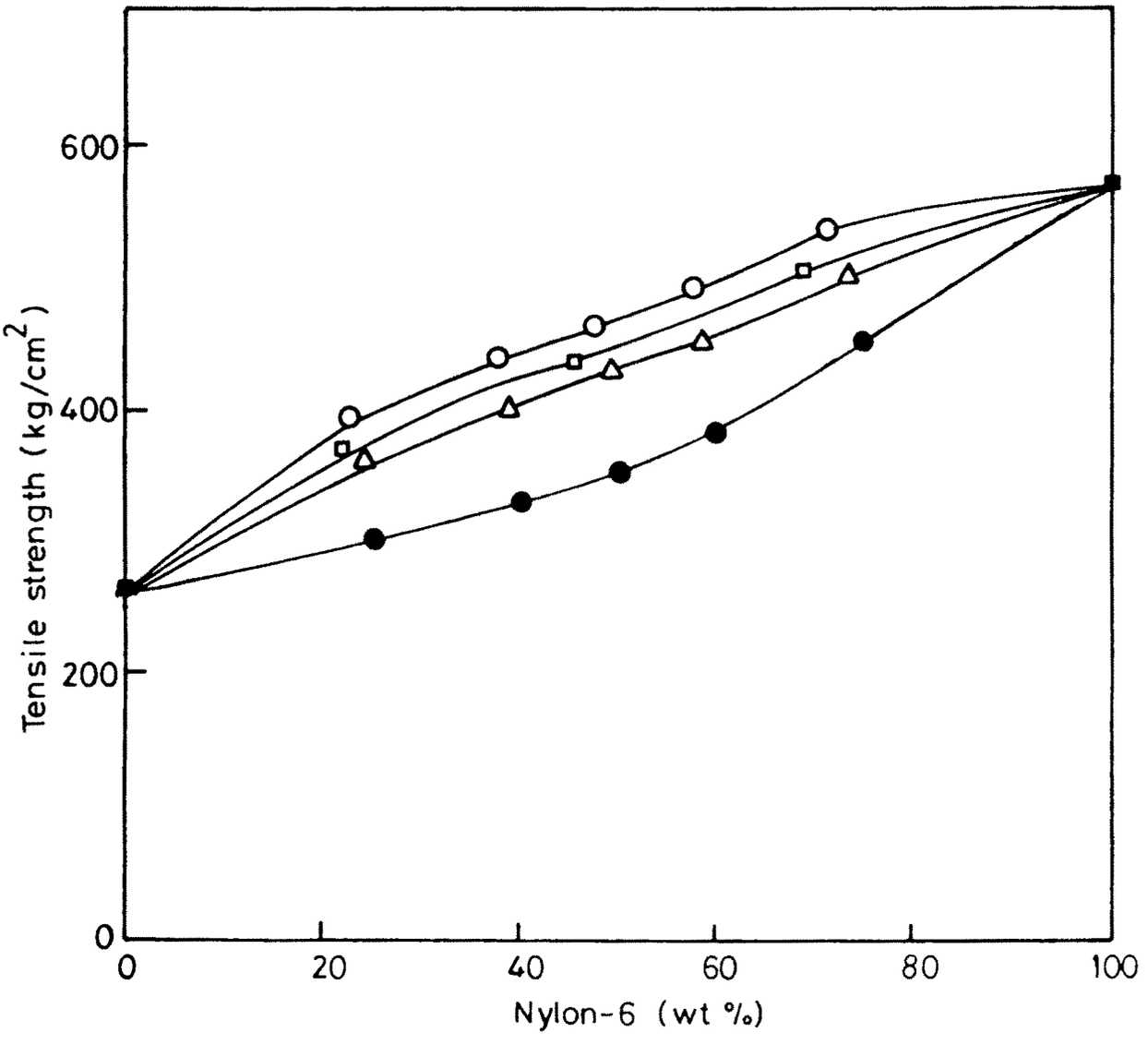

Fig. 4.43 Effect of blend composition on tensile strength for

□ PP/Ny-6/PP-g-MAH (9.1%) blends

○ PP/Ny-6/PP-g-MAH (4.8%) blends

△ PP/Ny-6/PP-g-MAH (2.4%) blends

● PP/Ny-6 blends

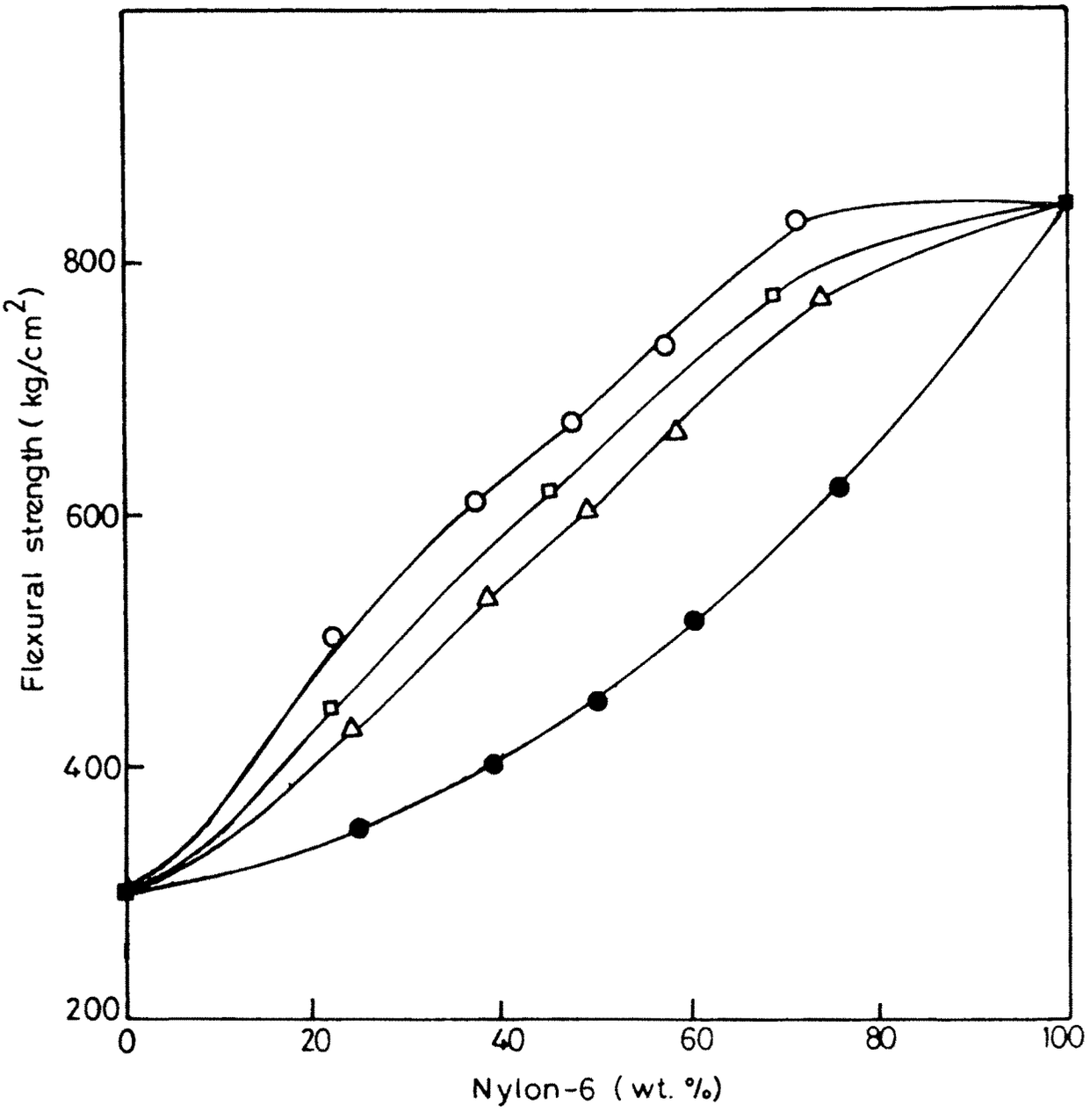

Fig. 4.44 Effect of blend composition on flexural strength for
□ PP/Ny-6/PP-g-MAH (9.1%) blends
○ PP/Ny-6/PP-g-MAH (4.8%) blends
△ PP/Ny-6/PP-g-MAH (2.4%) blends
● PP/Ny-6 blends

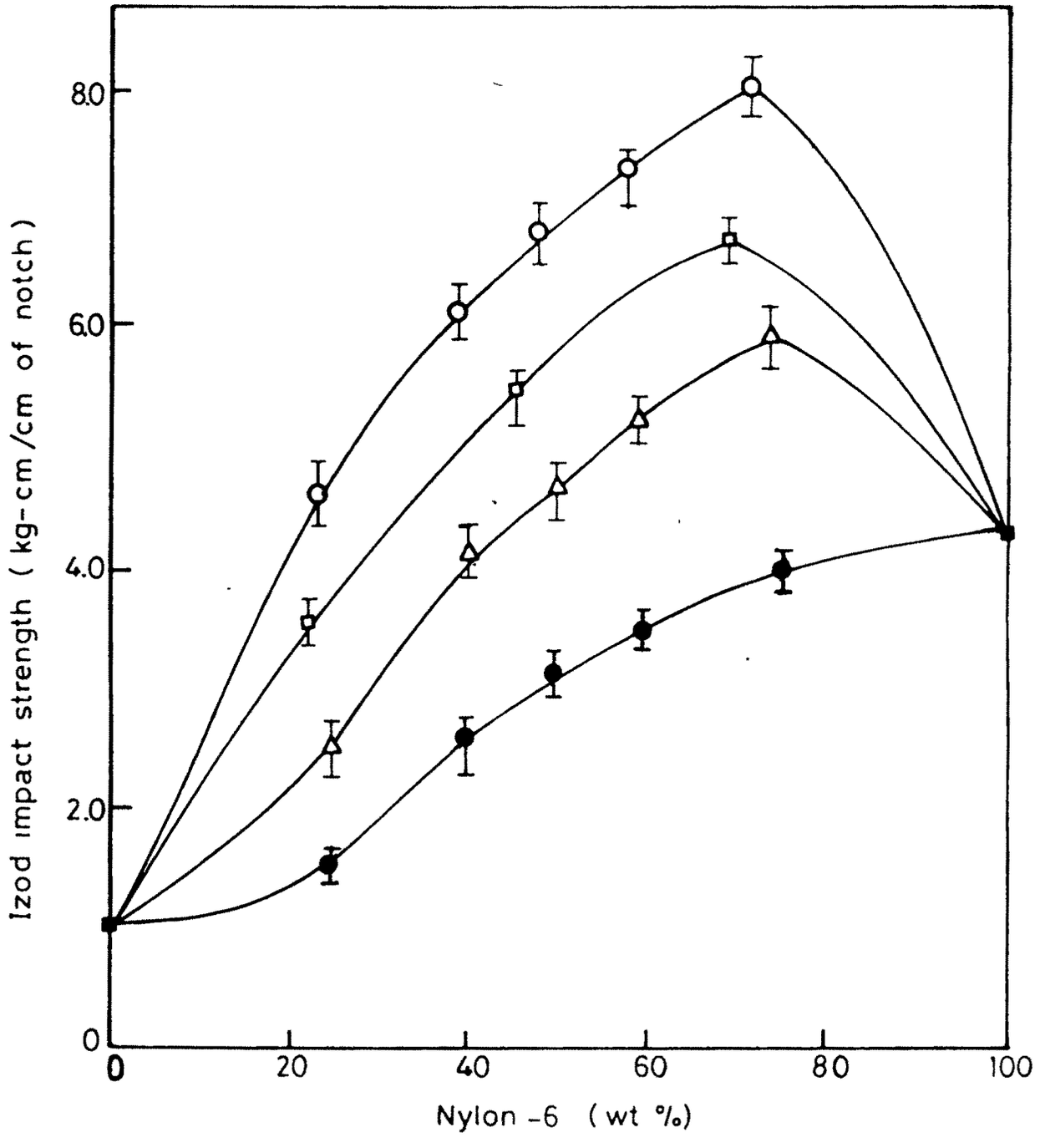

Fig. 4.45 Effect of blend composition on izod impact strength for

□ PP/Ny-6/PP-g-MAH (9.1%) blends

○ PP/Ny-6 /PP-g-MAH (4.8%) blends

△ PP/Ny-6/PP-g-MAH (2.4%) blends

● PP/Ny-6 blends

the SEM's (Fig.4.35 and 4.36) it is observed that addition of PP-g-MAH to PP/Ny-6 blends results in to reduction in the average dimention of the dispersed phase particles. The rough surface of the dispersed particles indicates the existance of adhesion between Ny-6 matrix and the dispersed phase PP or vice versa. As a result increased impact strength is observed for the ternary blends. Higher values of impact strength with increasing concentration of compatibiliser were observed due to improved homogenity which is discussed earlier, but for 9..1% compatibilised blend the observed decrease in impact strength may be due to the presence of higher amount of maleic anhydride producing chain breaking of the polymer as well as increase in domain size. The overall results of impact strength are higher when compared with the corresponding PP/Ny-6/PP-g-BA blends.

4.4.4.d Melt flow index

From Fig. 4.46 it can be inferred that all the blends have lower melt flow index than that of Ny-6. As observed in PP/Ny-6/PP-g-BA system, MFI of all ternary blends containing 2.4% and 4.8% of PP-g-MAH decreases with respect to the corresponding binary blend. The decreased MFI can be attributed to the higher reactivity of maleic anhydride resulting into formation of strong bond with Ny-6. However, higher concentration of compatibiliser (9.1%) shows increase in MFI than that for 4.8% and 2.4% compatibilised blends, emphasising the optimum concentration of the compatibiliser in the blends. Similar observation was made by Ide and Hasegawa [10] for Ny-6/PP/PP-g-maleic anhydride blends.

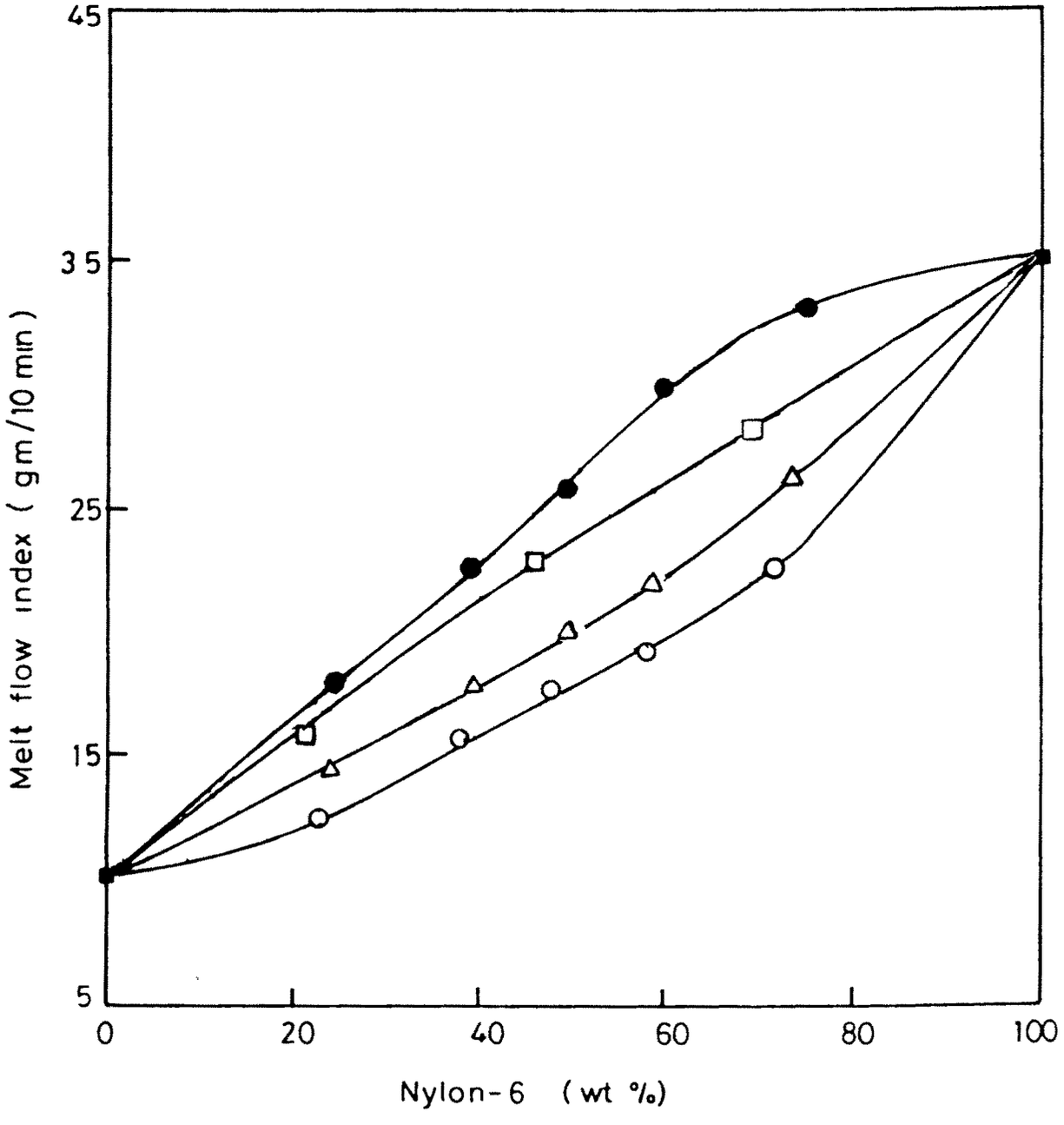

Fig. 4.46 Effect of blend composition on melt flow index for

□ PP/Ny-6/PP-g-MAH (9.1%) blends

○ PP/Ny-6/PP-g-MAH (4.8%) blends

△ PP/Ny-6/PP-g-MAH (2.4%) blends

● PP/Ny-6 blends

4.4.4.e Rockwell hardness

Table 4.9 shows the Rockwell hardness for PP/Ny-6/PP-g-MAH (2.4%) and PP/Ny-6/PP-g-MAH (4.8%) blends. It is observed that all the ternary blends have lower Rockwell hardness than Ny-6 but higher than binary blends. However, in case of PP-g-BA compatibilised blends very little difference in Rockwell hardness was observed for binary and ternary blends than the correspinding PP-g-MAH compatibilised blend.

4.4.4.f Heat deflection temperature (HDT)

Table 4.10 shows the effect of blend composition on the HDT values. As it is discussed earlier, in PP-g-BA compatibilised blends, HDT values of binary blends are lower than that of PP but those of ternary blends are slightly higher than PP. In case of PP-g-MAH compatibilised blends considerable increase in HDT values over PP-g-BA compatibilised blends was observed due to hardening effect of maleic anhydride. Similar observation was made by Nagao et al. [21] for Ny-66/PP/PP-g-maleic anhydride blend system.

4.4.4.g Thermal analysis

The representative melting curve for PP/Ny-6/PP-g-MAH (4.8%) is shown in Fig. 4.47. The results obtained from DSC analysis are given in Fig. 4.48 as melting temperature versus blend composition. It was observed that melting temperature (Tm) of Ny-6 as well as PP goes on decreasing as the extent of compatibiliser increases. Similar effect was observed in

Table 4.9

Rockwell hardness values of PP/Ny-6/PP-g-MA (2.4%) and PP/Ny-6/PP-g-MAH (4.8%), blend systems.

Code No.	Rockwell hardness (RHR)	Code No.	Rockwell hardness (RHR)
E_1	88	F_1	91
E_2	95	F_2	98
E_3	101	F_3	102
E_4	105	F_4	107
E_5	107	F_5	110

Table 4.10

Heat deflection temperature of various PP/Ny-6/PP-g-MAH blends.

Code	HDT (^{o}C)	Code	HDT (^{o}C)
E_1	79	F_1	84
E_2	83	F_2	87
E_3	80	F_3	89
E_4	79	F_4	85
E_5	76	F_5	81

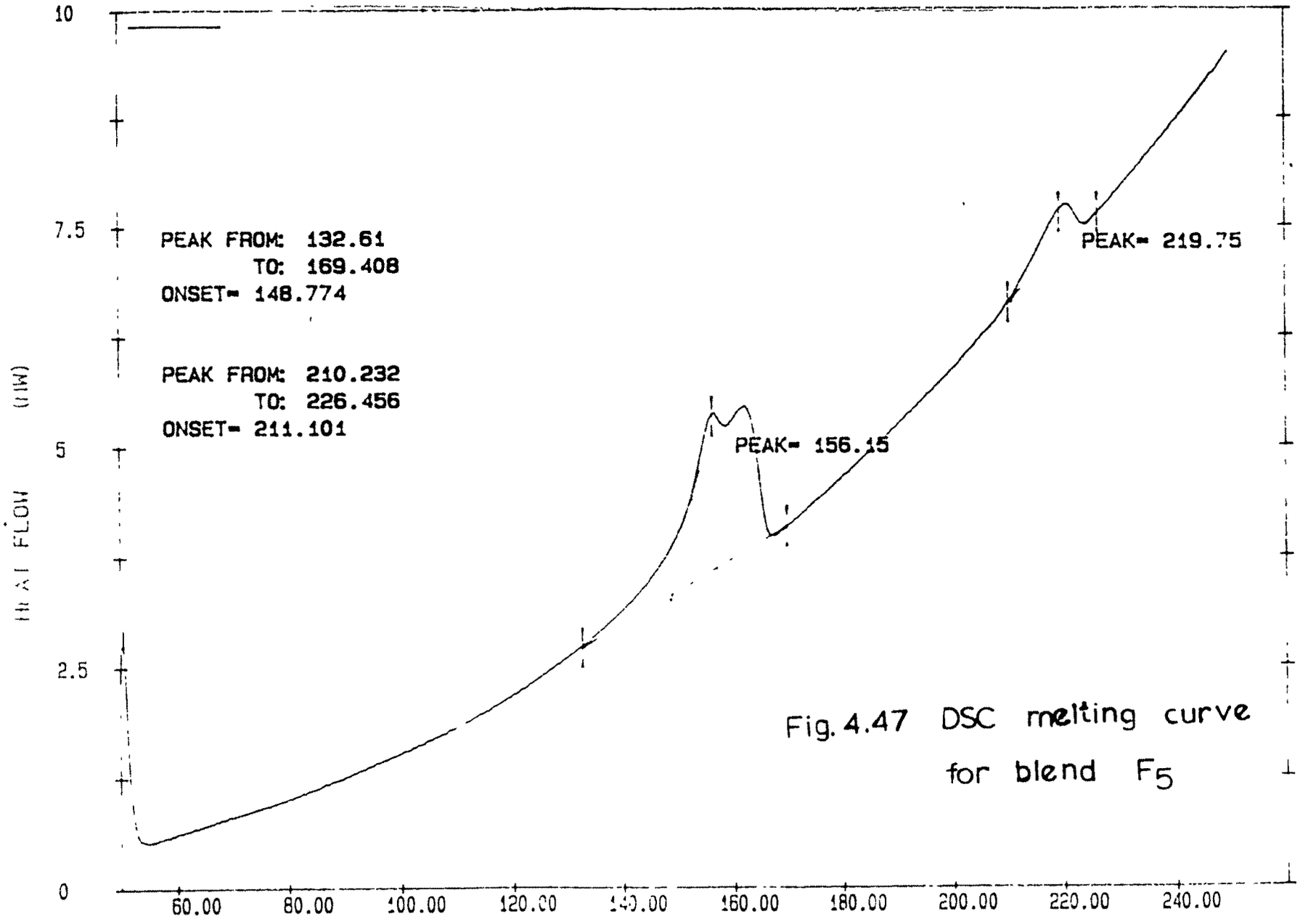

Fig. 4.47 DSC melting curve for blend F_5

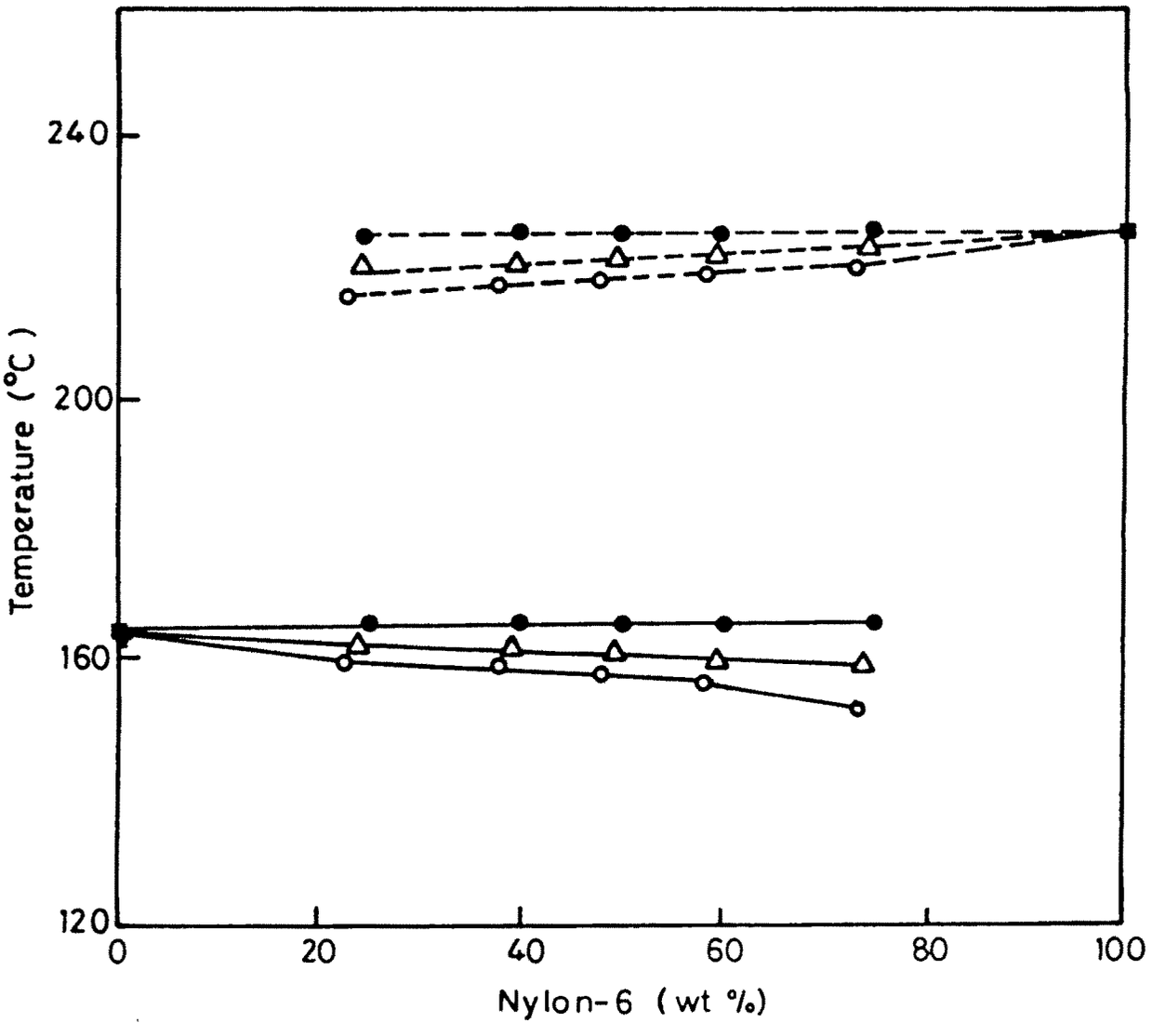

Fig. 4.48 Effect of blend composition on melting temperature : (●——●), Tm (PP) and (●----●), Tm (Ny-6) in PP/Ny-6 blends ; (△——△), Tm (PP) and (△----△) Tm (Ny-6) in PP/Ny-6/PP-g-MAH (2.4%) blends; (○—○), Tm (PP) and (○--○), Tm (Ny-6) in PP/Ny-6 /PP-g-MAH (4.8%) blends

PP/Ny-6/PP-g-BA blends as given and discussed in section 4.4.3.f. The per cent crystallinity of the ternary blends (Fig. 4.49) was observed to be lower than that of PP and Ny-6. As discussed in section 4.4.3.f, decreased percent crystallinity can be attributed to the increased hinderance of PP-g-Ny-6 to polymer chain packing. On comparision of results obtained for PP-g-BA and PP-g-MAH compatibilised blends, it is observed that reduction in percent crystallinity is higher for PP-g-MAH compatibilised blends. This may be due to the formation of higher amount of PP-g-Ny-6, which can be assigned to higher homogenity of blends as observed in various studies carried out for this system.

4.4.4.h Dynamic mechanical properties

The Figs. 4.50.a and 4.50.b summarise the loss modulus (E") data for PP/Ny-6/PP-g-MAH (2.4%) and PP/Ny-6/PP-g-MAH (4.8%) blends respectively. Here the blend containing 2.4% compatibiliser still shows broader peak around 60^{o}C for β-transition in Ny-6, but blends with 4.8% compatibiliser do not show any peaks at 60^{o}C indicating very strong chemical interaction between PP and Ny-6.

Figs. 4.51.a and 4.51.b show the loss factor tan δ (E"/E') versus temeprature. The results obtained indicate that the blends compatibilised with 2.4% and 4.8% PP-g-MAH differ very much from non compatibilised blends. The β-transition peaks for binary system are sharp, whereas those for ternary blends containing 2.4% compatibiliser are broader. In case of

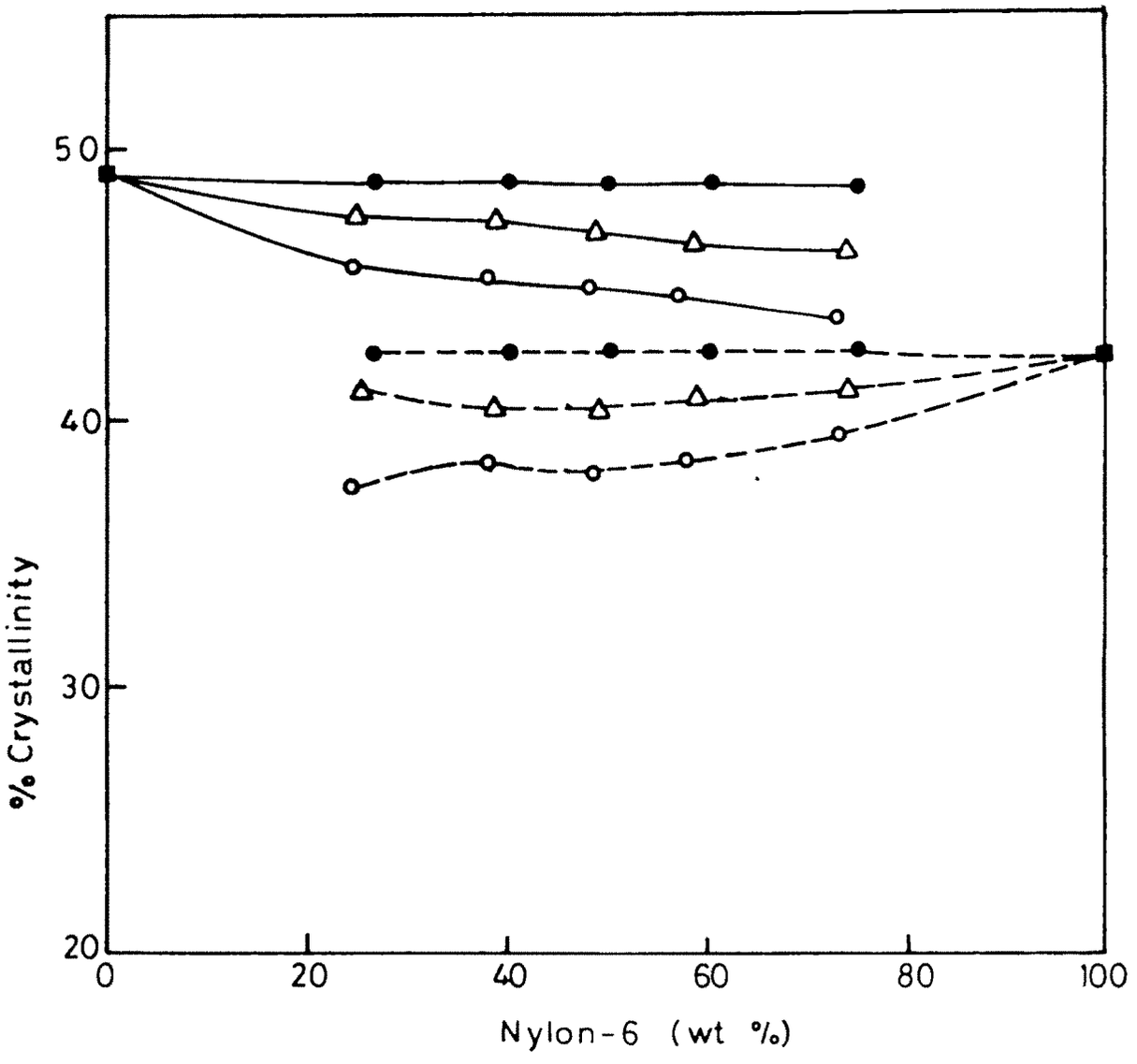

Fig. 4.49 Effect of blend composition on % crystallinity: (●——●), % crystallinity of PP and (●----●), % crystallinity of Ny-6 in PP/Ny-6 blends ; (△——△), % crystallinity of PP and (△----△), % crystallinity of Ny-6 in PP/Ny-6/PP -g-MAH (2.4%) blends; (○——○), % crystallinity of PP and (○----○), % crystallinity of Ny-6 in PP/Ny-6/PP-g-MAH (4.8%) blends.

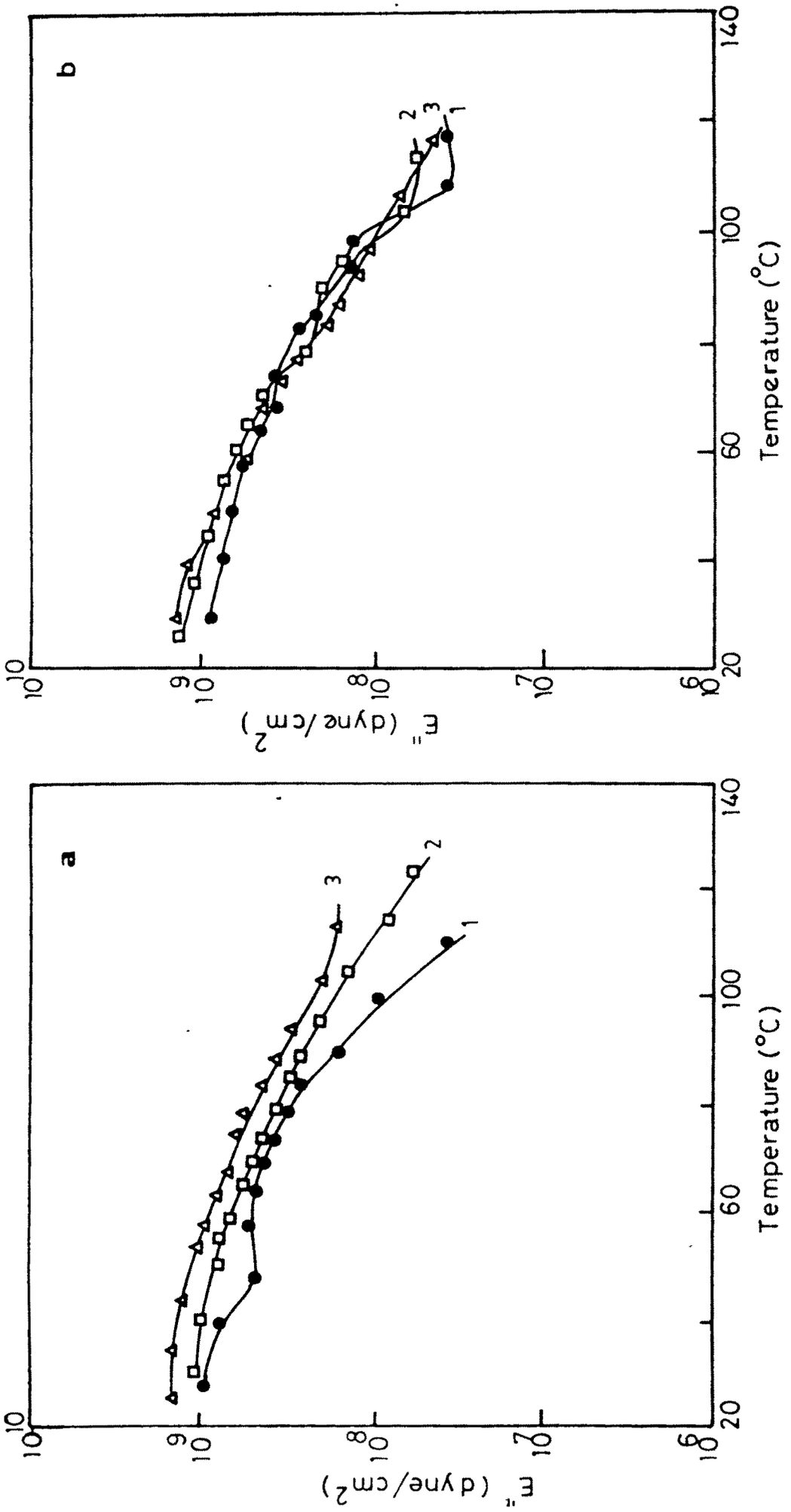

Fig. 4.50 Temperature dependence of loss modulus (E'') for (β-relaxation for Ny-6 phase)

a) PP/Ny-6/PP-g-MAH (2.4%) blends : 1, E_1 , 2, E_3 ; 3, E_5

b) PP/Ny-6/PP-g-MAH (4.8%) blends : 1, F_1 ; 2, F_3 ; 3, F_5

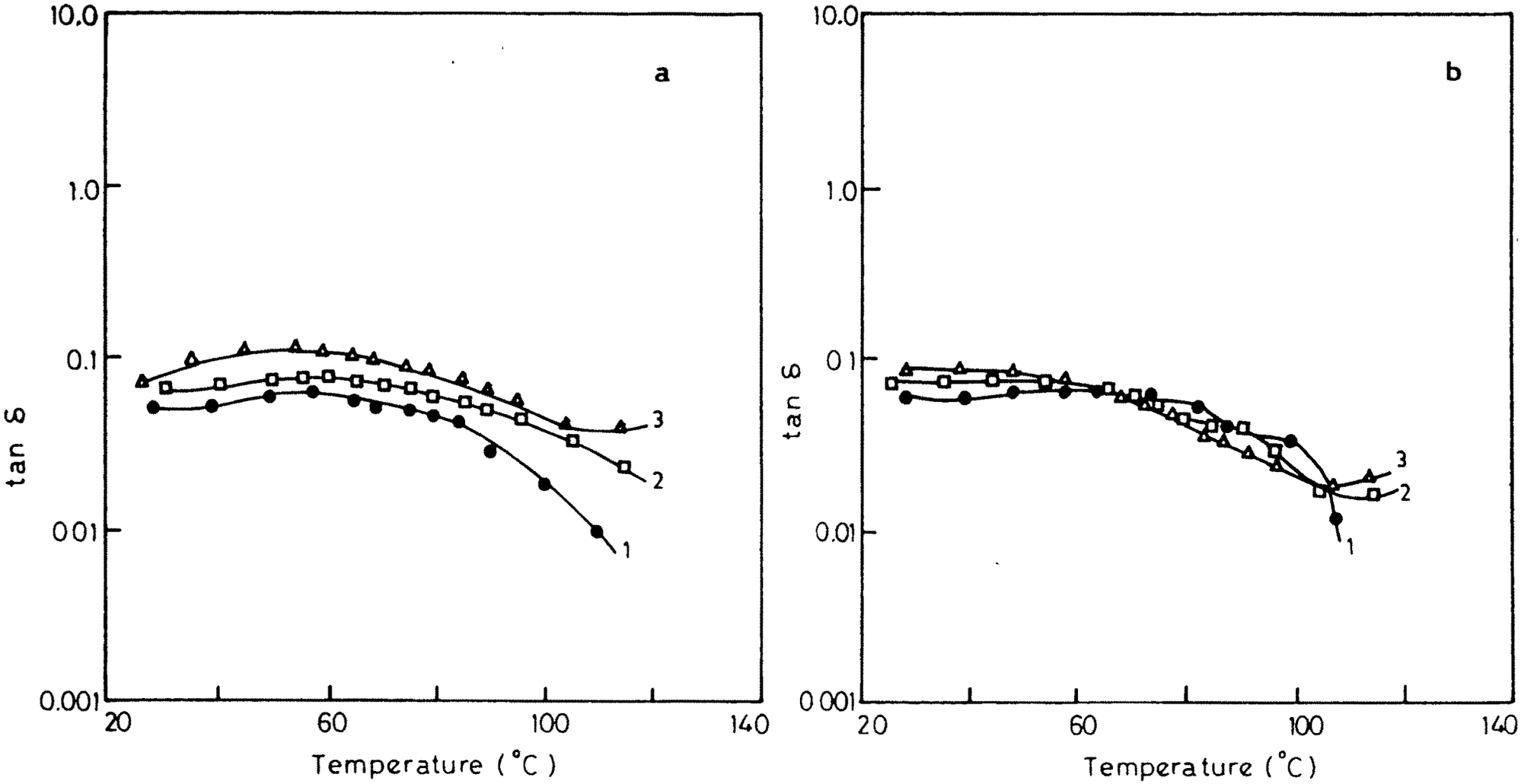

Fig. 4.51 Temperature dependence of loss factor (tan δ) for (β-relaxation for Ny-6 phase)

a) PP/Ny-6/PP-g-MAH (2.4%) blends : 1, E_1 ; 2, E_3 ; 3, E_5

b) PP/Ny-6/PP-g-MAH (4.8%) blends : 1, F_1 ; 2, F_3 ; 3, F_5

4.8% compatibilised blends β-transition peaks almost disappear indicating the complete miscibility of PP and Ny-6 phases.

In both types of ternary blends, compatibilised with PP-g-BA, and PP-g-MAH, the loss modulus (E") and loss tangent (tanδ) were higher than those for only mechanially blended polymers (binary blends). This may be due to the decrease in crystalline properties, as already discussed earlier. This also indicates good dispersibility of ternary blends in the amorphous area. Similar results were obtained by Ide and Hasegawa [10].

4.4.4.h Water absorption

From Fig. 4.52 it can be observed that the ternary blends have lower percentage water absorption values than that of Ny-6. On comparision with ternary blends containing PP-g-BA, these blends showed lower percentage of water absorption inspite of the presence of highly water suseptible maleic anhydride in the system. This can be attributed to the higher reactivity of MAH for Ny-6, resulting into the less availability of amine groups from Ny-6 for water absorption.

4.4.5 PP-g-(BA-co-MAH) as compatibiliser for PP/Ny-6 blends

The efficiency of the PP-g-(BA-co-MAH) as an compatibiliser in PP/Ny-6 blends is evaluated in this section.

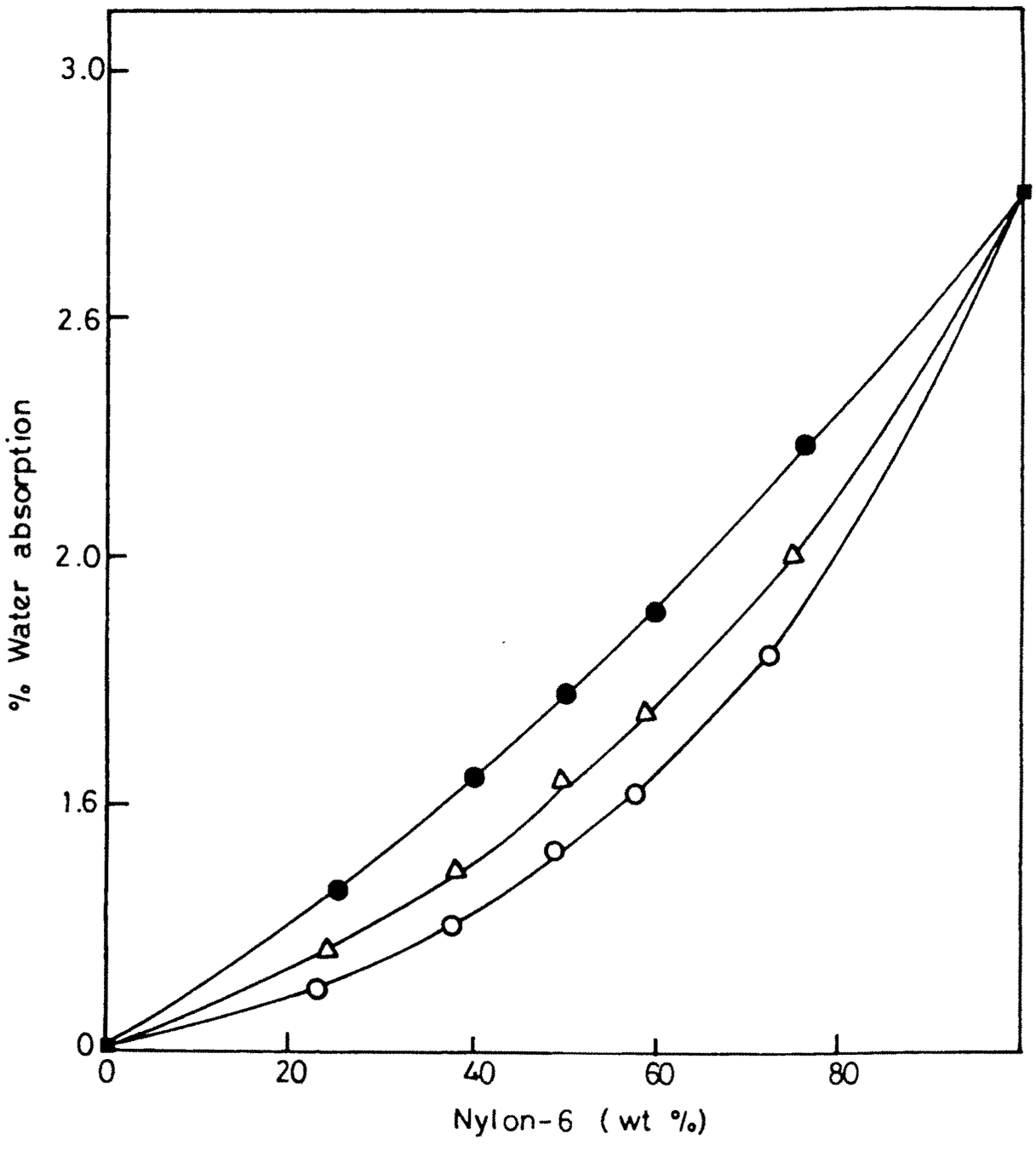

Fig. 4.52 Effect of blend composition on percent water absorption for

- ○ PP/Ny-6/PP-g-MAH (4.8%) blends
- △ PP/Ny-6/PP-g-MAH (2.4%) blends
- ● PP/Ny-6 blends

When PP-g-(BA-co-MAH) is added to PP/Ny-6 blends, the anhydride group of maleic anhydride and ester group of butyl acylate may react with the terminal amine group of Ny-6 during melt mixing at 235^{o}C. The reaction between free amine group of Ny-6 with the anhydride group of maleic anhydride has already been reported by various researchers [10,22] and the formation of PP-g-Ny-6 is assumed. In support to this statement Molau's test described earlier in section 4.4.2.a was carried out. On addition of formic acid to PP/NY-6/PP-g-(BA-co-MAH) blends, colloidal solution was obtained. This positive Molau's test indicates the presence of PP-g-NY-6 in the PP/NY-6/PP-g-(BA-co-MAH) blends which acts as an interfacial agent.

4.4.5.a Microscopy study

Figs. 4.53 and 4.54 show the micrographs of the fractured surfaces for BM_3 and BM_6 blends respectively. From Fig. 4.52, for 2.4% compatibilised blends, it can be observed that the dispersed particles have $\simeq 5\mu m$ diameter. But 4.8% compatibilised blends (Fig. 4.53) show no evidence of dispersed particles indicating good miscibility of two phases.

4.4.5.b Effect of PP-g-(BA-co-MAH) on tensile mechanical properties

The tensile modulus tensile strength flexural strength and impact strength values for 2.4% and 4.8%. PP-g-(BA-co-MAH) compatibilised blends are given in Table 4.11. From the

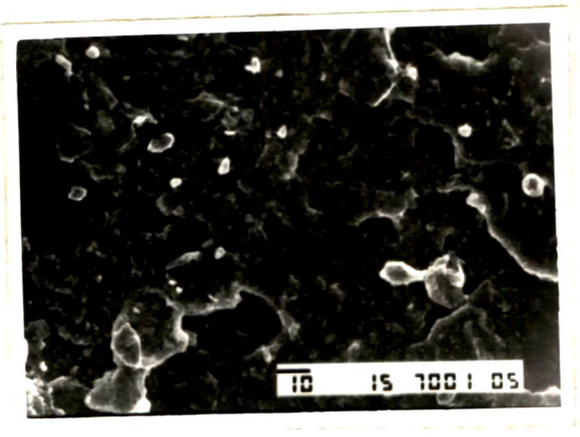

Fig. 4.52 SE micrographs of cryogenically fractured blend BM_3 (X 1000)

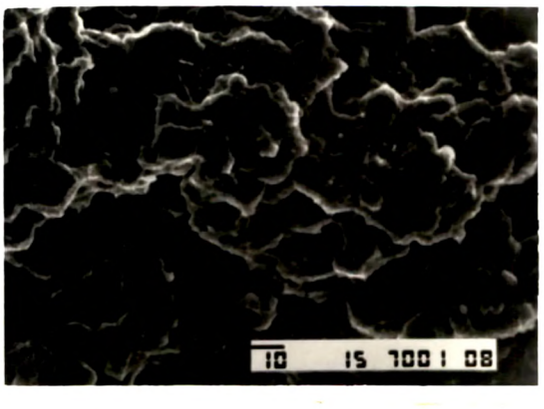

Fig. 4.53 SE micrographs of cryogenically fractured blend BM_6 (X 1000)

Table 4.11

Mechanical properties of the PP/Ny-6/PP-g-(BA-co-MAH) blends.

Code No.	Tensile modulus Kg/cm^2	Tensile strength Kg/cm^2	Flexural strength Kg/cm^2	Impact strength Kg-cm/cm
BM_1	13800	335	416	2.10
BM_2	14500	410	558	5.00
BM_3	15740	458	715	5.52
BM_4	14205	375	460	4.15
BM_5	14850	458	608	5.91
BM_6	16300	506	735	6.71

Table 4.11 it is seen that, all the values of the above mentioned properties are decreasing, when compared with the tensile mechanical properties of the corresponding PP/Ny-6/PP-g-MAH blends. But they are higher than those for PP/NY-6-PP/g-BA blends.

4.4.5.c Rockwell hardness and heat deflection temperature measurements

The Rockwell hardness and HDT values of 2.4% and 4.8% PP-g-(BA-co-MAH) compatibilised blends are given in Table 4.12. From the Table 4.12 it is observed that Rockwell hardness values of blends compatibilised with PP-g-BA, PP-g-MAH or PP-g-(BA-co-MAH) do not differ to a large extent.

There is some improvement in the HDT of these blends over the blends compatibilised with PP-g-BA.

4.4.5.d Water absorption

It can be observed from Table 4.12 that all PP/Ny-6/PP-g-(BA-co-MAH) blends have lower percentage water absorption. In this respect these blends resemble more to blends compatibilised with PP-g-MAH than to PP-g-BA.

4.4.5.e Thermal properties

The melting temperature and percent crystallinity of the PP/NY-6/PP-g-(BA-co-MAH) blends are listed in Table 4.13.

It can be inferred from Table 4.13 that the melting

Table 4.12

Rockwell hardness, HDT and percent water absorption of the various PP/Ny-6/PP-g-(BA-co-MAH) blends :

Code No.	Rockwell hardness (RHR)	HDT (^{o}C)	Water absorption (%)
BM_1	84.1	74.6	1.32
BM_2	93.7	72.3	1.70
BM_3	103.0	70.1	2.30
BM_4	85.0	82.4	1.25
BM_5	96.0	81.3	1.55
BM_6	106.0	83.1	1.92

Table 4.13

Melting temperatures (Tm) and % crytallinity values of various PP/Ny-6/PP-g-(BA-co-MAH) blends :

Code	PP		NY-6	
	Tm (^{o}C)	Crystallinity (%)	Tm (^{o}C)	Crystallinity (%)
BM_1	163.0	47.7	224.1	42.1
BM_2	162.1	46.8	223.5	41.0
BM_3	161.2	45.7	222.8	40.5
BM_4	162.4	47.2	223.8	41.8
BM_5	161.2	46.2	222.0	40.6
BM_6	160.1	45.6	220.3	39.6

temperatures and percent crystallinity of PP and Ny-6 in the ternary blends are lower than those in binary PP/NY-6 blends. Similar behaviour was observed for PP/Ny-6/PP-g-BA and PP/Ny-6/PP-g-MAH blends. The reasons for such behaviour have already been discussed earlier in section 4.4.3.f.

REFERENCE

1. R. J. Seward, J. Appl. Polym. Sci., **14**, 852 (1970).
2. C. B. Bulknell, Toughened Plastic, Applied Sci., London, 1977.
3. S. Wu, Polymer, **26**, 1855 (1985).
4. S. Wu, J. Appl. Polym. Sci., **35**, 549 (1988).
5. R. A. Dickie, J. Polym. Sci., Polym. Phys. Ed., **14**, 2073 (1976).
6. E. H. Kerner, Proc. Phys. Soc., **69B**, 808 (1950).
7. L. E. Nielsen, Mechanical Properties of Polymer and Composites, Marcel Dekker, New York, 1974.
8. B. Paul, Trans. Metallurgy. Soc., AIMI, **218**, 36 (1960).
9. T. Kunori and P. M. Geil, J. Macromol. Sci., **B18**, 135 (1980).
10. F. Ide and A. Hasegawa, J. Appl. Polym. Sci., **18**, 963 (1974).
11. R. Martuscelli, C. Silvestre and G. Abate, Polymer, **23**, 229 (1982).
12. Bo-RunLiang, J. L. White, J. E. Spruiell and B. C. Goswami, J. Appl. Polym. Sci., **28**, 2011 (1983).
13. N. K. Baramboim and V. F. Rakityanskii, Kolloidn. Zh., **36**, 129 (1974).
14. G. E. Molau, J. Polym. Sci., **A3**, 4735 (1965).
15. H. P. Schreiber and M. Kapuscinski, Polym. Eng. Sci., **21**, 433 (1983).
16. Z. Z. Liang and H. L. Williams, J. Appl. Polym. Sci., **44**, 699 (1992).

17. H. Rawal, Y. P. Singh, M. H. Mehta and S. Devi, Polymer, **32**, 493 (1991).

18. H. Rawal, Y. P. Singh, M. H. Mehta and S. Devi, J. Polym. Mater., **7**, 303 (1990).

19. T. Nishio, Y. Suzuki, K. Kojima & M. Kakugo, J. Polym. Eng., 10, 123 (1991).

20. L. A. Utracki and P. Sammut, A Poster Presented at the 33rd IUPAC International Symposium on Macromolecules, Montreal, July (1990).

21. T. Nagao, J. Nakamura and J. Takeda, Jpn. Pat. 01, 284, 553 (1989); Chem. Abstr. **113**, 7542p.

22. A. Y. Coran, R. Patel and D. Williame-Headd, Rub. Chem. Technol., **58**, 1014 (1985).